D 2021

U.PORTO
FEUP FACULDADE DE ENGENHARIA
UNIVERSIDADE DO PORTO

# AN OPTIMIZATION FRAMEWORK TO ESTIMATE THE ACTIVE AND REACTIVE POWER FLEXIBILITY IN THE TSO-DSO INTERFACE

**JOÃO PEDRO VASQUES VIEIRA DA SILVA**

TESE DE DOUTORAMENTO APRESENTADA
À FACULDADE DE ENGENHARIA DA UNIVERSIDADE DO PORTO EM
ENGENHARIA ELETROTÉCNICA E DE COMPUTADORES

June 01, 2021

Supervisor: Vladimiro Henrique Barrosa Pinto de Miranda

Co-Supervisor: Jean Sumaili Akilimali

The research leading to a part of this work has been carried out as a part of the evolvDSO, EU-SysFlex and TDX-ASSIST projects. The evolvDSO project was funded by the European Commission under the seventh framework program (FP7) under grant agreement number 608 732.The EU-SysFlex and TDX-ASSIST projects are part of the H2020 program and the corresponding grant agreement numbers are 773 505 and 774500.

This work was supported by the Portuguese Foundation for Science and Technology (FCT) under the grant SFRH/BD/124727/2016 and by the Centre for Power and Energy Systems of the Institute for Systems and Computer Engineering, Technology and Science – INESC TEC, Portugal.

Happiness can be found, even in the darkest of times, if one only remembers to turn on the light.

(J.K.Rowling)

To the ones that in the “darkest of times” encouraged me to continue this path

# Acknowledgments

First of all, I would like to acknowledge my thesis supervisor, Professor Doctor Vladimiro Henrique Barrosa Pinto de Miranda. Thanks to his ideas, support and guidance, this PhD thesis took the correct path. I also want to address a special appreciation to Doctor Jean Sumaili. He was the number one supporter, the person that guided me in my professional career as well as during this PhD thesis. I will never have enough words to express my gratitude to him. I also want to thank to the Centre for Power and Energy Systems (CPES) of INESC TEC. The persons working there became more than colleagues and I can fortunately call them friends. Here, I want to address a special appreciation to Ricardo Bessa, who has been a role model in my professional career.

# Abstract

The Distributed Renewable Energy Sources (DRES) connected to the distribution networks have been increasing their penetration for the last few years. Although necessary for environmental issues, this continuous growth has been leading to the arising of technical problems in both transmission and distribution grids. Historically, the overall system security is mainly ensured by the Transmission System Operators (TSOs). However, the foreseen increase of Distributed Energy Resources (DER) located in the distribution grids - whose flexibility might be exploited - is a clear sign that Distribution System Operators (DSOs) can play an important role and provide support in this task. The exploitation of flexibility services within a TSO-DSO coordination mechanism can become an effective procedure to keep the quality of supply service and security. Such exploitation should be ruled so that while TSOs become empowered with new mechanisms to deal with their inherent tasks, DSOs do no to have their operation jeopardized. Within this paradigm, knowledge regarding how DER flexibility would affect the TSO-DSO interface operating point, as well as the distribution side, is of utmost importance.

This PhD thesis focuses on the development of a methodology capable to estimate the active and reactive power flexibility ranges at the TSO-DSO boundary nodes while considering the DER flexibility costs and the technical constraints of the distribution grid. An optimization problem whose objective function automatically adapts itself to find the perimeter of the flexibility area is the core of the proposed approach. The results are compared with a sampling method and the outcome leads to clear conclusions: the proposed approach establishes the necessary conditions to promote the share of important information between both network operators without the need for disclosing confidential information.

# Resumo

As redes de distribuição de energia elétrica têm sofrido grandes alterações nos últimos anos, em particular no que se refere ao contínuo aumento de recursos distribuídos de origem renovável. Os planos mundiais e europeus apontam para a total descarbonização do setor elétrico mantendo, assim, a janela aberta para a integração de mais fontes renováveis. Apesar de necessária, particularmente por questões ambientais, este contínuo crescimento tem levado ao surgimento cada vez mais frequente de problemas técnicos, tanto nas redes de transporte como de distribuição. Historicamente, a segurança do sistema elétrico foi sempre uma tarefa levada a cabo pelo operador da rede de transporte. Contudo, o previsível aumento de recursos de energia distribuídos localizado nas redes de distribuição – cuja flexibilidade pode ser explorada – é um claro sinal de que os operadores da rede de distribuição poderão ter um papel importante no apoio a esta tarefa. A exploração de serviços de flexibilidade poderá dar um grande contributo para que se possa manter a segurança do abastecimento e a qualidade de serviço prestada aos clientes. Se, por um lado, os operadores da rede de transporte estarão certamente interessados na utilização deste tipo de serviços enquanto suporte às suas habituais tarefas, os operadores da rede de distribuição quererão assegurar que tal exploração não corresponderá a uma crescente instabilidade operacional nas suas redes. Será, então, crucial que ambos os operadores possam ter o conhecimento do impacto que o uso de flexibilidade pode ter nas suas interfaces enquanto garantem o cumprimento dos seus limites técnicos de operação.

A presente tese de doutoramento foca-se, assim, no desenvolvimento de uma metodologia capaz de estimar os limites de flexibilidade de potência ativa e reativa ao nível das interfaces entre os operadores. Tal estimação considera como restrições do problema, as restrições técnicas da rede de distribuição e os custos de flexibilidade. O ponto fulcral da abordagem desenvolvida está na construção de um problema de otimização, cuja função objetiva automaticamente se adapta para conseguir encontrar o perímetro da área de flexibilidade. Os resultados obtidos são comparados com um método de amostragem e a conclusão é clara: a abordagem proposta estabelece as condições necessárias para a partilha de informação de caráter importante para ambos os operadores, sem que para isso seja necessária a partilha de informação confidencial.

# Contents

**Acknowledgments** ..... **9**

**Abstract** ..... **11**

**Resumo** ..... **12**

**Contents** ..... **13**

**List of figures** ..... **16**

**List of tables** ..... **18**

**List of acronyms** ..... **20**

**Chapter 1** ..... **23**

Introduction ..... 23
1.1 Context and motivation ..... 23
1.2 Research question and hypothesis ..... 30
1.3 Dissertation outline ..... 32

**Chapter 2** ..... **33**

Flexibility Assessment and Exploitation ..... 33
2.1 Models and approaches to enable flexibility services exploitation ..... 33
2.2 A random sampling approach to identify the flexibility ranges ..... 34
2.3 Optimization methods applied to the OPF problem ..... 37
2.3.1 Linear Programming ..... 37
2.3.2 Non-linear Programming ..... 38
2.3.3 Quadratic Programming ..... 40
2.3.4 Newton-Raphson based category ..... 41
2.3.5 Mixture of programming categories ..... 43
2.3.6 Interior Point methods ..... 43
2.3.7 Artificial Intelligent methods ..... 46
2.3.8 Critical analysis: Conventional mathematical techniques Vs AI methods ..... 48
2.4 Primal-Dual IPM for NLP ..... 49

**Chapter 3** ..... **51**

Estimating the Flexibility Area at the TSO-DSO Interface ..... 51
3.1 Methodology framework ..... 52
3.2 The pathway towards an optimization framework ..... 53
3.3 The optimization problem formulation ..... 54
3.4 Flexibility area identification procedure ..... 57
3.5 Key Performance Indicators (KPI) ..... 60
3.6 Estimation of the flexibility range at the TSO/DSO boundary nodes ..... 61
3.6.1 Test Case Description - 210 nodes MV distribution network ..... 61
3.6.2 Results and Critical Analysis ..... 63
3.6.3 KPI evaluation ..... 66
3.6.4 Benefits assessment ..... 68
3.7 Estimation of non-convex flexibility areas ..... 69
3.8 Contributions to Goal 1 ..... 70

**Chapter 4** ..... **72**

Transmission network equivalents to support flexibility area computation ..... 72
4.1 Network equivalents – from the basis to an innovative approach..... 72
4.2 The Ward equivalent methods ..... 74
4.2.1 Linear Ward equivalent model ..... 74
4.2.2 Non-Linear Ward equivalent model ..... 76
4.2.3 Ward equivalent with PV nodes retention..... 77
4.2.4 Extended Ward equivalent ..... 78
4.3 Transmission network equivalents – a novel algorithm only dependent on historical data availability..... 80
4.3.1 Evolutionary Particle Swarm Optimization (EPSO)..... 84
4.3.2 Results for the IEEE-RTS 96 (single-area variant) ..... 87
4.4 Contributions to Goal 2 ..... 94

**Chapter 5** ..... **96**

The impact of discrete variables in the flexibility area ..... 96
5.1 The arising of disjoint flexibility areas ..... 97
5.2 Searching for sub-areas of flexibility via a metaheuristic approach ..... 99
5.2.1 Iterated local search ..... 101
5.2.2 Smoothing methods ..... 102
5.2.3 Simulate annealing ..... 104
5.2.4 Variable neighborhood search ..... 106
5.3 Ensuring the feasibility of the flexibility domain using a VNS ..... 108
5.3.1 Results for the IEEE-RTS 96 (single-area variant) ..... 113
5.4 Contributions to Goal 3 ..... 118

**Chapter 6** ..... **119**

Conclusions ..... 119
6.1 Meeting the goals ..... 119
6.2 Thesis main impacts..... 121
6.3 Impact on the state-of-the-art ..... 122
6.4 Future research lines..... 126

References ..... 129

**Annex I – List of Publications** ..... **140**

**Annex II – Load and DRES data** ..... **143**

# List of figures

Figure 1 - DSO roles and corresponding responsibilities ..... 25

Figure 2 – Conceptual framework to reinforce the cooperation between system operators ... 26

Figure 3 – Relevant interactions between stakeholders [4] ..... 27

Figure 4 – TSO-DSO interaction scheme to avoid line overloading [6] ..... 28

Figure 5 – Illustration of flexibility areas constrained by different maximum costs ..... 31

Figure 6 – A random sampling approach to identify the flexibility area ..... 35

Figure 7 – General architecture of the proposed methodology ..... 52

Figure 8 - Flexibility area neglecting the technical grid limitations (grey) and including them (blue) ..... 53

Figure 9 – The impact of the PQ interdependency upon the flexibility area shape ..... 54

Figure 10 – Illustration of the perimeter identification procedure ..... 59

Figure 11 – Optimization process step-by-step ..... 59

Figure 12 – Real Portuguese MV distribution network [107] ..... 61

Figure 13 - Flexibility area for the 210 Nodes MV distribution network ($\theta tol$ =10 degrees) ... 63

Figure 14 - Flexibility area for the 210 Nodes MV distribution network ($\theta tol$ =3 degrees) .... 64

Figure 15 – Flexibility areas constrained by different maximum flexibility costs ..... 65

Figure 16 – Random Sampling vs Proposed Methodology ..... 66

Figure 17 – Estimation of a non-convex area ..... 69

Figure 18 – Generic representation of a full network model ..... 73

Figure 19 – Linear Ward equivalent model ..... 76

Figure 20 - Network equivalent with PV nodes retained ..... 78

Figure 21 – Extended Ward equivalent ..... 79

Figure 22 – Network equivalent model with the respective TSO-DSO interfaces ..... 80

Figure 23 – EPSO applied to the fine-tune the equivalent model ..... 82

Figure 24 – Clustering procedure and the transmission network equivalents ..... 84

Figure 25 – EPSO movement rule ..... 87

Figure 26 - Single area IEEE RTS-96 ..... 87

Figure 27 – Impact of $\boldsymbol{VTSO - DSO}$ in the clustering procedure ..... 89

Figure 28 – PQ limits for all the TSO-DSO connections (Only Distribution) ..... 91

Figure 29 - PQ limits for each TSO-DSO connection (Only Distribution) ..... 92

Figure 30 - PQ limits for each TSO-DSO connection (fine-tuned grid equivalent)..... 93

Figure 31 - PQ limits for each TSO-DSO connection (equivalent of other cluster) ..... 93

Figure 32 - Flexibility areas fixing each one of the discrete variables combinations ..... 98

Figure 33 – Comparison of flexibility areas (step Nº1 – green areas vs step Nº2 – red area) ... 99

Figure 34 – Algorithms to escape from local optima.....101

Figure 35 – Illustration of the ILS principles.....102

Figure 36 – Search space smoothing .....103

Figure 37 - Illustration of the smoothing methods principles .....103

Figure 38 - Illustration of the SA principles .....105

Figure 39 - Illustration of the VNS principles .....107

Figure 40 – Changes applied on the discrete variables to create shaking neighborhoods.....111

Figure 41 – Random solution extracted from the $kth$ neighborhood $Nk(x)$ .....111

Figure 42 – Perturbation process during the local search.....112

Figure 43 – Continuous PQ Map for the updated IEEE RTS .....114

Figure 44 – Largest sub-flexibility area encompassing $PQTSO - DSO$ .....115

Figure 45 – Fitness function evolution during the search .....116

Figure 46 – Impact of maximizing the feasible flexibility area .....117

Figure 47 - Feasible regions within the continuous flexibility area.....117

# List of tables

Table 1 - Degrees of flexibility for each flexible resource and corresponding costs ..... 62

Table 2 – KPI computation ..... 67

Table 3 – Computation time of both methods ..... 67

Table 4 – Benefits associated to the flexibility area recognition ..... 68

Table 5 – Centroids composition ..... 89

Table 6 – Parameters of the reduce network models ..... 90

Table 7 - Combination of discrete variables for the largest sub-flexibility area ..... 115

Table 9 – Load hourly forecast for a specific time instant ..... 143

Table 10 – DRES/DG installed capacity ..... 145

# List of acronyms

**List of acronyms**

| | |
|---|---|
| AI | Artificial Intelligent |
| BaU | Business as Usual |
| BRP | Balance Responsible Parties |
| DE | Differential Evolution |
| DER | Distributed Energy Resources |
| DG | Distributed Generation |
| DRES | Distributed Renewable Energy Sources |
| DSO | Distribution System Operator |
| EV | Electric Vehicles |
| FACTS | Flexible AC Transmission Systems |
| GA | Genetic Algorithm |
| ICT | Information and Communications Technology |
| ILS | Iterated Local Search |
| IPM | Interior Point Method |
| KE | Kinetic Energy |
| KKT | Karush-Kuhn-Tucker |
| KPI | Key Performance Indicator |
| LP | Linear Programming |
| FMIP | Mixed-Integer Programming |
| NLP | Non-linear programming |
| OLTC | On-load Tap Changers |
| OPF | Optimal Power Flow |
| PSO | Particle Swarm Optimization |
| QP | Quadratic Programming |
| RTS | Reliability Test System |
| SA | Simulated Annealing |
| SCADA | Supervisory, Control and Data Acquisition |
| TEF | Transient Energy Function |
| TSO | Transmission System Operator |
| USEF | Universal Smart Energy Framework |
| VND | Variable Neighborhood Descent |
| VNDS | Variable Neighborhood Decomposition Search |

| | |
|---|---|
| VNS | Variable Neighborhood Search |

# Chapter 1

# Introduction

The main goal of this chapter is the contextualization of the subject under study in this PhD thesis. The research question and corresponding hypothesis assume a high importance in this chapter since they illustrate the starting point and one of the most important steps of any dissertation. An outline of the developed work is also presented.

## *1.1 Context and motivation*

The power systems and their operation strategies are constantly evolving. Nowadays, the two main driven forces of this changing environment are the increasing impact of Distributed Renewable Energy Sources (DRES) in the generation mix and the growing pro-active demand for electricity. Together with the benefits brought by these changes, some technical problems for both distribution and transmission grids arise. For the Transmission System Operators (TSO), the increasing penetration of DRES is a challenge in terms of ensuring frequency balance due to their fluctuant character. Concerning the Distribution System Operators (DSO), more voltage violations and/or branch congestions are expected in their networks, mainly related to the increased consumption for Electric Vehicles (EV) and residential heat pumps, together with increased local production (e.g. Photovoltaics).

Several studies focusing on how these challenges should be addressed have been carried, arriving to a common conclusion: flexibility services exploitation is the key to deal with this evolving grid structure. In fact, one of the sources of the issues described above is, at the same time, the solution to overcome them. DRES is one of the multiple Distributed Energy Resources (DER) available in the distribution networks, which, in response to an external signal (e.g. price signal or activation), can modify their injection and/or consumption patterns, thus providing a service to the system [1]. Flexibility may be characterized by several evaluation parameters such as the response time or the amount of power modulation. A list of typical flexible DER is given:

- On-load Tap Changers (OLTC), Reactive Power Compensators (usually owned by the DSO);
- Distributed Renewable Energy Sources / Distributed Generation (DG);
- Flexible loads (i.e. demand response services);

- Storage Devices.

In this context of increasing value concerning flexible DER located at the distribution grids, a wide spectrum of subjects needs to be clarified: which will be the roles of each stakeholder in this evolving environment? how to integrate DER flexibility services within a market perspective? and which technical problems should these services address? The FlexPower project [2] departs from the fact that, in Denmark, the system balance is mostly maintained via the regulating power market, which is provided, primarily, by central power plants in combination with import/export to Norway and Sweden. In practice, small-scale demands and small-scale generations are excluded from the market since a 10 MW minimum bid size exists. Therefore, the inclusion of aggregated small-scale DER in a real-time market for balancing power is studied. In the iPower Project [3], there is the description of the conceptual design of a flexibility marketplace, where the flexible DER of prosumers are mobilized by aggregators in order to provide flexibility services to the DSO. Possible DSO needs concerning flexible resources activation are analyzed and contractual prerequisites are defined (e.g. price calculation, quality and penalizations specifications) depending on the type of technical problem (e.g. voltage issues caused by local generation). The importance of consider demand side resources as market-based products is also addressed in [4] by defining a set of future flexibility services, relevant value chains, market arrangements and recommendations to overcome the current regulatory barriers.

As grid managers, both TSOs and DSOs are responsible for the secure operation of their respective networks. However, in a regulatory environment where some DSO can already contract flexibility (e.g. Sweden, Finland) [5], the TSO is still the main responsible to deal with most of the grid operation challenges (e.g. congestion management, voltage support) [6].In fact, in most countries, DER flexibility services are directly contracted by the TSO [7]. Historically, these tasks were assigned to the TSO due to the typical power system architecture, in which the generation sources were mainly connected at the transmission level. The foreseen growth of smart appliances, electric vehicles, storage and other DER connected to the distribution grid is an indication that the DSO should have a more participative role in ensuring system security. An active distribution management by the DSO side would allow to take advantage and optimize the use of DER flexibility. In order to accomplish it, several projects focused on the definition of future roles that the different stakeholders should have in a smart grid environment. The “Reforming the Energy Vision” plan [8] defines a new stakeholder category – the Distribution System Platform Provider – that ensures DER coordination in order to meet system needs. In [9], a conceptual role framework - the Universal Smart Energy Framework (USEF) - explains how DER flexibility services should be used and how the stakeholders should correlate in order to guarantee a secure operation of the system. In the USEF, the Balance Responsible Parties (BRP), DSOs and TSOs acquire flexibility from the

aggregator, which has a central role. The GridWise Council also contributed with a plan to an effective DER integration by developing the transactive energy architecture [10]. It is a conceptual and regulatory perspective that can be mapped into four fields: policy and market design, business models, architecture guidelines and cyber-physical infrastructures. The evolvDSO project [11] applied the IEC PAS 62559 use case methodology and defined future roles for DSO in several domains and timeframes (e.g. planning, operational, TSO-DSO cooperation). These roles were idealized to allow for an efficient DRES integration in distribution networks and their conception followed the ideas presented on two previous works [12] [13]. In [12], the implications brought by an increasing penetration of DRES/DER for the typical tasks of system operators are analyzed and new possibilities for system planning/operation as well as for information exchange are highlighted. On the other hand, [13] they focus on exploiting synergies with the Information and Communication Technologies (ICT) sector and details a regulatory assessment regarding incentives and obligations that would empower consumers.

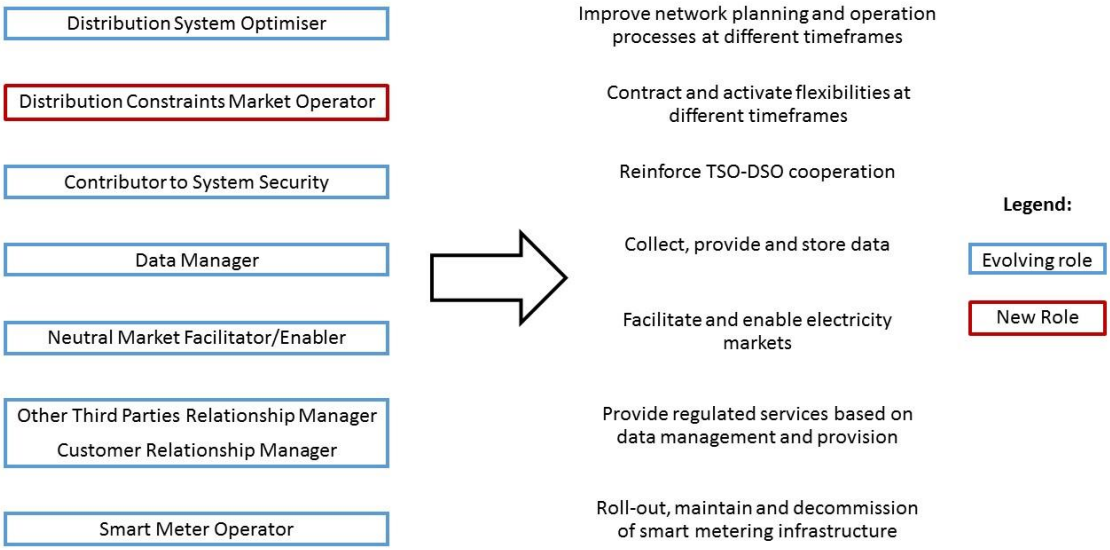


**Figure 1 - DSO roles and corresponding responsibilities**

Figure 1 shows the aim of each one of the potential DSO roles defined in [11]. The future DSO tasks are also analyzed in [14] in the context of different market structures and a similar conclusion is drawn: the DSO should move towards an active management of the grid – not only of the distribution grids, but also providing services to the TSO that support system security. Quoting [14], "From the point of view of DSO, smart grids are not a final goal, but a tool for efficient system management".

The "Contributor to System Security" is one of the evolving DSO roles presented in Figure 1. Its high importance is explained by three correlated facts:

1. DRES increase leads to technical problems not only in the distribution grids, but also in the transmission networks;

2. Flexible DER, which represent a solution to overcome these problems, are mostly located at the distribution grids;

3. Lack of power flow coordination at the system operator's interface.

Therefore, a close cooperation between TSOs and DSOs, characterized by a constant cross-actor exchange of information, is crucial to exploit flexibility benefits. Actually, the TSO-DSO coordination domain is an important part of the European Network of Transmission System Operators for Electricity (ENTSO-E) Network Code "Operational and Scheduling" [15], where it is stated that the power flows of active and reactive power in the primary substations should be monitored and controlled. In this coordination perspective, the DSO would have an important role in supporting the TSO fulfilling their responsibilities by managing their flexibility activation requests. To reach this goal, structural and forecast data needs to be exchanged between the system operators as well as between them and other market participants (e.g. flexibility operators).


**Figure 2 – Conceptual framework to reinforce the cooperation between system operators**

Figure 2 is a conceptual illustration of how DSOs can actively participate in the typical grid operational challenges. Therefore, in a TSO-DSO cooperation environment, the DSO would contribute to system security by managing the TSO requests. Nevertheless, a secure and safe operation of both grids while accessing flexibility is dependent of the arising of services conducted by the DSO (e.g. flexibility estimation, technical validation of flexibility activation). In order to deploy them, both practical methodologies and regulatory changes are mandatory. Regarding the latter, regulators have a key role to play in the definition of models that allow for the provision of these services. The differences amongst the European distribution systems

makes even more important their contribution to achieve a common standard. Although important, the regulatory framework update is not the motivation of this work, which clearly focus on a contribution at the algorithmic level.

In the literature, a wide spectrum of analysis regarding TSO-DSO coordination mechanisms and corresponding recommendations are described. As above mentioned, the work presented in [4] outlines relevant links between the different stakeholders present in a smart grid environment.

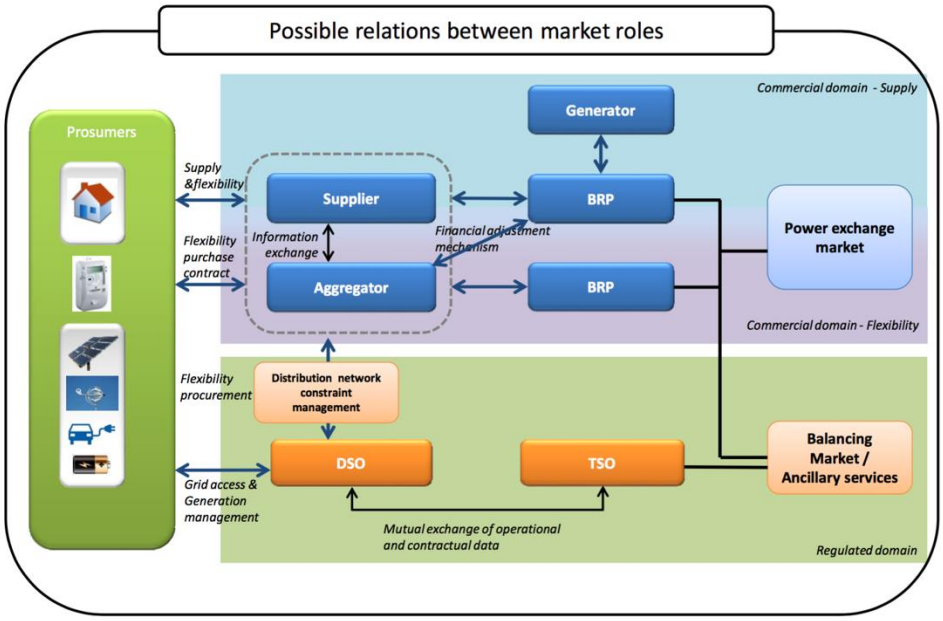


**Figure 3 – Relevant interactions between stakeholders [4]**

Figure 3 shows how complex these interactions can become. Particularly, in the distribution network constraint management the possible conflict of interests between the TSO and the DSO is clear. As an example, if a DSO needs to activate a certain amount of flexibility to address a technical problem in his grid, this would have an impact in the TSO network and at the system balance level. Once again, this points out to a path where the TSO and the DSO should exchange operational and contractual data. A state of the art concerning the current interactions between system operators analyzed six different grid operational challenges and concluded that cooperation processes are rarely observed [6]. Therefore, a two-way communication system ($\mathrm{DER} \leftrightarrow \mathrm{DSO} \leftrightarrow \mathrm{TSO}$) should be undertaken in order to guarantee system security near to real time. Conceptual cooperation models are also proposed in [6] for each one of the operational challenges. Figure 4 shows the proposed interaction scheme to avoid line overloading. It consists of three simple steps with only one requirement: exchange of information. After performing a power flow calculation to detect a possible line overloading, the TSO, which already knows the available flexibility in the distribution grid (i.e. service provided by the DSO), makes an activation request to the DSO.

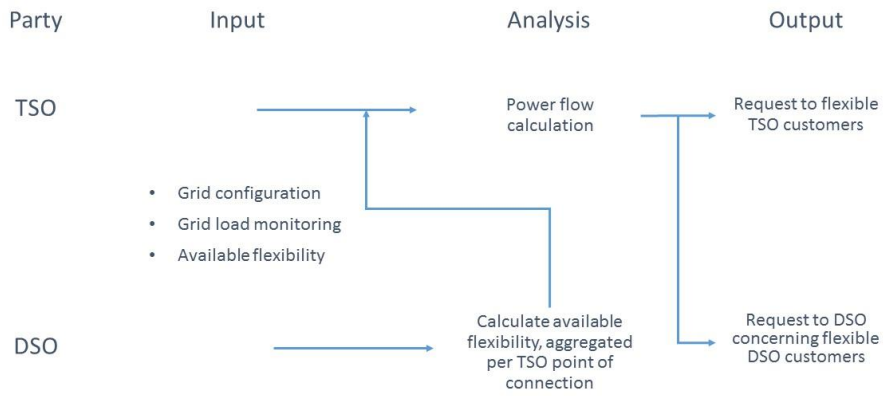


**Figure 4 – TSO-DSO interaction scheme to avoid line overloading [6]**

Several other projects contributed with a variety of interaction processes that try to rule the TSO-DSO interaction. What is interesting to observe across these projects is the different opinions regarding which would be the best-suited model. The SP Energy Networks, which is the DSO for central and southern Scotland, Merseyside and North Wales, and owns the transmission grid in south Scotland, points out to a vision where the DSO manages all DER located downstream the Transmission-Distribution boundary [16]. The DSO would be responsible for recruiting and dispatching flexibility services in order to deliver the response required by the TSO. At the same time, the DSO would also carry out local system balancing measures. However, if both networks operators have flexibility needs, it is not clear who would have the activation priority. This topic is of utmost importance and is well addressed in the SmartNet project [7]. Five different TSO-DSO cooperation structures are proposed covering different degrees of involvement by system operators regarding prequalification, procurement, activation and settlement of ancillary services. The outcome of a consultation process developed within this project highlighted the benefits of a common ancillary services market model, in which none of the system operators has priority. In this scheme, the activation of flexible resources is the result of an optimization process that considers the needs of both TSO and DSO while aiming to minimize the global operation cost. The hybrid VPP4DSO project addresses the same scope, but in a slightly different perspective. The concept of a hybrid virtual power plant arises in order to ensure that the exploitation of flexible resources does not create technical problems on the distribution networks [17]. Thus, this virtual power plant, which aggregates the capacity of diverse DER, participates in the ancillary services market while grid limits are respected. If a critical situation is identified, a dedicated algorithm is responsible for limiting its participation.

Regardless of the chosen cooperation model, insights concerning ICT technologies are necessary to apply it. The SmarterEMC2 project [18] focuses in this field and its framework is

divided into three main processes: technical validation of the flexibility offers, selection and activation of flexible resources in a local constraint management market and operation of a capacity market mechanism linked to the DSO planning tools. ICT solutions developed in this project support the inclusion of consumers through demand response services and the inclusion of RES flexibility through virtual power plants in the delivery of flexibility services.

Public authorities already started to acknowledge the need to foster better cooperation between system operators. The Council of European Energy Regulators (CEER) [19], the Agency for the Cooperation of Energy Regulators (ACER) [20], the European Distribution System Operators for Smart Grids (EDSO) [21] and ENTSO-E (in collaboration with other entities) [22] in their respective position papers propose a set of guidelines that help to understand which are the common barriers that need to be overcome. After analyzing these works, the need for practical approaches to realize the theoretical TSO-DSO cooperation models becomes clear. Particularly, the TSO-DSO data management report [22] defines the following concrete recommendations:

1. The DSO should be allowed to offer services to the TSO (e.g. technical management of flexibility activation in the distribution network);

2. Both TSO and DSO should have details concerning the users connected to the distribution networks: forecast of the PQ operating point and the flexibility available for a pre-defined time horizon;

3. Storage activities should be market-based [23] in order to make them available to the TSO and DSO for manning tasks;

4. The appearance of new market players should be facilitated through an efficient process of data exchange;

5. The data exchange should be standardized, i.e. protocols, standards and type of data;

6. The DSO should have access to the forecasted State of Charge curve.

Regarding the two first recommendations, their importance to put in place any of the mentioned cooperation schemes is undeniable. *How would it be possible to ensure that no technical problems arise on the distribution grids due to flexibility usage if neither of the system operators have knowledge on its availability/impact?* This question opens the door to the research study we intend to develop in this thesis.

Summarizing, flexibility is not an end in itself but rather a mean to deliver a more affordable, secure and efficient whole power system. However, to exploit DER flexibility capacity, an extensive cooperation and clear boundaries between TSO and DSO rights and duties are required. The solution to achieve the necessary level of coordination is, therefore, the

development of practical tools that support the operators in managing the flexibility available across their networks.

## *1.2 Research question and hypothesis*

Regardless of the user (TSO or DSO), if no data are available concerning the impact of flexibility for the network operation, its secure management cannot be ensured. Therefore, the research question of this thesis addresses this problem from the TSO-DSO cooperation perspective.

- ***Research Question:*** How can the TSO request a change in the operating point at the TSO-DSO interface by knowing, in advance, that it will not cause technical problems at the distribution level?

From the TSO point of view, what matters is the impact of flexibility activations in the operating points at the interfaces with the DSO (primary substations). Thus, their requests are set in terms of variation of the operating points at the TSO-DSO boundaries. This means that for the TSO is not important which DER are providing the needed flexibility (considering that all DER have the same flexibility activation costs). Considering this, the DSO need to evaluate the feasibility of these requests. Bearing this in mind, this thesis will focus on developing a method capable of estimating the active and reactive power limits that the power flow at the TSO-DSO interface can assume through feasible activations of DER flexibility. Such an assessment will take into account the distribution network technical limits. Moreover, the maximum cost that the user is willing to pay for the flexibility activation will also constrain the so-called flexibility area. This concept of flexibility area was firstly introduced in [24] and inspires this dissertation.

- ***Research hypothesis:*** Investigating the possibility of developing a robust, reliable and efficient method capable of accurately estimating the aggregated flexibility at TSO-DSO interconnections.

Figure 5 is a simple illustration of the flexibility area concept. Each colored flexibility area characterizes different regions of feasible PQ power exchanges that can be achieved by paying, at most, the corresponding maximum costs. For instance, in this particular case, the user knows that by paying a maximum of 25€/hour, there is the guarantee that any PQ point inside the yellow area can be exchanged at the TSO-DSO interface through, at least, one combination of DER flexibility activations and without violating the technical grid limits. The white point displayed in Figure 5 illustrates the scheduled PQ operating point that results from market dispatch and DRES/load forecasts.

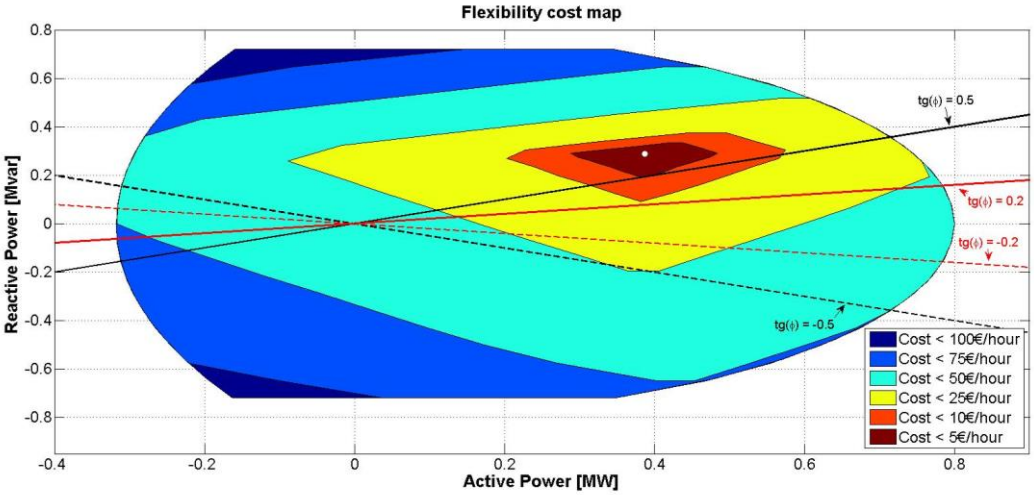


**Figure 5 – Illustration of flexibility areas constrained by different maximum costs**

The confirmation of the research hypothesis will leverage the TSO-DSO cooperation by clearly showing the benefits of an increased coordination. By promoting the cross-actor exchange of information, the flexibility area endows the TSO with better means to satisfy their own needs (e.g. system balance) without compromising the normal operation of the distribution network. In addition, it clearly supports the fulfilment of regulatory requirements in terms of reactive power ratio in the TSO-DSO connection points. In Portugal, if the reactive power flow at the TSO-DSO boundary nodes exceeds certain limits, which are dependent in the period of the day and on the tan $\Phi$ range, the DSO incurs in penalties [25]. Figure 5 shows a scenario in which the system will work outside the tan $\Phi$ limits. Thus, the DSO knows, in advance, that it needs to pay at most 10€/hour to move the operating point to a feasible zone (orange area). Moreover, in Italy, the possibility to implement a scheduled cumulative program with regards to each single HV/MV substation is being discussed or to one zone that includes more than one HV/MV substation [26]. The DSO would be obliged to follow this schedule, otherwise being penalized.

The research hypothesis will be verified through a roadmap with several stages, which are tackled in Chapter 3, 4 and 5. In each one of them, a more ambitious goal is addressed and new research gaps are identified. Throughout these three chapters, the main objectives are always clear as well as the path to achieve them. However, the choice of the "back-end algorithms" (e.g., interior point method, variable neighborhood search) can be matter of discussion. Although a detailed revision of the state-of-the art is performed in every Chapter, it is not the intention of this PhD thesis to claim that the most effective methods were used. In fact, this research work does not aim to carry a benchmarking analysis, but rather to provide an actual answer to an innovative topic while never neglecting the minimum requirements of an industrial solution (e.g., computational performance).

## 1.3 Dissertation outline

In Chapter 2, a comprehensive literature review is carried out. Three important topics are addressed:

- Flexibility coordination/aggregation approaches in different contexts e.g. planning domain;
- Random sampling approach to estimate flexibility ranges in primary substations;
- Optimization approaches in order to find the most suitable way to address the proposed hypothesis.

In Chapter 3, the optimization problem formulated in this thesis is described. The mathematical description is addressed as well as the flexibility area identification procedure, which constitutes the novelty behind this methodology. The outcomes of the developed approach are also analyzed and compared against the random sampling method proposed in [24].

Chapter 4 and 5 are responsible to continue the storyline of this thesis focusing on gaps that arise from the observation of Chapter 3 results. The estimation of flexibility areas in meshed grids and the inclusion of discrete variables in the optimization process are accessed in these two Chapters.

Chapter 6 presents general conclusions of the research study and indicates perspectives of future work.

# Chapter 2

# Flexibility Assessment and Exploitation

The development of the Smart Grid concept was responsible for a significant increase in terms of observability and controllability of the distribution system, which led to the possibility of bi-directional control of DER [27]. Within this new paradigm, DSOs are looking forward to investing in new ICT [28]. Therefore, the requirements to exploit DER flexibility are being met.

The following sections provide a literature review that analyzes a wide variety of studies concerning flexibility management, enabling to identify the correct path to answer the proposed research question. Since the OPF algorithm is in the core of this research study, several different optimization techniques are also detailed.

## *2.1 Models and approaches to enable flexibility services exploitation*

Flexibility exploitation options have been extensively studied and a particular focus has been given to the inclusion of DER flexibility in ancillary services. In [29], a geometric approach to aggregate flexibility of thermostatically controlled loads is presented. It is based on the Minkowski sum of individual polytopes [30] and has as its main goal the provision of regulation services to the TSO. The coordination and aggregation of DER is also studied in [31] with the main goal of provide demand response services. To do so, it makes use of a "virtual" battery model together with a Nash-bargaining based coordination strategy [32].The work presented in [33] is a step forward regarding flexibility estimation approaches and paves the way to include DER flexibility in the transmission level dispatch. The proposed methodology approximates the aggregate feasible regions of active and reactive power consumed by a set of DER to an ellipsoid in the PQ domain.

The usage of flexibility is also addressed in the planning field. In [34], the concept of flexibility envelopes is presented. These envelopes allow to understand if the available flexible resources are capable to meet the reserve requirements not only in terms of capacity, but also regarding time, ramping rate and stored energy. Still in the planning domain, [35] addresses the need of considering the operating reserve as deployable energy. The typical reserve studies only consider it as deployable power; however, the high variability and uncertainty arising from DRES demands for the inclusion of flexible resources capable of providing ample ramping e.g. storage devices and demand response.

The different types of flexibility services are affected by forecast uncertainty. Potential flexibility shortage events are measured through an innovative flexibility metric that assesses the largest variation range of uncertainty within which the system remains stable [36]. In [37], a robust procurement algorithm is developed to guarantee that, even in a worst-case scenario of uncertainty, technical grid problems are overcome resorting to local flexibility. This concept of using DER flexibility located near the area where the grid issue occurs (i.e. local flexibility) led to the arising of new market platforms - local flexibility markets [38].

The importance concerning the existence of coordinated actions between the different stakeholders is studied in several works. On the one hand, the reserve operation is not independent of the control area and, for this reason, the activation of flexibility should be coordinated between the different TSO [39]. On the other hand, the cooperation between TSOs and DSOs is also crucial to avoid situations where both activate flexibility services, but in opposite directions [40].

Considering what is stated above, it becomes clear that the coordination/aggregation of flexibility resources is already a widely studied topic. However, in which concerns the cooperation between the system operators, most of the works focus on conceptual and regulatory contributions. As proposed in the formulated *research hypothesis*, this thesis aims to materialize some of these concepts, such as estimate the PQ limits that the power exchange in the primary substations can assume through feasible flexibility activations. Studies on how to control the power flow at the TSO-DSO interface are few. Pudjianto *el al*. [41] developed a conceptual framework called "technical virtual power plant", whose main goal is to help the DSO in control and keep a fixed active and reactive power profile at the primary substations. Schwerdfeger and Westermann [42] make use of distributed storage to allow the TSO and the DSO to negotiate a power flow schedule for each primary substation. Although meritorious, these two works did not consider the impact of the flexible resources in the power flow exchanged at the TSO-DSO boundary nodes. In fact, to my knowledge, only one approach tried to estimate the active and reactive power flexibility ranges at the connection points between transmission and distribution networks [24]. However, the random nature of this methodology led to significant limitations both in terms of finding the "true" flexibility limits and in terms of computational performance. These limitations established the starting point of my research study. Therefore, the following section is dedicated to a more detailed analysis of the approach proposed in [24].

## *2.2 A random sampling approach to identify the flexibility ranges*

The work described in [24] is more extensive than the simple, although meritorious, description of the flexibility area concept. In fact, a methodology aiming to estimate these areas is presented. It consists of the simulation of a pre-defined number of power flow scenarios

in which the DER power output is randomly selected from the corresponding flexibility bands. For each scenario, if the technical and contractual constraints of the distribution network are respected, a new operating point is plotted on the flexibility area. The process stops after the evaluation of all the extracted samples. Figure 6 summarizes, through a flowchart, the main steps of this random sampling approach.

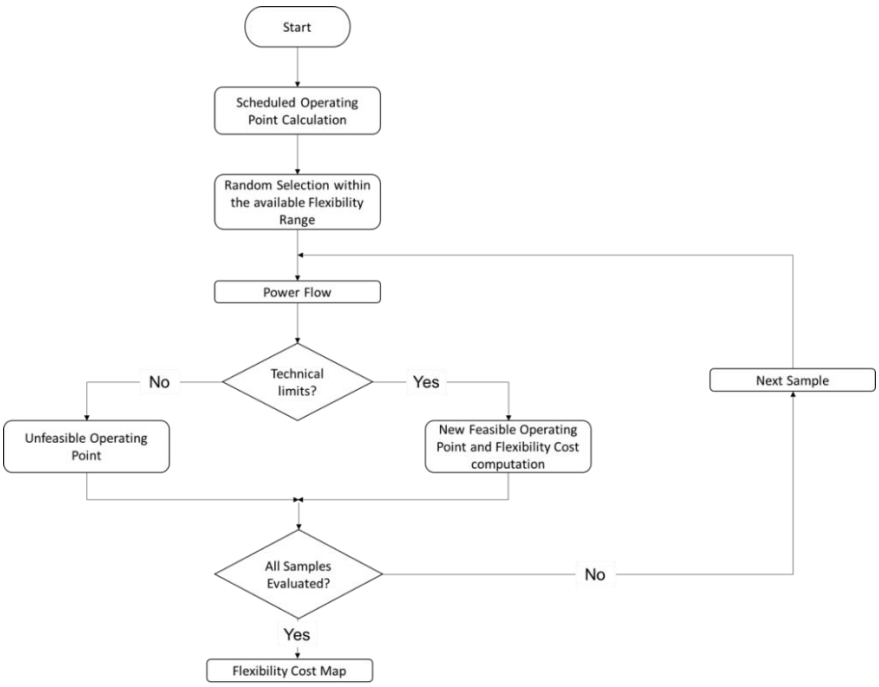


**Figure 6 – A random sampling approach to identify the flexibility area**

The key to understand this method is to comprehend how the activated flexibility in each DER is selected. Two approaches are followed: an independent random variable is associated to each flexible resource (DRES and loads); a negative correlation between DRES and loads connected to the same bus is used (i.e. these two DER have opposite growth trends). The former is ruled by the following equations:

$$P_{n,i}^{flex} = ({P_{gen}}_{n,i}^{max} - {P_{gen}}_{n,i}^{min}).\varphi_{n,i}^{P_{gen}} + {P_{gen}}_{n,i}^{min} - ({P_{Ld}}_{n,i}^{max} - {P_{Ld}}_{n,i}^{min}).\varphi_{n,i}^{P_{Ld}} + {P_{Ld}}_{n,i}^{min} \quad (2.1)$$

$$Q_{n,i}^{flex} = ({Q_{gen}}_{n,i}^{max} - {Q_{gen}}_{n,i}^{min}).\varphi_{n,i}^{Q_{gen}} + {Q_{gen}}_{n,i}^{min} - ({Q_{Ld}}_{n,i}^{max} - {Q_{Ld}}_{n,i}^{min}).\varphi_{n,i}^{Q_{Ld}} + {Q_{Ld}}_{n,i}^{min} \quad (2.2)$$

Four independent variables ($\varphi_{n,i}^{P_{gen}}$, $\varphi_{n,i}^{P_{Ld}}$, $\varphi_{n,i}^{Q_{gen}}$, $\varphi_{n,i}^{Q_{Ld}}$), which are obtained from uniform distributions between 0 and 1 are responsible for sorting the active and reactive power flexibility activated in each DRES and load. This random selection is performed within the flexibility bands of each flexible resource, as shown in (2.1) and (2.2). Therefore, $P_{n,i}^{flex}$ and $Q_{n,i}^{flex}$ illustrate the PQ flexibility activated in each MV node $n$, for each sample $i$. Regarding the later, only two random variables are used ($\varphi_{n,i}^{P}$, $\varphi_{n,i}^{Q}$). This allows to establish the aforementioned negative correlation.

$$P_{n,i}^{flex} = (P_{gen}{}_{n,i}^{max} - P_{gen}{}_{n,i}^{min}).(1 - \varphi_{n,i}^{P}) + P_{gen}{}_{n,i}^{min} - (P_{Ld}{}_{n,i}^{max} - P_{Ld}{}_{n,i}^{min}).\varphi_{n,i}^{P} + P_{Ld}{}_{n,i}^{min} \quad (2.3)$$

$$Q_{n,i}^{flex} = (Q_{gen}{}_{n,i}^{max} - Q_{gen}{}_{n,i}^{min}).(1 - \varphi_{n,i}^{Q}) + Q_{gen}{}_{n,i}^{min} - (Q_{Ld}{}_{n,i}^{max} - Q_{Ld}{}_{n,i}^{min}).\varphi_{n,i}^{Q} + Q_{Ld}{}_{n,i}^{min} \quad (2.4)$$

Therefore, by using the same variables to select the flexibility provided by DRES and loads, the random process is no longer independent.

By analyzing the results of both sampling techniques, some limitations are easily noticeable. In the first case, a trend to generate values around the scheduled operating point can be identified. DRES and load flexibilities are independently generated, which explains the absence of the extreme values of power injection in the flexibility area. Although following uniform distributions, this sampling process due to its independency leads to an injected power in the TSO-DSO boundary node, which is not ruled by the same probability distribution. Another drawback of this first approach regards to the high number of samples needed to find the lowest cost that allows for a specific change on the operating point. Several different combinations of flexible resources activations can lead to the same operating point variation. Thus, when considering an independent sampling process, all the available possibilities can occur, which dramatically increases the search space. This problem would have been even more highlighted if the tests had been performed in a meshed network with a high number of OLTC (i.e. higher number of possibilities leading to the same TSO-DSO operating point changes).

The negative correlation forced in the second method proves its ability to overcome these limitations. As immediate consequence, it refines the search space. Exemplifying, it avoids the activation, at the same time, of significant upward generation and downward load (or vice versa) that would lead to small or even no changes in the operating point. Therefore, it promotes the search for “extreme” values of injected power in the TSO-DSO interface. Nevertheless, with this correlation, it is not possible to achieve a specific dispatch by only activating a part of DRES or load flexibility. Even if 80% of the available flexibility of a specific load was enough to meet the dispatch requirement, this approach would not lead to this solution. Instead, it would also activate flexibility from DRES connected to the same node. Thus, despite the better performance, this sampling strategy might lead in some cases to more expensive solutions.

Independently from the sampling method, two parameters should be evaluated to assess their adequacy: delivery of the expected output and fulfilment of network operation time constraints (non-functional requirement). Concerning the flexibility area estimation, even applying the second sampling approach, it is not possible to ensure that the extreme points are present in the computed flexibility area perimeter. In Chapter 3, a comparison between the sampling method and the developed methodology supports this statement since a flexibility area increase is achieved. Moreover, the computational effort required to capture a representative approximation of the flexibility area is not compatible with the time constraints imposed by

the network operation. This is explained by the significant number of samples that fall in unfeasible operating points, not contributing for the flexibility ranges estimation.

Departing from the limitations found in [24],it is clear the need to develop a methodology capable of "guiding" the search only to the PQ points belonging to the flexibility area perimeter. The formulation of an optimization model capable to update its objective, thus allowing to explore this entire perimeter seems to be an interesting option. This optimization problem obviously needs to consider the electric power flow equations as well as the technical limits of the distribution networks, which leads us to the OPF basic concepts (non-linear and non-convex problem). In the available literature, a wide range of optimization variants tried to solve it. This way, the next section aims to identify which one of them best suits the OPF problem.

## *2.3 Optimization methods applied to the OPF problem*

The OPF is one of the most important and well-researched problems of constrained non-linear optimization. Carpentier [43] introduced it as an extension of the typical economic dispatch problem. The Gauss-Seidel method is employed to represent the load flows as power injections in the voltage polar form. One of the main contributions of this method is the inclusion of the electric power flow equations. As matter of fact, OPF is a generic term used to describe a broad class of optimization problems that are constrained by the physical and operational limits of a power system. The conventional formulation sets as objective function the minimization of the system operation costs or the minimization of the active power transmission losses. The range of applications of this problem in the decision support field is vast and nearly covers the entire planning horizon e.g. transmission network capacity planning, reactive power dispatch. Generally, the OPF is defined as a large-scale highly constrained non-convex non-linear optimization problem. Since Carpentier's contributions, a wide variety of techniques has been developed aiming to improve both optimality and computational time.

### 2.3.1 Linear Programming

The application of linear programming (LP) approaches to the OPF problem requires the linearization of the objective function as well as the inclusion of non-negative variables in the constraints. Therefore, piecewise linearization or successive linearization are usually used to approximate the non-linear functions. In [44], Wells develops a LP approach to solve the economic dispatch problem while considering network security requirements. After linearizing the objective function and constraints, the simplex method [45] is applied, which is known to be quite effective for solving LP problems. This first attempt to exploit LP merits to answer to this non-linear problem had two main limitations: the final result may not be the optimum for

infeasible conditions and computing rounding errors may lead to overloaded constraints. Shen and Laughton [46] tried to overcome these drawbacks by proposing a dual LP technique and promising results were obtained. Both primal and dual problems are formulated and the revised simplex method is used to solve them. This revised methodology is mathematically equivalent to the original simplex method. However, it takes advantage of a sparse matrix to increase the computational performance. In fact, this is the most commonly used LP technique to address the OPF problem.

Several other works based on the OPF concepts aim to avoid and/or overcome insecure system operating conditions (e.g. branch overloads). Through different LP approaches, [47], [48] and [49] define the appropriated control actions to ensure system security. A LP iterative technique for network sparsity selection of binding constraints is employed in [47]. The method comprises six prioritized objective functions and uses heuristic approaches to deal with infeasible situations. Although robust, this methodology only handles linear objective functions. Housos and Irissari [48] propose a Quasi-Newton LP method, which also involves multiple objective functions while uses variable weights coefficients to treat the linearized constraints as a set of penalty functions. Two interesting characteristics are presented: the full Hessian matrix is replaced by the corresponding sparse, which improves computational performance and a "guiding" function to preserve feasibility is employed. This approach has proven its merits in small size systems. The method developed in [49] describes a real time control algorithm to work under emergency state. It includes ramp rate constraints and a fast-decoupled load flow is used. Moreover, its effectiveness is proven for online operation.

LP approaches are reliable and present a high computational performance, which makes them suitable for real-time purposes. However, this class of optimization algorithms suffer lack of accuracy. When using a piecewise linear cost approximation, even small changes of the control variables may lead to significant oscillations in the final solution. This is explained by the discrete jumps between segment breakpoints of the piecewise curve. Therefore, the application of LP techniques in the OPF field has remained mainly restricted to the PQ dispatch problems, whose objective functions are modulated by the sum of convex cost curves. The issues caused by the approximations applied in LP methods are studied and partially overcome in [50]. The developed methodology proved to be able to deal with non-separable objective functions and the results showed to be quite effective when compared with the typical Newton method (non-linear category). Nevertheless, the convergence performance is a clear drawback.

### 2.3.2 Non-linear Programming

By analyzing the physical models of the electric networks, it becomes easy to realize why non-linear programming (NLP) was the earliest formulation category tested to solve the OPF problem. NLP is divided in two sub-groups: constraint and unconstraint NLP. Moreover, the first

sub-category can be converted into the second one through the Lagrangian or penalty-function methods.

Dommel and Tinney [51] applied an NLP technique based on the penalty-function optimization approach to minimize the system operation cost and the active power losses. This methodology employs the Lagrangian multiplier approach to check boundary violations. Its application was tested in large-scale power systems (up to 500 nodes). Although the convergence process is impacted by the penalty-function used, the main limitation of the method regards to the modelling of components such as transformer taps. This type of resources is excluded from the optimization routine, only being considered in the power flow simulation. In [52] an iterative indirect method that accounts for the Lagrange-Kuhn-Tucker conditions of optimality is proposed to minimize the system operation cost. For some specific conditions (tolerance parameter of 0.001) and when compared to other penalty-function techniques, this method proved its improved computational performance. The methodology presented in [53] extends the work of [51] by improving the convergence procedure. The Powell and Fletcher-Powell algorithms are used and the convergence is checked at every stage of the optimization. The main goal is achieved, but this method is only capable to handle a maximum of two constraints per node. As in [51], the methodology described in [54] applies the penalty-function technique and the Lagrange multiplier to the optimization problem. In addition, it incorporates exact outage-contingency constraints in order to provide an optimal steady-state-secure system operating point. The algorithm accuracy is closely dependent on the gradient step size choice. Aiming to overcome the main drawback of standard penalty methods, a shifted penalty-function approach is suggested [55]. A method based on a reduced gradient concept and on an adapted version of Fletcher's Quasi-Newton technique optimizes the shifted penalty-functions thus allowing to effectively deal with the ill-conditioning of the Hessian matrix. The convergence rate and the accuracy of the results were improved for the specified test systems. The choice of the slack bus proved to be critical to achieve these outcomes. More recently, an NLP model based on a combination between quadratic and network flow programming was developed to solve the security-constrained multi-area economic dispatch [56]. Therefore, it includes the tie-line security and transfer constraints in each area. This method uses the concept of maximum basis in the network flow graph to formulate an unconstrained quadratic programming (QP) model, which can be solved through a typical reduced gradient method.

The spectrum of available NLP techniques is, therefore, characterized by high accuracy, but slow convergence especially when near the optimal solution. The accuracy of the OPF solution increases with the gradient dimension. On the other hand, two aspects negatively affect the convergence procedure: the gradient direction, often changed during the optimization procedure, and the matrices sparsity, which is reduced due to the inclusion of penalty factors.

### 2.3.3 Quadratic Programming

QP is a special form of NLP applicable to optimization problems with quadratic objective functions and linear constraints. The first effort to solve the economic dispatch problem through a QP approach is assigned to Reid and Hasdorff [57]. To do so, help variables are used to approximate the objective function to a quadratic form and Taylor series expansion is employed to linearize the constraints. Neither the gradient step length nor the penalty factors impact on the convergence procedure; however, the computational time is significantly influenced by the system size increase. Moreover, this method does not consider the existence of resources that follow a discrete behavior. After this first exploitation of QP merits, a growing interest emerged and, in the following year, one of the pioneering works regarding the application of the decomposition algorithm in the economic dispatch was proposed [58]. Thanks to it, contingency requirements were met. The implementation of sparsity matrix techniques allowed to achieve reliable and satisfactory results. In another work, the original non-linear OPF is decomposed in a sequence of QP problems i.e. not all the control variables are simultaneously optimized [59]. The method shows its capability to provide the OPF solution within a maximum of 5 minutes for a network size up to 2000 nodes. In addition, the feasibility of the starting point does not need to be ensured. This explains why it was considered a technology break through at that time. The obtained improvements concerning computational time and robustness were demonstrated by comparing it with a method considering an augmented Lagrangian i.e. the Lagrangian function with a quadratic penalty term [60] [61]. While the algorithm presented in [59] uses the exact second derivative, the augmented Lagrangian-based only uses first derivative information. However, this innovative methodology is unable to decide which constraints should be included in the active set. Two years later, the same authors implemented modifications in their original method [62]. Sparsity techniques are employed and the method converges quadratically. Even under power flow divergence i.e. singularity of the Jacobian matrix, a feasible solution is obtained by adding capacitor banks. These resources due to their inherent flexibility adjust the physical conditions of the system until a solution is found. The decomposition of the OPF problem into two sub-problems – real and reactive - is also a valid possibility [63]. Both are converted in QP problems at each iteration by using Z-matrix techniques to compute the network losses and generalized distribution factors to linearize the branch flows. An optimization technique called Beale's method is then employed since it is appropriate to solve QP problems with linear constraints. Until the final solution is not obtained, the outcome of the real sub-problem feeds the reactive one, ensuring the effectiveness of the method.

In the last twenty years, the power systems architecture has been suffering significant modifications, leading to key changes on the typical and well-studied procedures of network operation and at the market structure level. One of them was the emergence of an open access

environment, which caused a dangerous approximation between the operating conditions and the security boundaries. Specifically, the topic of voltage security and the role of reactive power to ensure it under the new conditions became of particular interest [64]. A unified OPF formulation is employed to ensure voltage security while minimizing the reactive power support costs. The main novelty of this work regards to the consideration of support provided by private reactive compensators i.e. ancillary services provision. The problem is solved through a sequential QP model. Several tests under different voltage margin requirements in both normal and outage conditions are analyzed. Voltage problems might cause significant bottlenecks in the electrical grids thus appealing for an increase of the total transmission capability among areas. TSO are paying attention to this problem and solutions based on exploiting flexible AC transmission system (FACTS) devices are being studied [65]. This paper presents a compact and reduced security-constrained OPF capable to deal with the convergence problems introduced by the strong nonlinearities of FACTS models. The Han-Powell algorithm [66] is used to optimize the operation of FACTS devices due to its recognizable merits in dealing with optimization problems with these characteristics. To do so, it solves successive quadratic problems with linear constraints. The method presented in [65] also proposes new techniques to overcome the local minimum problem caused by the non-convex characteristic of the problem. Particularly, the objective function incorporates a quadratic penalty term related to the FACTS control variables.

In general, QP allows a fast convergence procedure mainly because does not require the use of penalty factors or the computation of gradient step size. Additionally, these approaches are effective when facing ill-conditioned matrices. Although QP allows to overcome some problems assigned to NLP, it also suffers from some similar drawbacks associated to LP - piecewise quadratic cost approximation.

### 2.3.4 Newton-Raphson based category

In the power systems field, the application of the Newton-Raphson method is typically associated to the power flow assessment. Thanks to its flexible formulation, it can also be used to solve a wide variety of OPF problems. The methodology convergence is fast when near the optimal solution due to its quadratic properties. In this approach, the Karush-Kuhn-Tucker (KKT) optimality conditions need to be satisfied.

As an extension of Tinney's work [51], a method to minimize the loss and cost functions is proposed in [67]. It is an NLP approach based on the homotopy continuation algorithm. The Lagrangian multipliers and the Newton method (with the Hessian matrix replacing the Jacobian) are also employed, while an acceleration factor is used to compute the update controls. The tests on a 179-bus system showed a good convergence performance. A methodology also using the Lagrange multipliers and the Newton-Raphson load flow is detailed in [68], aiming to solve

the economic dispatch problem. As in most studies concerning the real power dispatch, this methodology includes the impact of incremental power losses through the so-called penalty factors. Nonetheless, and contrary to what happens in the classical approach [69], this method uses the Jacobian formed in the Newton-Raphson method to compute the incremental losses. The simplicity and fast convergence associated to this approach makes it suitable for on-line implementation. Under the same topic, in [70] a new technique to calculate the penalty factors and the incremental losses is detailed. Sensitivity factors are included in the Newton-Raphson method to express the B-coefficients (transmission loss formula constants) and the Jacobian matrix. Therefore, an improved real-time emission-dispatch in terms of computational time is achieved. When including security constraints in the economic dispatch, some works do not include system corrective actions after outage events. Monticelli et al. [71] propose a technique to incorporate these capabilities, composed of two main separated steps: an iterative procedure to solve a "base case" economic dispatch and a contingency analysis considering generation re-scheduling. The later defines preventive control actions, which are sent to the economic module. Through this model, an effective procedure to eliminate constraints violation is achieved. Mathematically speaking, a Bender's decomposition algorithm is used to separately deal with both sub-problems. Its convergence is dependent on some convexity assumptions.

The application of explicit Newton formulations to large-scale non-linear problems are usually too burdensome. However, the OPF problem differs from this typical situation due to the sparse Hessian matrix of the Lagrangian function. Network sparsity techniques are thus used in the Newton method to solve reactive power optimization problems [72]. Independently from the set of binding constraints, this approach evidences a very fast convergence to the KKT conditions. The main problem reported in this paper is the efficiency regarding the identification of binding inequalities. An interesting approach to address this recognition drawback is available on the literature [73].

In this state-of-the-art revision, a common point is highlighted: the Newton-Raphson method allows for a fast convergence to the optimal solution. Its quadratic convergence properties are the main cause of this characteristic. In addition, the impact of the number of control variables or inequality constraints upon the computational effort is minimum. Instead, the increase of the network size has a significant influence. As main drawbacks, the determination of the binding constraints and the need for employing sparsity techniques are usually assigned to this method. The "sparse Newton methods" shows a superior performance when comparing with the Quasi-Newton, which are characterized for avoiding the inversion of the Hessian matrix.

### 2.3.5 Mixture of programming categories

OPF studies also encompass the usage of hybrid techniques composed of different types of programming approaches. The Mixed Integer Programming (MIP) is probably the most well-known. It is a LP method involving integer decision variables, with an important role to play in the power systems field e.g., OLTC, reactive power compensators. MIP is also known for the level of computational effort required, which is related to the number of discrete variables considered. A recent method applied to the OPF problem, allowing for the representation of discrete decisions via integer variables still deals with the computational time problem [74]. As reported, the binary variables, which illustrate the discrete decisions, are the reason behind this obstacle. In [75], LP and QP are both used to solve the OPF problem depending on a particularity of the objective function. As in a previous work of the same author [63], the decoupling characteristics between network voltages and phase angles are exploited to separate real and reactive problems. A QP method is used to solve both sub-problems when a quadratic function is able to approximate the cost function of each generator i.e. without considering the valve-point loading. The consideration of this effect in the objective function demands for the application of a LP approach.

### 2.3.6 Interior Point methods

Interior Point Methods (IPM) are considered one of the most efficient algorithms to solve both linear and non-linear optimization problems. It is a very robust method, which, when compared with the approaches already mentioned, shows similar accuracy, but great advantages regarding computational speed. As reported in several works, the computational effort is 50 times lower that the required when applying the simplex method. The name of this methodology itself explains the novelty behind it – IPM, in contrast with the simplex method, only move in the interior of the feasible region, which allows to by-pass a great number of solutions on the boundary region. IPM focus on finding the best direction to the next move. By properly choosing the step lengths, the optimal solution is found in a low number of iterations.

The first IPM dates back to the early 50's with Frisch contribution [76], which considers a logarithmic barrier method. Fiacco and McCormick [77] intensively studied Frisch's method and applied it to non-linear inequality constrained problems. In the later 60's and during the 70's, the IPM lost favor due to convergence problems caused by the ill-conditioning in the Hessian matrix as the optimum is approached. A new era concerning the IPM began with Karmarkar's algorithm to LP problems [78], whose core is made of non-linear projective transformations. This method is characterized for avoiding too many visits to points located in the search space boundaries. The fact that it showed a higher computational efficiency when compared with the

simplex method placed the IPM at the top of researching agenda. Currently, the IPM can be divided into three different categories:

- Projective methods [78][79];
- Affine-scaling methods [80][81];
- Primal-dual methods [82][83].

While projective methods include Karmarkar's original idea, the affine-scaling add some simplifications to it. As a result, the later provides a computational time decrease, but does not exploit the same theoretical qualities of the former. Within IPM, it is broadly accepted that Primal-dual methods are the most efficient. Their main advantages are derived from Megiddo's work [82], which applied a logarithmic barrier to the primal and dual problems at the same time. The Primal-dual methods keep both primal and dual feasibility while working towards complementarity. Two main classes characterize this method category: the path following [83] [84] and the potential reduction [85].

The deployment of Primal-dual techniques to solve optimization problems has been vast and with proved merits. However, these methods also have some drawbacks that were surpassed over the time. As already mentioned, the ill-conditioning of the Hessian matrix associated to barrier-based methods is one of them. Such methods are also very sensitive to the initialization and reduction of the barrier parameter as well as to the step size. In [86], the initial infeasibility problem is overcome thanks to a modified barrier method. On the other hand, Mehrotras's predictor-corrector mechanism [87] is seen as a very effective contribution to promote global convergence. It employs factorization strategies, which allow to reduce the number of matrix factorizations when determining the search directions. In generic terms, this mechanism finds two different optimization directions: a predictor and a corrector. The former is obtained by only considering a first order term, while the latter is based on the Cholesky decomposition achieved in the predictor step. By summing both, a new search direction is found, which is responsible for reducing the number of iterations required to converge. Departing from the basic concepts proposed in [87], new techniques using multiple corrector steps were developed to reduce even more the computational effort [88].

Even though the research concerning IPMs was intensified during the 80's, their application to the power systems field began later. In 1991, a non-linear IPM was developed to solve power system state estimation problems [89]. The proposed scheme allows the integration of inequality constraints e.g. generators var limits by exploiting a logarithmic barrier function and uses an iterative Gauss-Newton method to achieve the KKT conditions. The initialization of the barrier parameter is identified as a potential obstacle. In order to reduce the convergence time, this methodology takes advantage of the already mentioned Cholesky technique. The security-constrained economic dispatch is also one of the optimization problems assessed by IPM [90]. In this case, a dual affine version of the IPM is used and a comparison with the simplex

method performed. The algorithm shows its efficiency while proves to be two times faster than the simplex method. The power flow and the optimization routine are separately solved in this problem. During the same time period, an IPM variant was proposed to solve the var planning, a non-convex, non-linear problem with non-linear constraints [91]. More specifically, a Primal-dual approach based on the methodology described in [84] was employed. However, the application of the method detailed in [84] refers only to LP and QP problems. Besides showing superior computational performance when applied to these programming problems categories, the technique developed in [91] presents interesting results. In order to solve the problem for both loss and reactive injection cost minimization, proper weights need to be specified. Tests on large-scale networks (1832 and 3467 network nodes) were carried and a Bender's decomposition scheme was incorporated to handle contingencies. In addition to the standard version of the Primal-dual method, its variants covering global convergence improvements are also applied to the OPF problem [87] [88]. When using voltages in rectangular coordinates, the OPF formulated in [92] has quadratic features i.e. objective function and respective constraints are quadratic. These characteristics allow an easy matrix setup and a smooth integration of higher-order information in a predictor-corrector approach. The computational tests carried proved the capability of Mehrotra's method in reducing the number of iterations to achieve the OPF convergence. Motivated by the impressive performance of this algorithm, the same authors also assessed the performance of Gondzio's multiple centrality corrections when employed in the OPF problem [93]. In this work, an extension to non-linear problems of Gondzio's original technique is therefore proposed. The performed tests allow to conclude that the multiple centrality approach outperforms in terms of robustness and convergence speed the typical predictor-corrector method. Moreover, it suggests that the impact of centrality corrections is more evident in NLP than in LP. The work of Yan et al. [94] is the proof that the research concerning the application of the Primal-dual methods to the OPF did not stuck in time. Despite the proven merits, the OPF formulation in [92] is not completely quadratic due to the existence of tap ratio variables in the load tap changing branch power equations. To overcome this drawback while improving convergence performance, the method proposed in [94] uses an ideal transformer to illustrate the load tap changing branch and its series impedance is represented by a fictitious node. Thus, the branch power can be expressed by the voltages of the two sides of the ideal transformer instead of using the tap ratio. This approach was applied to the optimal reactive power flow problem and interesting results were obtained.

This literature review shows that the application of IPMs is extended to all sorts of practical problems, even when including non-convex characteristics. This category of optimization methods has been reported as one of the most efficient to deal with the OPF problem and the interest in it goes far beyond its theoretical complexity. The similar accuracy when compared with other classical methods together with the significant improvements demonstrated in terms of computational efficiency are its key achievements. However, IPMs also have their own

weaknesses, namely the incorrect choice of step size. This can lead to severe convergence problems.

### 2.3.7 Artificial Intelligent methods

Independently from the type of classical optimization method, they all share a common limitation: handle the dynamic characteristics of a power system e.g. transient stability events. Artificial Intelligent (AI) techniques appear as an interesting solution to deal with this aspect. Therefore, the application of heuristic-based approaches - which are derivative-free - to the OPF problem is described in this sub-section.

Genetic Algorithms (GA) are a particular category of evolutionary algorithms, whose inspiration is derived from the bio-natural selection process. Mutation, crossover and selection operators that act upon each chromosome characterize this population-based method. The incorporation of FACTS devices e.g. thyristor controlled phase shifter, thyristor-controlled series compensation in the OPF problem is not straightforward. The inclusion of their controllable parameters in the conventional OPF method causes the change of the admittance matrix. In order to overcome this problem and therefore allow the introduction of FACTS injection model, a hybrid GA is proposed in [95]. In this approach, the GA is integrated with a conventional OPF to control the phase shifters and the series compensators while aiming to minimize the generation costs. The OPF method is seen as a black box that evaluates each chromosome and whose solutions are ranked according to their fitness - generation costs. The GA applies then its typical operators in order to find the best control parameters. In another scope and as already mentioned, the inclusion of discrete decisions in the classical OPF methods is also a challenging task. A real-coded mixed-integer GA, which tries to provide to network operators' optimal controls for discrete DER, is described in [96]. This optimal management aims to fulfill several requirements: bus voltage profile improvement, total generation cost and transmission losses minimization. Moreover, this GA takes into account the valve-point loading effect of thermal units. The population individuals are real-coded illustrations of the DER state and are therefore composed of a mixture of continuous and discrete control variables. Depending on the variable type, different crossover and mutation schemes are employed, which allow to simulate the natural evolution of the population. The proposed approach shows superior performance when compared with evolutionary programming techniques in terms of accuracy, convergence rate and computational time.

Differential Evolution (DE) is also a class of evolutionary algorithms, which deserves attention due to its proven merits in searching for the global optimum solution of non-linear and non-convex optimization problems [97]. An application of a DE approach to the transient stability constrained OPF is presented in [98]. In its formulation, the transient stability is seen as a condition to be reached and not as a parcel of the fitness function. Considering this, each

individual is characterized by a “stability” index, which is responsible to evaluate the capability of maintain system stability after a contingency. Thus, this index is a key part of the individual selection procedure. More concretely, the transient stability assessment is carried through a hybrid method that combines time-domain simulation and Transient Energy Function (TEF) methods. After performing the transient time-domain simulation for each individual, the system Kinetic Energy (KE) is compared with the TEF. If a KE larger than the TEF is observed, an unstable situation is identified. The results of this method not only ensure system stability as well as show a lower cost solution in comparison with other approaches. However, due to the computational burden, the parallelization of the DE algorithm is mandatory.

Before moving forward to a critical analysis regarding which of the mentioned methods fits better in this thesis research problem, it is important to explore the application of a last population-based algorithm – the Particle Swarm Optimization (PSO). This stochastic method is widely used to solve optimization problems mainly due to its flexible and well-balanced mechanism, which allows the intelligent movement of a swarm of particles over the search space. Each particle's movement is not only influenced by its own memory (i.e. local best position), but it also takes into account the best-known position found by other particles of the swarm. One of the first works that exploits PSO merits to solve the OPF problem is detailed in [99]. The optimal set of the control variables is evaluated for different types of objective functions: cost minimization, voltage profile improvement and voltage stability enhancement. Besides the classical PSO structure, this study adds some new features, which mainly aim to enhance the trade-off between global and local exploration thus avoiding a premature convergence. First, an annealing procedure is included in the algorithm. Through it, the search procedure suffers variations as the process progresses: from a uniform search to a more local one over the space. Moreover, the velocity of the moving particles is constrained by a maximum, also contributing to a local exploration of the search space. This last aspect illustrates the incremental changes of human learning. In order to avoid the existence of particles outside the feasible regions of the search space, a feasibility check mechanism assesses each particle position in each iteration. With all these control aspects, the method proves its robustness and superiority when compared with an evolutionary programming technique. The main drawback assigned to this method is the impact of the penalty terms in its convergence. The proposed approach includes these terms in the objective function to convert the OPF in an unconstrained problem. Nevertheless, high penalty factors may lead to the local optima trap while low values do not guarantee that the algorithm finds a feasible solution. In [100], a methodology driven by this issue is proposed. It is also a PSO algorithm, but composed of reconstruction operators for the continuous variables, aiming to limit the heuristics dependency concerning the penalization terms. These operators are used to ensure that the units’ operative constraints - slope restrictions, generating limits for the pre- and post-contingencies states - are respected. On the other hand, when a power flow constraint is

violated, the particle is penalized. Besides this improvement and as well as in [99], a varying weight allows to begin the process with a global search and finish with a more focused one, which improves PSO effectiveness. As final remark, the goal of this method is to solve a security constrained OPF with continuous and discrete control variables for the operation cost minimization.

### 2.3.8 Critical analysis: Conventional mathematical techniques Vs AI methods

One of the first steps in order to confirm the proposed *research hypothesis* is the selection of the optimization method that best suits the problem under discussion. From the literature review detailed in the previous sections, it became clear the difficulties associated to this task. Conventional mathematical methods have an extensive application to the OPF problem, are usually very robust and their merits are recognized. However, these approaches have several limitations, which are mostly related to their derivative dependency. AI algorithms overcome some of these drawbacks since only use the objective function information to guide the search. Therefore, in theory, AI is able to effectively deal with non-differentiable and non-convex objective functions. Nevertheless, it is a hard task to ensure convergence towards the global optima, even for the AI techniques. The standard versions of GA are a perfect example of methodologies that easily get stuck in local optima. Furthermore, in the context of electricity markets, AI methods are not able to provide the economic information i.e. shadow prices. In the classical optimization methods, the Lagrangian multipliers illustrate these values.

This critical analysis thus leads to a deadlock since is impractical to grade the optimization methods from the best to the worst. There are methods that have better optimality convergence characteristics while others are more focused in getting a good trade-off between optimality and computational burden. As matter of fact, research studies in both categories still struggle to achieve a method capable to ensure that the global optimum is obtained. In [101], a hybrid PSO showing two interesting aspects is presented: incorporation with the Newton-Raphson method in order to minimize the power mismatch in the power flow equations and the implementation of a mechanism to handle inequality constraints based on the memory element of each particle. Therefore, this hybridization allows to keep “alive” particles that at a specific moment of the search become infeasible. This highly contributes to a diversified population thus improving the search towards the global optima. More recently, Steven Low and its convex relaxation of the OPF showed a step forward regarding this topic. The work is divided into two complementary parts: Part I [102] formulates the OPF, details two power flow models and, for each one of them, describe the convex relaxations while Part II [103] is responsible to ensure their exactness. Part II is necessary in order to provide the sufficient conditions under which an optimal solution of the original OPF can be recovered. The key feature of this convex relaxation is the capability to verify if a solution is globally optimal.

Unlike other approximations (e.g., DC OPF), an infeasible relaxed problem also illustrates the infeasibility of the original OPF. Despite the importance of this work, it does not cover several important aspects such as what to do when relaxation fails.

That being said, the *research question* and corresponding *research hypothesis* of this thesis have no ambition to develop an optimization algorithm with a better accuracy. Instead, they should exploit the merits of a specific optimization method in order to achieve their real goal: explore the entire flexibility area perimeter through an adaptive OPF-based problem. As presented in the following chapter, inside the whole perimeter drawing process, several OPF-based problems are solved, which demands for a robust optimization methodology with proven merits in terms of both optimality and computational effort. The Primal-dual version of the IPM fulfill these requirements. Moreover, when applied to the OPF, these methods show numerical stability, as reported in [104]. Therefore, there are some reasons that justify the application of the Primal-dual IPM. However, the developed methodology is flexible enough to allow for the application of other optimization algorithms without affecting its effectiveness and possibly improving the global solution. Before advancing to the novel aspects of this thesis, some brief details concerning the chosen method are provided.

## 2.4 Primal-Dual IPM for NLP

The main steps of the Prima-dual methods are described in this section, departing from a generic formulation of a non-linear problem.

$$minimize\ f(x) \tag{2.5}$$

$subject\ to$:

$$h(x) = 0 \tag{2.6}$$

$$g_{-} \leq g(x) \leq g^{-} \tag{2.7}$$

$$x_{-} \leq x \leq x^{-} \tag{2.8}$$

where:

- $x \in R^n$ is the vector of the decision variables - activated flexibilities and voltage magnitude at the reference node;
- $f: R^n \rightarrow R$ is a scalar function that illustrates the optimization goal. In the proposed methodology, this function is adaptive since it aims to explore the entire flexibility area perimeter;
- $h: R^n \rightarrow R^m$ is a vector function composed of the equality constraints - active and reactive power balance equations;

- $g: R^n \rightarrow R^p$ is a vector function composed of the inequality constraints – power system operating limits and flexibility ranges.

The first stage of this approach employs the conversion of the original problem into an equality-constrained problem. To achieve this change, two non-negative slack vectors are included in the formulation. Their non-negative characteristics are ensured by logarithmic barriers terms. Moreover, the so-called barrier parameter ($\mu^k$) whose initialization and update are among the most discussed issues in the IPM field, is also introduced in the objective function. Following these modifications, the Langrage-Newton method is used to solve the "new" formulated problem. The KKT optimality conditions need therefore to be satisfied allowing to find a local minimizer of the objective function. The following steps briefly detail how the KKT system is solved:

1. Initialization ($k = 0$) – Accordingly to strict positivity conditions define $\mu^0$ and choose the starting point $y^0$;

2. Newton Direction Calculation – Apply the Newton's method at the current point. In other words, solve the KKT system for the Newton direction;

3. Update Variables – The primal and dual variables are updated using the step length parameters;

4. Convergence Test – The process stops if the new point satisfies the convergence criteria. Otherwise, iterate again which means: $k = k + 1$, update the barrier parameter $\mu^k$ and go to step 2. Repeat this process until all the convergence criterions are met.

Since the purpose of this thesis is not the description of the primal-dual methods, detailed insights concerning each one of these steps are presented in [105]. The following chapter is the key to understand the novelty behind the flexibility area identification procedure.

# Chapter 3

# Estimating the Flexibility Area at the TSO-DSO Interface

Through the in-depth literature review carried in Chapter 2, it became clear that the sampling approach proposed in [24], where originally the flexibility area concept was described, is not an efficient solution to estimate it. Realizing what is really necessary to capture these flexibility ranges should thus be the first objective of this Chapter. Thankfully, the answer is simple: capturing the maximum and minimum of PQ exchange in the TSO-DSO interface while respecting the technical constraints. Although the answer is straightforward, the road to find these extreme points is not, since they are not only defined by the sum of the flexibility available in each DER – the technical network constraints and the interdependency between active and reactive power have their own impact. Therefore, and as already mentioned in Chapter 2, the formulation of an optimization problem shows the proper characteristics to find the power exchange limits.

- ***Goal 1:*** Formulation of an optimization problem that, iteratively, changes its own objective function in such an intelligent way that allows to estimate the entire flexibility area perimeter

The idea behind this optimization problem formulation is to use the basic concepts of the OPF algorithm, which already considers the distribution network constraints, and set an objective function that illustrates a family of straight lines. The definition of their slope is the key to explore the different extremes of the flexibility area perimeter.

By achieving this goal, it is expected to obtain a set of flexibility areas associated to different maximum costs, for each time interval of the forecast horizon. As an additional feature, the scheduled PQ operating point is computed, which constitutes a valuable information for the TSO in order to accurately calculate the power flow on the transmission network nodes.

Focusing on fulfilling *Goal 1* and thus providing an effective answer to the research question, the following sections show the details concerning the implementation of the optimization problem.

## 3.1 Methodology framework

At this stage, it should already be clear that the focus of this thesis is the development of a method capable to estimate, from the TSO point-of-view, the degree of flexibility in the distribution grid. To accomplish this objective, an approach that encompasses the solution of a set of optimization problems is proposed. Its formulation, detailed in the following sections, needs to be accurate and robust thus demanding for a proper framework. Figure 7 provides a general overview of the context in which this methodology is applied.

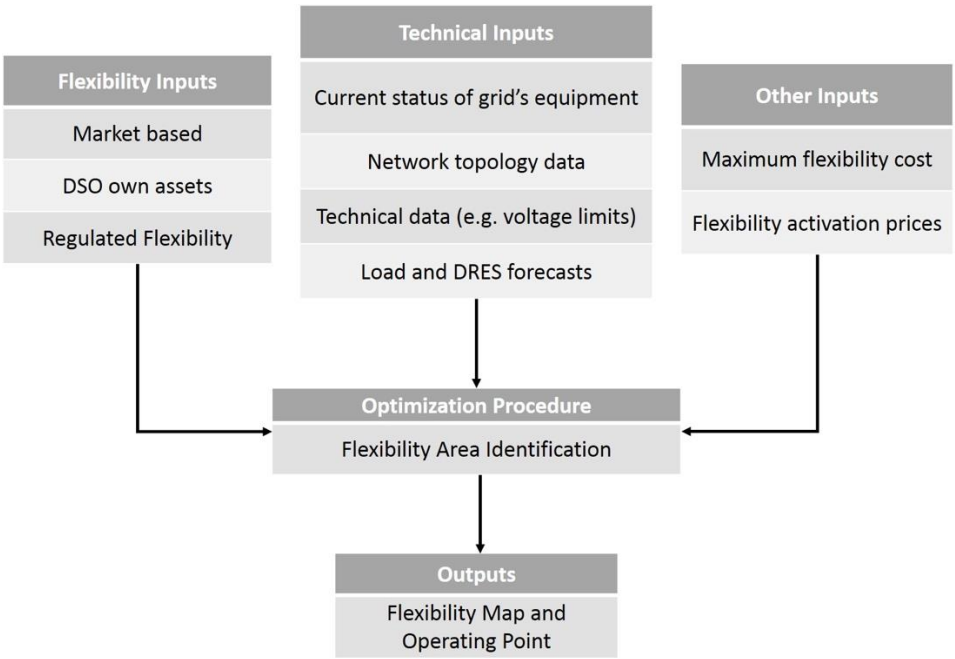


**Figure 7 – General architecture of the proposed methodology**

Regarding the market context, this thesis assumes that DSOs are allowed to purchase or require flexibility volumes whether through flexibility contracts or through participating in flexibility markets. Therefore, the definition of the flexibility availability and corresponding activation costs rely on the type of scheme associated to each flexible resource – market-based, DSO own assets or "regulated" flexibility. The first scheme consists of a short-term market platform (e.g., traditional reserve markets) or in flexibility tenders for a mid-term horizon, where aggregators or other stakeholders (e.g., storage and DRES owners) offer active power flexibility. If any other type of market platform arises due to changes on the regulatory frameworks, it can be smoothly included in the proposed methodology. Additionally, the DSO also have their own resources that can provide flexibility to the grid (e.g., OLTC, reactive power compensators). The "regulated" flexibility is illustrated through the establishment of non-firm connection contracts. Typically, these are based on agreements with large consumers and DRES. By providing them a connection license, they allow their power output to be curtailed during a couple of hours per year. Within an operational context, the expected outputs should be

computed for a pre-defined time horizon in order to support the network operator in their planning tasks. Therefore, load and DRES forecasts are crucial to construct future operating scenarios. Moreover, the current status of grid's equipment as well as the topology data are necessary to provide reliable snapshots of the network. The optimization procedure also needs to be fed with the grid technical limits in order to comply with the network constraints.

Since the approach main goal goes far beyond the achievement of a theoretical result, this overview of the methodology framework is of utmost importance. It provides fundamental insights to system operators concerning the minimum requirements to exploit the approach. One simple example is the need for an efficient integration with the DSO operational systems such as the Supervisory, Control and Data Acquisition (SCADA) system and the forecasting tools.

## *3.2 The pathway towards an optimization framework*

One of the first questions that might arise in the reader's mind is: "Why is an optimization approach employed to estimate the flexibility area?". There are two factors that significantly contributed to the arising of *Goal 1*: the drawbacks highlighted in the random sampling approach [24] and the "irregular" limits of the flexibility area perimeter. While the former was already studied in the previous chapter, the latter needs additional explanations. Each flexible resource connected to the distribution grid has their own amount of available flexibility. However, the technical network constraints (e.g., voltage and branch flow bounds) might limit the activation of this volume. Without this influence, the flexibility area would be obtained as an outcome of simply adding the flexibility provided by each resource to the scheduled operating point. Figure 8 clearly shows that, when considering the technical limits impact, the process of finding the flexibility area bounds becomes much more challenging.

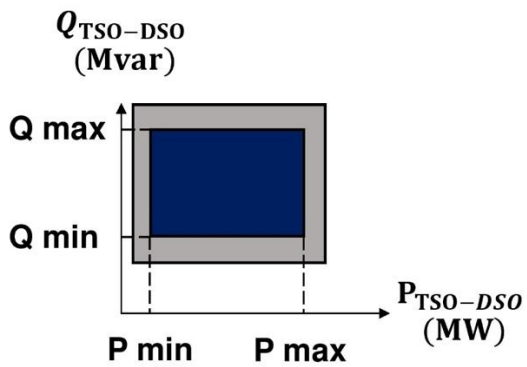


**Figure 8 - Flexibility area neglecting the technical grid limitations (grey) and including them (blue)**

As expected, when including the grid limits, the original rectangle that illustrates the activation of all the available flexibility (upward and downward) becomes smaller. Moreover, the bounds of this new rectangle are now unknown. Besides this first obstacle, there is an inherent

interdependency between the active and reactive power, also impacting on the flexibility area shape. This means that the effect of the technical network constraints upon the active and the reactive power is not the same. Therefore, the flexibility area perimeter has now "irregular" limits, whose estimation becomes even harder.

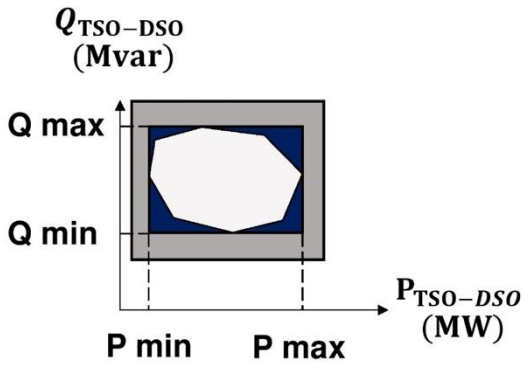


**Figure 9 – The impact of the PQ interdependency upon the flexibility area shape**

Figure 9 indicates that the answer to the research question of this thesis is based on finding out the several extreme points of the light grey flexibility area. The development of an optimization model capable of changing its objective function in such an intelligent way that allows to completely explore the flexibility area perimeter seems a suitable idea (i.e. *Goal 1*). By doing so, it becomes possible to empower both TSO and DSO with the knowledge regarding the feasible points that can be exchanged at their interconnections.

## *3.3 The optimization problem formulation*

The formulation of the optimization model needs to account with the obstacles previously mentioned. As observed in Figure 9, their disregard would lead to an over-estimation of the flexibility area. Therefore, the maximization and minimization of the active and reactive power in the TSO-DSO interface are not enough. Instead, the development of a single optimization problem that by being run several times (with updated objective function) allows to estimate the extreme points of power injection is mandatory. The objective function formulated below is the key to fulfill this goal:

$$\min \ \alpha \, P_{DSO \to TSO} + \beta \, Q_{DSO \to TSO} \tag{3.1}$$

where $P_{DSO\rightarrow TSO}$ and $Q_{DSO\rightarrow TSO}$ are the active and reactive power flows at the TSO-DSO connection points. $\alpha$ and $\beta$ are two coefficients that together form the tangent of the slopes $\theta$ of a straight-line family.

$$\tan\theta = -\alpha/\beta \tag{3.2}$$

The minimization of the objective function for different slopes illustrates therefore a set of tangent lines that intersect the $P_{DSO\rightarrow TSO}$ / $Q_{DSO\rightarrow TSO}$ plan of the flexibility area perimeter through all the possible angles. Thus, the flexibility area identification procedure and the precision in identifying its shape is dependent on the intelligent control of the coefficients $\alpha$ and $\beta$. A more detailed description of this specific topic is performed in the following section.

The complete description of the optimization model requires the definition of the decision variables and constraints.

$$V_{ref} \; - \; Voltage\ magnitude\ of\ the\ reference\ node \tag{3.3}$$

$$\Delta P_j^G, \Delta Q_j^G \; \forall j \in T_G \quad - \quad Flexibility\ activated\ through\ DRES/DG \tag{3.4}$$

$$\Delta P_i^L, \Delta Q_i^L \; \forall\, i \in T_L \quad - \quad Flexibility\ activated\ through\ \ demand\ response \tag{3.5}$$

$$\Delta Q_s^{shunt} \; \forall s \in T_{shunt} \; - \quad Reactive\ power\ compensation\ flexibility \tag{3.6}$$

$$\Delta OLTC_{ij}^t \; \forall t \in T_{OLTC} \; - \; Variation\ of\ OLTC\ positions \tag{3.7}$$

where $j$ illustrates each DRES/DG, $i$ each load, $s$ each reactive power compensator and $t$ each OLTC of the corresponding sets ($T_G$, $T_L$, $T_{shunt}$ and $T_{OLTC}$). Therefore, the decision variables are the activated flexibilities within the available ranges and the voltage magnitude of the reference node. The voltage magnitudes and angles of the remaining nodes are considered state variables of the optimization problem, which is subjected to the typical OPF constraints:

$$\theta_{ref} = 0 \; - \; Reference\ node\ angle \tag{3.8}$$

$$V_{bb,min} \leq V_{bb} \leq V_{bb,max}\ , \forall bb \in T \; - \; Voltage\ magnitude\ limits\ in\ the\ nodes \tag{3.9}$$

$$(\Delta P_{bb}^G + P_{bb}^G) - (\Delta P_{bb}^L + P_{bb}^L) - P_{bb} = 0, \forall bb \in T \; - Active\ power\ balance \tag{3.10}$$

$$(\Delta Q_{bb}^G + Q_{bb}^G) + \left(\Delta Q_{bb}^{shunt} + Q_{bb}^{shunt}\right) - (\Delta Q_{bb}^L + Q_{bb}^L) - Q_{bb} = 0 \tag{3.11}$$

$$\forall bb \in T \; - \; Reactive\ power\ balance$$

$$Q_{bb}^{shunt} \in \left\{Q_{bb}^{shunt}\right\}, \forall bb \in T_{shunt} \; - \quad Reactive\ power\ compensators\ (discretized\ values) \tag{3.12}$$

$$OLTC_{ij}^t \in \left\{OLTC_{ij}^t\right\}, \forall t \in T_{OLTC} \; - \quad On - load\ tap\ changer\ (discretized\ values) \tag{3.13}$$

$$\left[S_{ji}^b\right]^2 \leq [S_{max}^b]^2, \forall b \in B \; - \; Branch\ flow\ limits - Inverse \tag{3.14}$$

$$\left[S_{ij}^b\right]^2 \leq [S_{max}^b]^2, \forall b \in B \; - \quad Branch\ flow\ limits - Direct \tag{3.15}$$

where:

$$P_{bb} = |V_{bb}| \sum_{k=1}^{T} [|V_k|(G_{bbk} * \cos\theta_{bbk} + B_{bbk} * \sin\theta_{bbk})] \tag{3.16}$$

$$Q_{bb} = |V_{bb}| \sum_{k=1}^{T} [|V_k|(G_{bbk} * \sin\theta_{bbk} - B_{bbk} * \cos\theta_{bbk})] \tag{3.17}$$

$\Delta P_{bb}^{G}$, $\Delta Q_{bb}^{G}$, $\Delta P_{bb}^{L}$, $\Delta Q_{bb}^{L}$, $\Delta Q_{bb}^{shunt}$ illustrate the flexibility activated in node *bb*. The operating points from the market-clearing mechanism, the DRES and the net-load forecasts are denoted by $P_{bb}^{G}$, $Q_{bb}^{G}$, $P_{bb}^{L}$, $Q_{bb}^{L}$, $Q_{bb}^{shunt}$. $P_{bb}$ and $Q_{bb}$ represent the active and reactive power flows in node *bb*. In addition to these constraints, which mostly show the technical limits imposed by the grid characteristics, the decision variables also have their own bounds – the flexibility bands.

$$\Delta P_{jmin}^{G} \leq \Delta P_{j}^{G} \leq \Delta P_{j,max}^{G} \; \forall j \in T_G \quad - \quad Active\ power\ DRES/DG\ flexibility\ band \tag{3.18}$$

$$\Delta Q_{jmin}^{G} \leq \Delta Q_{j}^{G} \leq \Delta Q_{j,max}^{G} \; \forall j \in T_G \quad - \quad Reactive\ power\ DRES/DG\ flexibility\ band \tag{3.19}$$

$$\Delta P_{i,min}^{L} \leq \Delta P_{i}^{L} \leq \Delta P_{i,max}^{L} \; \forall i \in T_L \quad - \quad Active\ power\ demand\ flexibility\ band \tag{3.20}$$

$$\Delta Q_{i,min}^{L} \leq \Delta Q_{i}^{L} \leq \Delta Q_{i,max}^{L} \; \forall i \in T_L \quad - \quad Reactive\ power\ demand\ fexibility\ band \tag{3.21}$$

$$\Delta Q_{s,min}^{shunt} \leq \Delta Q_{s}^{shunt} \leq \Delta Q_{s,max}^{shunt} \tag{3.22}$$

$$\forall s \in T_{shunt} \quad - \quad Reactive\ power\ compensation\ flexibility\ band$$

This mathematical formulation meets the necessary conditions to estimate a specific point on the flexibility area perimeter. In addition, and under a convenient update of the coefficients $\alpha$ and $\beta$, the entire area can be drawn.

The activation of flexibility is a service provided by a specific resource, which means that its owner needs to be monetary compensated[1]. These costs can vary between different resources, as reported in the following formulas:

- *Load and DRES/DG flexibility cost:*

$$Cost_{LoadFlex} = \sum_{i=1}^{T_L} \left[c_i^{PL}(\Delta P_i^L) + c_i^{QL}(\Delta Q_i^L)\right] \tag{3.23}$$

$$Cost_{GenFlex} = \sum_{j=1}^{T_G} \left[c_j^{PG}(\Delta P_j^G) + c_j^{QG}(\Delta Q_j^G)\right] \tag{3.24}$$

where $\Delta P_i^L$, $\Delta Q_i^L$, $\Delta P_j^G$ and $\Delta Q_j^G$ show the flexibility activated in each load $i$ and DRES/DG $j$. The activation cost function correspondent to each MWh or Mvarh of flexibility provided by these resources is illustrated by $c_i^{PL}$, $c_i^{QL}$, $c_j^{PG}$, $c_j^{QG}$. From the offer submitted to the flexibility market

[1] Assumption: only a price per activation in m.u./MWh (or Mvarh) is paid. Therefore, a price per flexibility capacity in m.u./MW (or Mvar) is not used in this thesis. Its inclusion in the model would be straightforward.

by the market agent, it is possible to obtain the activation price.

- *OLTC transformer flexibility cost:*

$$Cost_{OLTC} = \sum_{t=1}^{T_{OLTC}} \left[c_t^{OLTC}(\Delta OLTC_{Position_{ij}^{t}})\right] \tag{3.25}$$

where $c_t^{OLTC}$(in m.u.) is the cost function associated to the variation of the tap position. In [106], the inclusion of this cost in the objective function of an optimal reactive power dispatch is investigated aiming to avoid excessive maneuvers in the control devices.

- *Reactive power compensation flexibility cost:*

$$Cost_{shunt} = \sum_{s=1}^{T_{shunt}} \left[c_s^{QC}(\Delta Q_s)\right] \tag{3.26}$$

where $\Delta Q_s$ is the change of position of each reactive power compensator $s$. The corresponding cost function is defined by $c_s^{QC}$ (in m.u.). This cost function only relates to based power compensators since for synchronous compensators with continuous variation, the formulas defined in (3.23) and (3.24) can be used. All the defined cost functions consider the variation in terms of direction i.e., upward or downward and magnitude of the flexibility requested. At the current state, the methodology uses a quadratic cost function. Nevertheless, a different relation would be easily included without affecting its effectiveness.

The sum of all these flexibility costs provides the total expense that the user needs to pay to activate the required flexibility. Thus, it makes perfect sense to add a cost constraint to the optimization problem in order to limit the flexibility usage to a maximum cost that the user is willing to pay.

$$\sum_{j=1}^{T_G}\left[c_j^{PG}(\Delta P_j^G) + c_j^{QG}(\Delta Q_j^G)\right] + \sum_{i=1}^{T_L}\left[c_i^{PL}(\Delta P_i^L) + c_i^{QL}(\Delta Q_i^L)\right] + \sum_{t=1}^{T_{OLTC}}\left[c_t^{OLTC}(\Delta OLTC_{ij}^{t})\right] + \sum_{s=1}^{T_{shunt}}\left[c_s^{QC}(\Delta Q_s)\right] \leq C_{max} \tag{3.27}$$

This constraint ensures, therefore, that any change of the scheduled operating point inside the flexibility area do not overcome the maximum predefined cost.

The following section takes responsibility for detailing how the coefficients $\alpha$ and $\beta$ are managed in order to allow an effective identification of the flexibility area.

## 3.4 Flexibility area identification procedure

The identification process that allows to draw the flexibility area is described focusing on three aspects: interaction between the outputs of the several optimization problems, initialization/update of $\alpha$ and $\beta$ coefficients and definition of the convergence criteria.

Highlighting again that $\alpha$ and $\beta$ together illustrate the tangent of the slopes of a straight-line family, the following steps show how the optimization procedure is carried.

1. Perform the optimization for $\theta = 0°$ and $\theta = 180°$ ($\alpha = 0$ and $\beta = \pm 1$). By doing so, the active power parcel is excluded from the objective function. Therefore, the extreme values $Q_{min}$ and $Q_{max}$ as well as the corresponding active power injections that can be exchanged at the TSO-DSO connection are estimated.

2. Perform the optimization for $\theta = \pm 90$ ($\alpha = \pm 1$ and $\beta = 0$). By doing so, the reactive power parcel is excluded from the objective function. Therefore, the extreme values $P_{min}$ and $P_{max}$ as well as the corresponding reactive power injections that can be exchanged at the TSO-DSO connection are estimated.

These two first steps provide a first idea of which will be the flexibility area perimeter. However, the four obtained points are not totally representative of the flexibility area shape. Thus, the following steps belong to a closed loop that only stops when the exploration of additional extreme points does not lead to significant changes on the perimeter.

3. For each two consecutive points on the area perimeter, obtain the straight line that connects them and compute $\theta_{new} = \tan^{-1}\left(\frac{Q_i - Q_{i+1}}{P_i - P_{i+1}}\right)$. This slope is then compared with the ones that provided the $i$ and $i+1$ points according with the following inequalities:

$$|\theta_{new} - \theta_i| > \theta_{tol} \tag{3.28}$$

$$|\theta_{new} - \theta_{i+1}| > \theta_{tol} \tag{3.29}$$

where $\theta_{tol}$ is the tolerance angle. If these two conditions are respected, a new optimization process for $\theta_{new}$ is carried, which estimates a new point between $i$ and $i+1$. The identification of the flexibility area only stops if there is a clear sign that the space between each pair of consecutive points is no longer valuable (i.e., violation of any convergence criterion by all $\theta_{new}$). In other words, (3.28) and (3.29) allow to understand if exploring the space between $i$ and $i+1$ would lead or not to a significant change on the flexibility area shape.

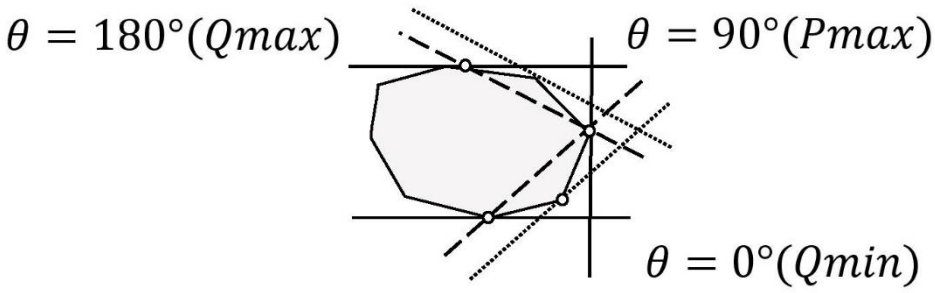


**Figure 10 – Illustration of the perimeter identification procedure**

In Figure 10 a very simple, but highly illustrative example of the process carried is provided. As it is possible to observe, three tangent straight lines (solid lines - $\theta = 0, 90, 180°$) allow to obtain $Q_{min}$, $P_{max}$ and $Q_{max}$. For each pair of consecutive points, the slope of the straight line joining them (dashed lines) is obtained. Considering that both $\theta_{new}$ fulfill equations (3.28) and (3.29), two new tangent lines (dotted lines) are available to intersect the PQ perimeter. Thus, by running optimization processes for both $\theta_{new}$, two new operating points lying on the perimeter of the flexibility region are obtained. The closed loop comes to an end when all $\theta_{new}$ are so similar to the corresponding $\theta_i$ and $\theta_{i+1}$ that exploring them would also lead to extreme points similar to $i$ and $i + 1$.

This model is based on solving a set of optimization problems in an intelligent and automatic manner. This means that the capability to control the slopes is crucial to avoid unnecessary computational burden. Figure 11 is a flowchart that sums up every detailed step.

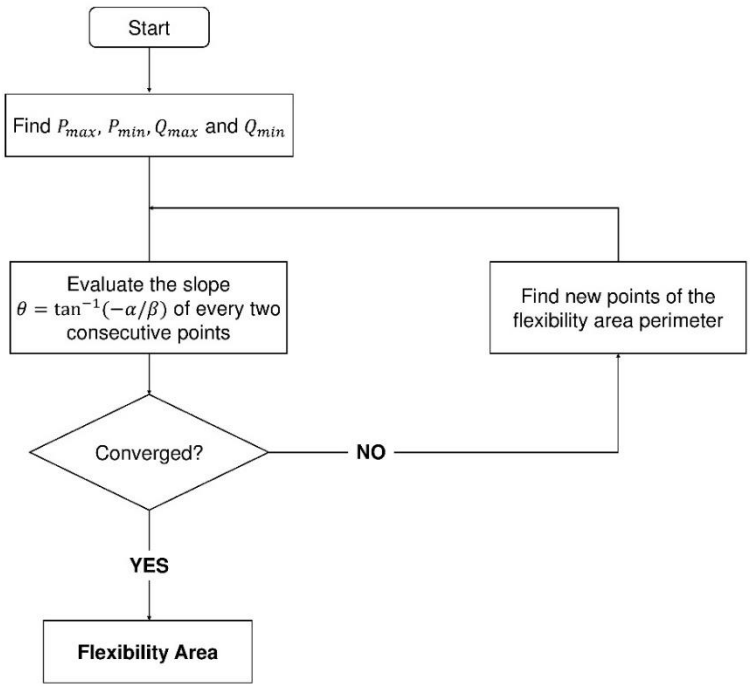


**Figure 11 – Optimization process step-by-step**

## 3.5 Key Performance Indicators (KPI)

Still in this chapter, results evidencing the capability of the algorithm to estimate the flexibility area are presented. The effectiveness of those results needs to be accessed through a comparison with a business as usual (BaU). Since the random sampling approach proposed in [24] is, to my knowledge, the only available study regarding this topic, it was used as baseline. The definition of the Key Performance Indicators (KPI) is the starting point to allow for a fair comparison.

- ***Increase of the size of the estimated flexibility area***

1) Run the sampling approach (for 1000, 10000, 100000 and 1000000 randomly extracted samples) to draw the flexibility area;

2) Run the approach proposed in this thesis to estimate the flexibility area;

3) Compute the flexibility area increase ((%) of [MW×Mvar]) through the following expression:

$$AI = 100 \times \frac{A_{ICPF} - A_{MCS}}{A_{MCS}} \tag{3.30}$$

- ***Reduction of the computational time***

1) Considering the execution times of both approaches, compute the reduction achieved with the proposed methodology using the following expression ((%) of seconds):

$$TR = 100 \times \frac{T_{MCS} - T_{ICPF}}{T_{MCS}} \tag{3.31}$$

By assessing these two KPI, it is possible to observe if the main drawbacks assigned to the sampling approach are overcome by the innovative methodology – finding the extreme points of the flexibility area within a computational time compatible with the operational requirements.

## 3.6 Estimation of the flexibility range at the TSO/DSO boundary nodes

This section evaluates the algorithm effectiveness by testing it in a modified version of the real MV network described in [107]. The obtained flexibility maps are shown, analyzed and compared with the baseline scenario.

### 3.6.1 Test Case Description - 210 nodes MV distribution network

The carried test cases are based on a real Portuguese MV distribution network with 210 nodes, which illustrates a typical rural grid. The one-line diagram of the network is presented in Figure 12.

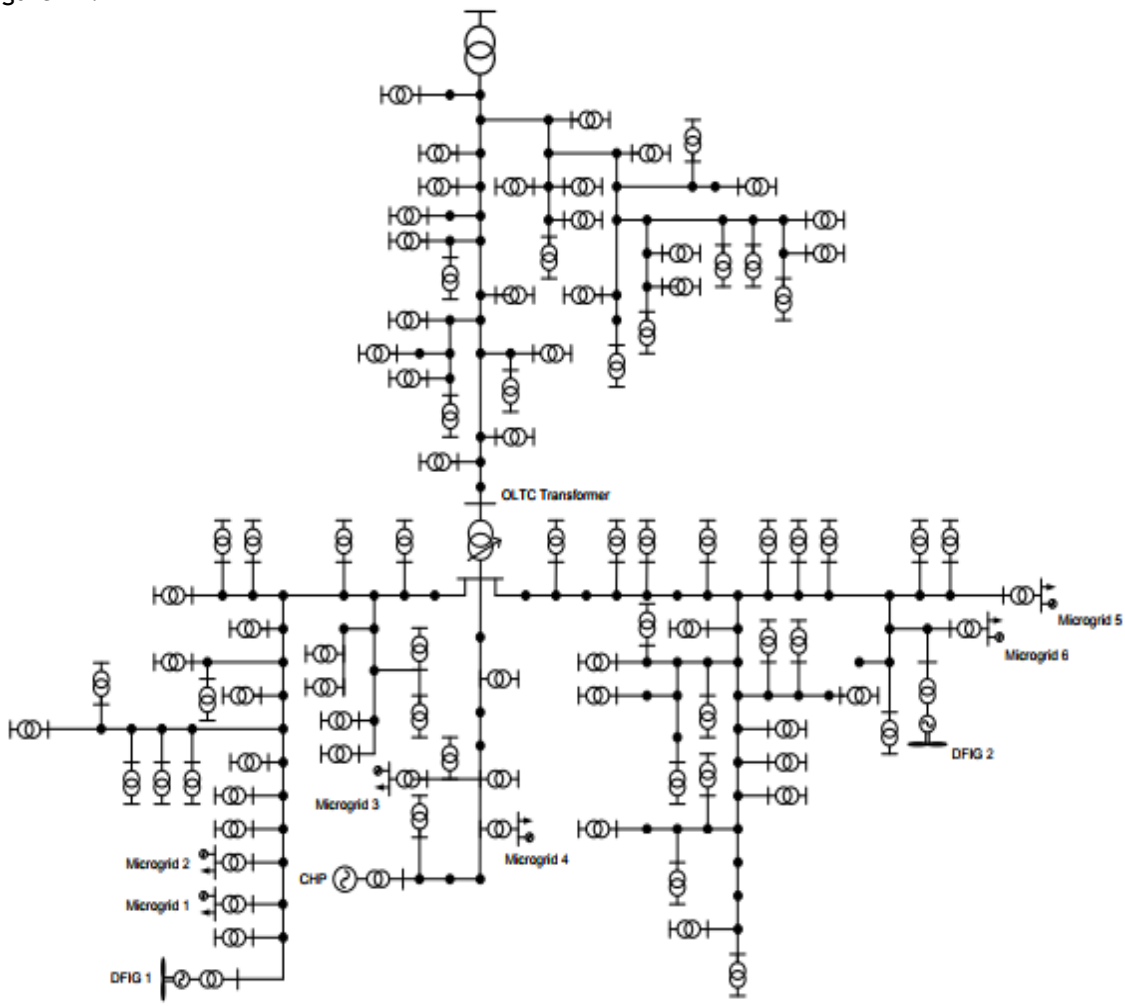


**Figure 12 – Real Portuguese MV distribution network [107]**

210 branches and 1 OLTC compose this network. This transformer, which has taps on the secondary side, divides two different voltage areas (30/15 kV). Following the modifications proposed in [107], DG units and "active" LV networks (microgrids) were added to this grid so that the flexibility estimation performance can be evaluated. As can be observed in Figure 12, the microgrids were modulated as a single bus with an equivalent generator and an equivalent

load. Thus, six interruptible consumers, six micro sources (totalizing 1.065 MW of installed capacity) and three DG units (totalizing 4 MW of installed capacity) compose the majority of the available flexible resources. In addition, a synchronous compensator (1 unit of 1 Mvar) was also connected to the grid.

**Table 1 - Degrees of flexibility for each flexible resource and corresponding costs**

| Resource | Flexibility Direction/Amount | | Cost |
|---|---|---|---|
| *Synchronous compensators* | $Q_{injection}$ | 100% Installed Capacity | 5€/Mvarh |
| | $P_{curtailment}$ | - | - |
| *DRES/DG* | $Q_{injection}$ | 6,67% Installed Capacity | 5€/Mvarh |
| | $P_{curtailment}$ | 100% Available Power[2] | 5€/MWh |
| *Interruptible consumers* | $Q_{curtailment}$ | 10% Reactive Load | 10€/Mvarh |
| | $P_{curtailment}$ | 10% Active Load | 10€/MWh |

Table 1 shows the flexibilities that would be activated in the grid if the technical constraints did not play their role. In other words, it details the flexibility that is available along with the cost to pay per MW/Mvar activated. For instance, if the current network conditions allow, DRES/DG are willing to see their active power output fully curtailed in exchange for a payment of 5€/MWh. In the following test cases, the same DRES/DG units are also able to provide reactive power support services through an additional $Q_{injection}$ that can reach 6.67% of the installed capacity. The DRES/DG installed capacity as well as the load forecast for the time instant considered in the test cases are exhibited in Annex II. The choice for the flexible resources presented in Table 1 took into account the current Portuguese regulatory framework - existence of interruptible consumers [108], possibility of DRES curtailment [109]. In other countries, the type and amount of controllable flexibility units can significantly vary [110]. However, this does not constitute an obstacle to the developed algorithm. In [111] and [112], the proposed approach was tested considering distinct operating conditions (RES penetration level and load growth) and different flexible sources (e.g., storage devices). These scenarios were built for Portuguese, French and German distribution grids and none of them led to problems in the methodology performance.

Due to its particular characteristics, the impact of discrete variables upon the flexibility area estimation requires a separate analysis. Therefore, in the following section, the test cases are carried without considering the tap changing capability - the transformer works with a fixed tap. Two tolerance values and three different maximum costs for flexibility activation were used in these test cases. In Chapter 5, the tap changing capability is enabled and the

[2] In the following test cases, DRES/DG units will be injecting in the grid at their maximum capacity (Annex II)

synchronous compensator is replaced by a capacitor bank thus allowing to explore their influence.

### 3.6.2 Results and Critical Analysis

Figure 13 shows the flexibility area obtained for the 210 Nodes MV distribution network. It can be seen as the maximum achievable flexibility area since is constrained by a cost that cannot be overcome, even if all the available flexibility was activated. This is similar to have an unconstrained problem regarding the flexibility activation costs. More precisely, this area shows the flexibility available from the transmission network point of view (i.e. at the TSO/DSO connection) considering the technical limits in the distribution grid.

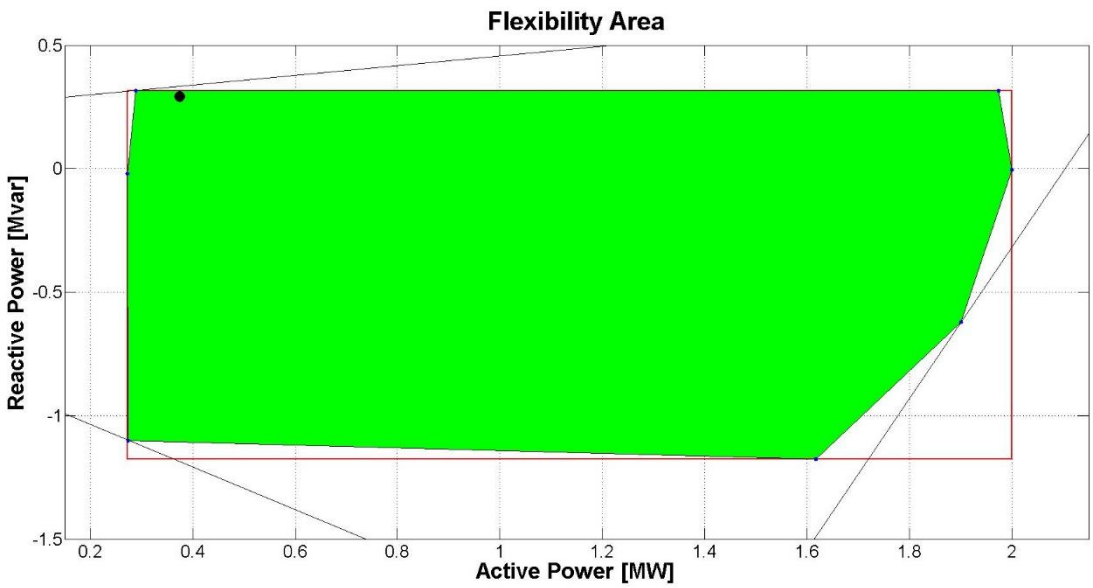


**Figure 13 - Flexibility area for the 210 Nodes MV distribution network ($\theta_{tol}$ =10 degrees)**

The flexibility area shows both active and reactive power ranges expected, considering the available resources. The location of the scheduled operating point (black point) in the PQ plan is also an indication of the method accuracy. As detailed in Table 1, the reactive power flexibility only has the downward direction. Regarding the active power, a higher amount of flexibility in the upward direction was expected due to the available power of DRES/DG in comparison with the load values (see Annex II). The estimated flexibility area clearly complies with these expectations. Another clue about the methodology effectiveness is provided by the fact that not all the available flexibility is being activated. For instance, the constraint imposed by the branch that connects the primary substation to the distribution network (2 MVA of maximum branch flow capacity) is perfectly visible in the active power upper limit of Figure 13.

The red rectangle that joins the extreme points of the perimeter illustrates an over estimation of the flexibility area. As already shown in Figure 9, the PQ interdependency has a

significant impact in the flexibility area shape. Therefore, other points on the area perimeter besides the maximum and minimum values of active and reactive power need to be estimated (blues points in Figure 13). To do so, the tangent straight lines of each two consecutive points (black lines in Figure 13) are used until the convergence criteria is met. The tolerance value is set at $\theta_{tol} = 10\, degrees$ thus allowing to catch a representative idea of the flexibility area shape.

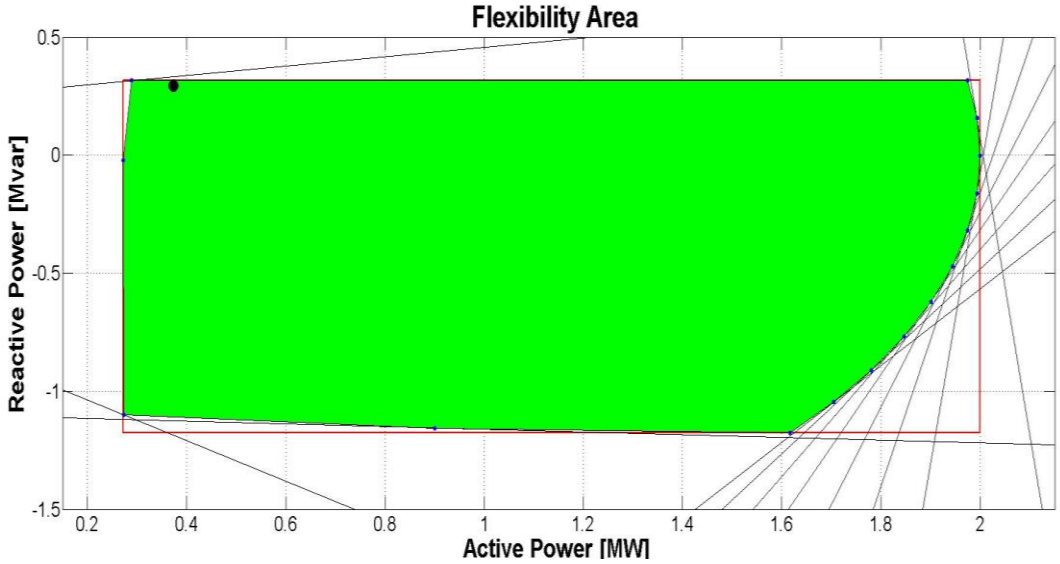


**Figure 14 - Flexibility area for the 210 Nodes MV distribution network ($\theta_{tol}$ =3 degrees)**

Figure 14 shows the flexibility area for the same 210 Nodes MV distribution network, but using $\theta_{tol} = 3\, degree$. By reducing the tolerance value, the search for new points continues even when they will probably not lead to significant changes on the flexibility area perimeter. The definition of a good tradeoff between the area representation and the computational effort is, therefore, of utmost importance. Figure 13 and Figure 14 show a clear example in which the time invested in exploring new zones of the perimeter is not compensatory.

Aiming to test the flexibility cost constraint, three different maximum costs were set. Their definition considered the cost that the user would need to pay if all the flexibility available was activated (excluding simultaneous activations of active/reactive flexibilities in opposite directions) – 32.06€. Therefore, one of the maximum costs is equal to 32.06€ while the remaining two are set below this value (5€ and 3€). Without the impact of the network constraints and the PQ interdependency, a small downward variation regarding the 32.06€ cost would lead to changes on the flexibility area. Nevertheless, this impact is real and for this particular test case, the maximum flexibility that can be activated has a total cost much lower than 32.06€. This way, in order to observe the effect of the flexibility cost constraint, it was necessary to set the remaining maximum costs far below from this one. From this explanation, it can also be expected that the area corresponding to the 32.06€ is equal to the one in Figure 13 and Figure 14.

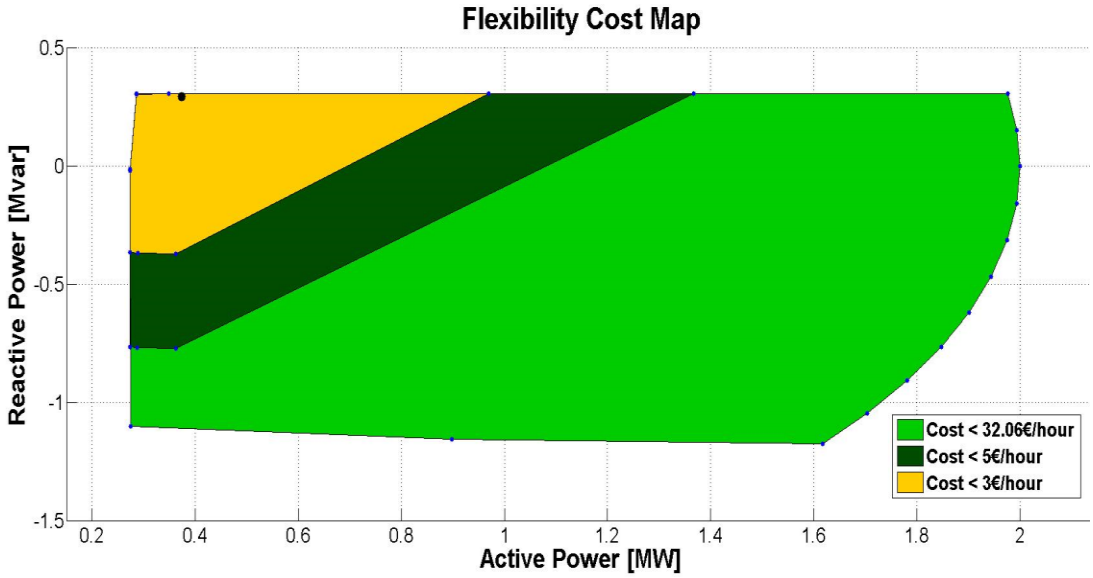


**Figure 15 – Flexibility areas constrained by different maximum flexibility costs**

Figure 15 depicts three different flexibility areas corresponding to the maximum flexibility costs defined, as detailed in its label. As expected, if the user is not willing to pay a high cost for the flexibility activation, the margin in which the scheduled operating point can be moved becomes narrower. Inside each one of these colored areas, the flexibility activator knows that the scheduled operating point can take any position by paying, at most, the respective maximum flexibility cost. The optimization model ensures that exists, at least, one combination of flexibility activations that allow for these changes while respecting the technical network constraints. As mentioned before and confirmed in Figure 15, the flexibility area constrained by 32.06€ is equal to the one in Figure 13 and Figure 14.

The flexibility area identification procedure fulfils the expectations by providing the feasible region of PQ points that can be exchanged at the TSO-DSO boundary nodes, independently from the maximum cost defined. Therefore, the automatic update of the objective function through the coefficients $\alpha$ and $\beta$ is an effective technique. It obtains the tangent straight lines that intersect the PQ plan thus allowing to completely explore the flexibility area perimeter.

The proposed methodology was tested during several months in two demonstration sites by the Portuguese and French DSO (EDP and Enedis). Four distribution networks (two in Portugal/two in France) connected upstream, to the corresponding national transmission grids were considered. During the field-tests, the method performance was evaluated concerning three different aspects: expected output, computational performance and integration with DSO operational tools (e.g., SCADA/DMS, forecasting systems). The tests were performed in open loop, allowing an experienced network operator to validate the results. The real-world implementation thus highlighted the capability of this methodology to provide the expected

flexibility areas within the network operation time constraints (non-functional requirement). In addition, a smooth integration with the DSO operational systems was observed.

### 3.6.3 KPI evaluation

The performance of the optimization model is assessed in this section. A comparison between the BaU and the proposed method was carried. In [113], the BaU is also known as "control state" and illustrates the benchmark model that should be used to evaluate the effectiveness of a new methodology. Thus, the flexibility areas for the 210 Nodes MV distribution network were also obtained through the random sampling approach [24] and the KPI were computed.

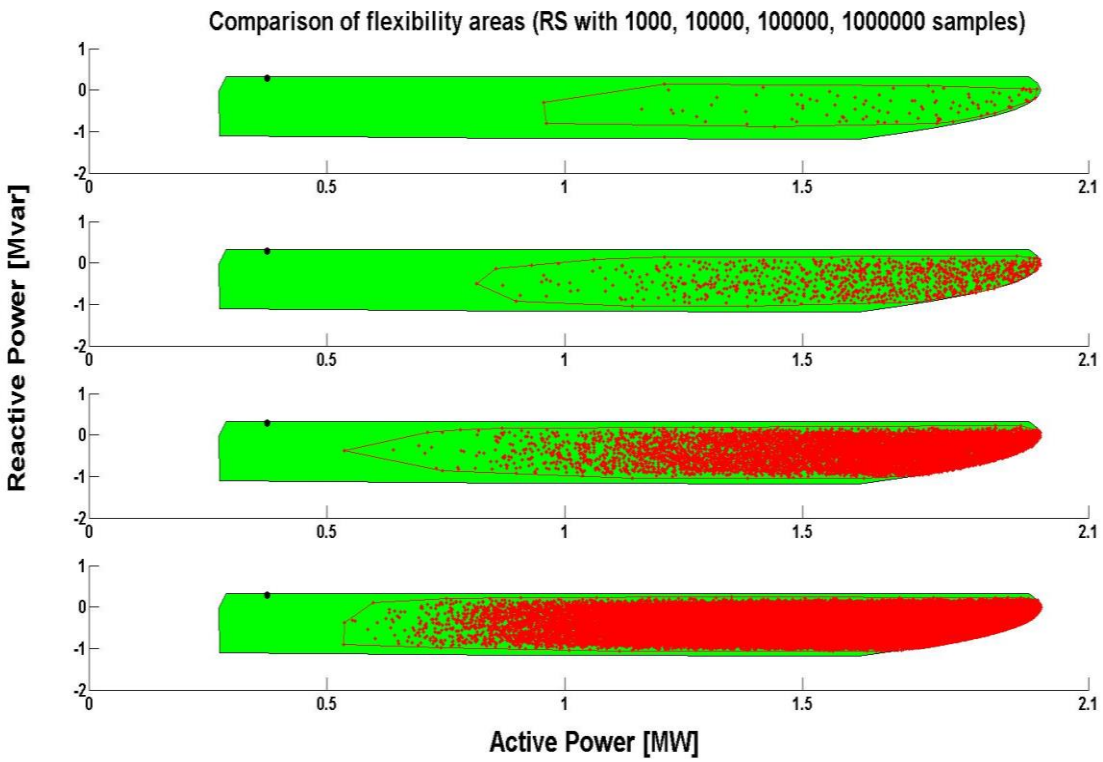


**Figure 16 – Random Sampling vs Proposed Methodology**

Figure 16 shows the flexibility area obtained with the proposed methodology ($\theta_{tol}$ =3 degrees) as well as the ones computed through the random sampling approach (1000, 10000, 100000 and 1000000 samples). This means that a total of 1000000 power flow calculations were executed. Among them, only a % leads to feasible results, which are illustrated in Figure 16 by the red points. The convex hull of these points thus characterizes the flexibility area obtained with the random sampling approach. As expected, the operating point has lower variation margins due to the limitation of this approach in finding some extreme values of power injection. In this particular case, the random sampling method was incapable of finding lower values of active power injection, irrespective of the corresponding reactive power. To achieve

them, two conditions would have to be observed in the sampling process: $P_{curtailment}$ of each DRES/DG close to zero and $P_{curtailment}$ of each interruptible consumer near their maximum. However, as already mentioned, the flexibility provided in each node by these two types of resources is independently created using uniform distributions. In addition, the volume of flexibility offered by each type is quite different - a small $P_{curtailment}$ of DRES/DG can cover the $P_{curtailment}$ of all interruptible consumers. Therefore, the fulfillment of both conditions is a rare event, not illustrated by any of the 1000000 samples. Figure 16 clearly shows that the optimization model developed overcomes this drawback.

**Table 2 – KPI computation**

| No. samples | Flexibility area increase (%) | Computational time reduction (%) |
|---|---|---|
| **1 000** | 171,33 | 15,09 |
| **10 000** | 100,01 | 91,06 |
| **100 000** | 58,46 | 99,07 |
| **1 000 000** | 39,49 | 99,91 |

Table 2 highlights that the methodology here described allows a reduction of the computational effort while achieves a significant increase in the identification of the flexibility area. Through its optimization model, the innovative method catches the full contribution that the available flexible resources have for the power exchanged at the TSO-DSO interface. Thanks to that, both TSO and DSO know which changes can be carried in the operating point.

In order to support the information provided by Table 2, the solution times of the proposed method and the random sampling approach are shown in Table 3.

**Table 3 – Computation time of both methods**

| No. samples/Proposed method | Computational time (s) |
|---|---|
| **1 000** | 6,08 |
| **10 000** | 57,75 |
| **100 000** | 554,84 |
| **1 000 000** | 5579,18 |
| **Proposed Method** | 5,16 |

The time needed to draw the flexibility area through the proposed methodology is compliant with the real network operation, where the existence of time constraints is a reality. In other words, if more accurate forecasts are available or a change in the network topology is observed, the methodology can quickly display an updated flexibility area. The KPI detailed in Table 2

refer only to the maximum flexibility area $C_{max}$= 32.06€/hour, since the comparison for other maximum flexibility costs would lead to similar conclusions.

As final remark, the improvement achieved in the flexibility area identification may be even more noticeable depending on the available flexible resources. Let us imagine the same 210 MV distribution network, but with OLTC's connected to it. In this case, the number of combinations of tap positions would lead to a huge increase of the available operating points, most of them potentially infeasible. Contrary to what would happen with the optimization model, the random sampling approach would frequently fall in these infeasible points. This once again highlights the need for an effective flexibility area estimation procedure.

### 3.6.4 Benefits assessment

The awareness of the flexibility area produces highly valuable information for both system operators. Table 4 shows a set of benefits that can be derived from the proposed methodology.

**Table 4 – Benefits associated to the flexibility area recognition**

| Benefits |
|---|
| It contributes to increase the information exchange |
| It enhances the accuracy of the definition of contractual values of electrical energy exchange |
| It provides valuable data for the future planning of distribution network |
| It separates the contributions of each type of flexible resource |

The results presented in the previous sections clearly illustrate how the developed method contributes to increase the information exchange between the TSOs and the DSO. Through the flexibility areas, the TSO knows exactly the impact of a flexibility activation by the DSO on the operating point margins. This information supports the TSO when requesting flexibility from the DSO side. Without these insights, the system operators would be incapable to coordinate their flexibility activation procedures. In addition, the knowledge of the scheduled PQ operating point helps to forecast the power exchanges in the transmission network nodes without depending on the existence of a distribution network equivalent (or complete topology description). The recognition of the operating point margins is also valuable when defining the contractual values of electrical energy exchange between the TSO and the DSO. By combining areas constrained with different maximum flexibility costs - Figure 15 -, the system operators become able to identify the minimum cost to pay for a specific power exchange at their interface.

This methodology provides the network planner with

the awareness regarding the impact of future scenarios (e.g., with more DER, with an increased DRES penetration) in the current flexibility area. If no changes are observed, this might indicate that network reinforcements are necessary in order to take advantage of the additional flexible resources. A similar situation is described in the results section – the grid through their DER has more flexibility to offer, but the technical constraints are limiting its exploitation. The areas of a flexibility map can also be divided by type of resource. This functionality allows to observe the influence of each DER thus helping to identify which flexibility resources might be activated to fulfill a specific variation of the operating point.

## *3.7 Estimation of non-convex flexibility areas*

The fulfillment of *Goal 1* turned into a method that identifies flexibility areas at the TSO-DSO interfaces by searching for their vertex points. As it is further discussed in Chapter 5, the area obtained by the envelop of the vertex points is totally valid only when considering continuous variables. In addition, relying only on changing the slope $\theta$ of the straight line that geometrically illustrates the objective function, can lead to over estimations of the flexibility area. Such situations could arise when in the presence of non-convex flexibility areas. In these cases, the straight lines that intersect the $P_{DSO\rightarrow TSO}$ / $Q_{DSO\rightarrow TSO}$ plan would not be able to capture the non-convexities.

Despite this problem, slight modifications to the current methodology are capable to enable a reliable estimation of both convex and non-convex areas. The idea behind this update is to constrain the optimization to a straight line that intersects a specific $P_{DSO\rightarrow TSO}$ / $Q_{DSO\rightarrow TSO}$ point inside the flexibility area. Then, similarly to the methodology proposed in *Goal 1,* the slope of this line is iteratively updated in order to capture the several extreme points. Therefore, the coefficients $\alpha$ and $\beta$ are now part of a constraint that helps in the identification of non-convex areas, instead of being used to update the objective function. Figure 17 shows a real-test case applying this updated method, but it also provides a very good illustration of the described problem.

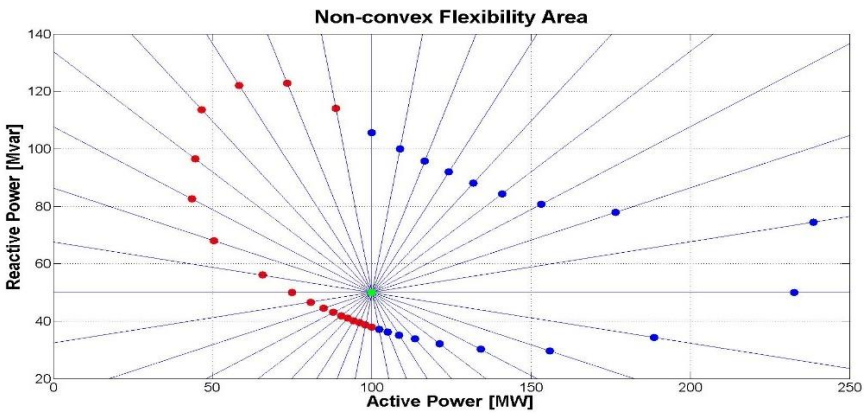


**Figure 17 – Estimation of a non-convex area**

The updated methodology is therefore mainly composed of two steps:

1. Running a single execution of an OPF in order to define a $P_{DSO \rightarrow TSO} / Q_{DSO \rightarrow TSO}$ point inside the flexibility area (green point in Figure 17). Since there is no preference concerning the estimated point, the OPF objective function can take different formulations e.g., maximization of the reactive power flow at the TSO-DSO interconnections

2. Adding a new constraint to the optimization problem, which is geometrically described by a straight line that intersects the $P_{DSO \rightarrow TSO} / Q_{DSO \rightarrow TSO}$ point. At each iteration, the slope of this line is updated and the objective function is maximized and minimized. These two independent processes allow to obtain the red and blue points depicted in Figure 17, which together form the flexibility area.

In the test-case that led to the result observable in Figure 17, the active power was the variable chosen to be maximized and minimized during the estimation process.

## *3.8 Contributions to Goal 1*

- ***Goal 1:*** Formulation of an optimization problem that, iteratively, changes its own objective function in such an intelligent way that allows to estimate the entire flexibility area perimeter

This chapter proposed the use of an entirely new algorithm developed within the scope of this dissertation to estimate the active and reactive power ranges that can be exchanged between the transmission and distribution networks by exploiting the flexibility provided by different types of DER. The tests performed in the simulation environment as well as the real-world experience validated the methodology effectiveness thus providing an effective answer to the *research question*. Despite the importance of these conclusions, the realization of *Goal 1* had a broader impact. It defined the foundations for an improved cooperation between system operators where a new concept called flexibility takes the main role. By estimating its impact at their interface, both the TSO and the DSO have the necessary information to carry internal studies on the same basis, but without sharing confidential information. As such, the contributions of fulfilling *Goal 1* go far beyond a theoretical analysis. They can have a direct impact on energy field players, as demonstrated by the tests described in following articles.

- *Detailed methodology description and demonstration carried together with EDF, the French DSO:*

- J. Silva, J. Sumaili, R.J. Bessa, L. Seca, M. Matos, V.Miranda, M.Caujolle, B. Goncer-Maraver and M. Sebastian-Viana, “Estimating the Active and Reactive Power Flexibility Area at the TSO-DSO Interface,” *IEEE Trans. Power Systems, vol. 33 (5)*, pp. 4741- 4750, Sept., 2018.

- *Test trials carried together with EDF, the French DSO:*
  - M. Sebastian-Viana, M. Caujolle, B. Goncer-Maraver, J. Sumaili, J. Pereira, P. Barbeiro, J. Silva and R.J. Bessa, "LV state estimation and TSO-DSO cooperation tools: Results of the French field tests in the evolvDSO project," presented at the CIRED 2017, Glasgow, Scotland, 12-15 June, 2017.

- *Test trials carried together with EDF and EDP, the French and Portuguese DSOs:*
  - N. Fonseca, J. Silva, A.C. Silva, J. Sumaili, L. Seca, R.J. Bessa, J. Pereira, M. Matos, P. Matos, C. Morais, M. Caujolle and M. Sebastian-Viana, "evolvDSO grid management tools to support TSO-DSO cooperation," presented at the CIRED 2016, Helsinki, Finland, 14-15 June, 2016.

- *Test trials carried together with Innogy, a German DSO:*
  - A.C. Silva, J. Sumaili, J. Silva, L. Carvalho, L. Seca, M. Matos, R.J. Bessa, G. Schaarschmidt and R. Hermes, "Assessing DER flexibility in a German distribution network for different scenarios and degrees of controllability," presented at the CIRED 2016, Helsinki, Finland, 14-15 June, 2016.

These same tests also highlighted some limitations concerning potential over-estimations of the flexibility area. Some of them such as the estimation of non-convex flexibility areas were already addressed in this Chapter, while others are matter of discussion in the following chapters. These drawbacks are analyzed while trying to find potential solutions.

# Chapter 4

# Transmission network equivalents to support flexibility area computation

Despite the progress achieved by the method previously proposed, some limitations arose during the on-going process of this dissertation. More specifically, when dealing with mesh distribution grids with multiple connections to the transmission network, the knowledge of the operating point in N-1 substations is a requirement to estimate the flexibility area in the N primary substation. Since the approach assumes independency between the different primary substations, without the knowledge of these operating points the flexibility area would be over-estimated. The inclusion of the existent mutual dependencies between the different TSO-DSO connections is thus mandatory in order to overcome this input dependency – the power exchanged in the N-1 substations. Two different options are capable of fulfilling this requirement: the full knowledge of the transmission network or an equivalent of it. The next sections detail why the second option is more valid thus allowing to formulate *Goal 2* of this dissertation.

- ***Goal 2:*** to model and integrate a network equivalent for the transmission network to fully tackle the problem of managing the active and reactive power flows in the TSO-DSO boundaries

## *4.1 Network equivalents – from the basis to an innovative approach*

Figure 18 divides the full network model into three distinct parts – internal and external grids and their boundaries – so that is easier to illustrate the idea behind the development of network equivalents.

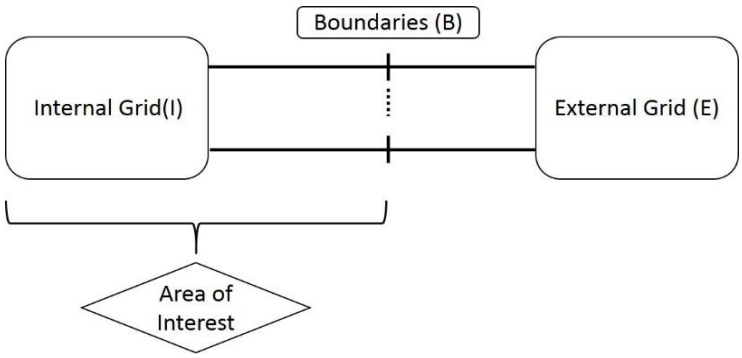


**Figure 18 – Generic representation of a full network model**

Their definition is closely dependent on the type of network study to be carried. For the specific case of this dissertation, the following correspondence should be considered:

- Internal Grid = Distribution Network
- External Grid = Transmission Network
- Boundaries = TSO-DSO connection nodes

Most of the times, these three different parts do not need to be entirely represented since the analysis only focus on a specific part of the electrical grid - the area of interest. Load flow studies in the distribution network are an example of this. However, in the presence of disturbances and/or perturbations (e.g., line and/or transformer contingency) in the area of interest, is of utmost importance to understand how the external network reacts. If the electrical behavior of the external network is not taken into account, then power exchanges between the boundaries and the external grids are taken as constant, which do not illustrate most of the real situations. Therefore, is clear that the inclusion of the full external network model would be the most straightforward solution. Despite this, not always the simplest solution is the best choice. For the particular case of this dissertation, where the transmission grid represents the external network, two main reasons validate this assumption: confidentiality and technical issues. While the former is a classical problem of sharing information with third-parties, the latter concerns the additional computational effort that the inclusion of the external network would have for an algorithm that is expected to run in real-time operation. Thus, the remaining option to model the behavior of voltage and power injections at the boundary nodes is the development of transmission grid equivalents. Although quite advanced, the state-of-the-art in this field only partially solves the aforementioned drawbacks. If it is true that the existing methods provide reliable results, it is also known that the external grid topology data is an input requirement. In other words, the computation of network equivalents is dependent on the knowledge of the external grid (at least, one time). In addition, the majority of the available methods assume a reference operation scenario, i.e., one specific snapshot of the grid operation. *Goal 2* seeks the development of a reliable approach

valid for a wide range of operation conditions while only using, as input data, historical data collected at the TSO-DSO boundary nodes.

## 4.2 The Ward equivalent methods

The study of network equivalents is a very specific topic within the power systems field. Nevertheless, a vast range of studies is available due to its utmost importance. In spite of not being recent, the discussion concerning their development is up to date, even more in an environment increasingly concerned with data privacy issues. The state-of-the art shows several different options and results, but the Ward equivalents are the ones that stand out. Their core procedure is the manipulation of the nodal admittance matrix of the entire network model – Y-Bus – so that the external grid can be represented by a set of series impedances and shunt admittances between the interface nodes and by current injections at these buses [114]. Four different variants compose the so-called Ward equivalents: the linear model [114], the non-linear approach [114][115], the Ward equivalent with PV nodes retention [116] and the extended version [115].

### 4.2.1 Linear Ward equivalent model

This version of the Ward equivalent is based on the following linear expression:

$$Y * U = I \tag{4.1}$$

where $Y$ illustrates the nodal admittance matrix, $U$ concerns to the complex bus voltage vector and $I$ is the current nodal injections vector. Being this a linear model, the loads and/or generating sources are represented by a constant current and/or a constant admittance. To understand how the equivalent model is deducted, expression (4.1) needs to be expanded. Throughout this procedure, the nomenclature defined in the Figure 18 should be followed.

$$\begin{bmatrix} \boldsymbol{Y_{EE}} & \boldsymbol{Y_{EB}} & \\ \boldsymbol{Y_{BE}} & \boldsymbol{Y_{BB}} & \boldsymbol{Y_{BI}} \\ & \boldsymbol{Y_{IB}} & \boldsymbol{Y_{II}} \end{bmatrix} * \begin{bmatrix} \boldsymbol{U_E} \\ \boldsymbol{U_B} \\ \boldsymbol{U_I} \end{bmatrix} = \begin{bmatrix} \boldsymbol{I_E} \\ \boldsymbol{I_B} \\ \boldsymbol{I_I} \end{bmatrix}$$

Focusing on the first equation of this linear system, $\boldsymbol{U_E}$ is evidenced:

$$\boldsymbol{U_E} = \frac{(\boldsymbol{I_E} - \boldsymbol{Y_{EB}} * \boldsymbol{U_B})}{\boldsymbol{Y_{EE}}} \tag{4.2}$$

A reduced system can then be obtained by replacing $\boldsymbol{U_E}$ in the second system equation.

$$\begin{bmatrix} \boldsymbol{Y_{BB}^{eq}} & \boldsymbol{Y_{BI}} \\ \boldsymbol{Y_{IB}} & \boldsymbol{Y_{II}} \end{bmatrix} * \begin{bmatrix} \boldsymbol{U_B} \\ \boldsymbol{U_I} \end{bmatrix} = \begin{bmatrix} \boldsymbol{I_B^{eq}} \\ \boldsymbol{I_I} \end{bmatrix}$$

where

$$Y_{BB}^{eq} = Y_{BB} - \frac{(Y_{BE} * Y_{EB})}{Y_{EE}} \tag{4.3}$$

$$I_B^{eq} = I_B - \frac{(Y_{BE} * I_E)}{Y_{EE}} \tag{4.4}$$

These two simple steps provided a reduced system where the knowledge of the state variable associated to the external grid - $U_E$ - is not necessary. Focusing on expression (4.3), $Y_{BB}^{eq}$ is responsible for modelling the admittance between the interface nodes as well as their shunt admittances. Going further on the analysis of (4.3), $Y_{BB}$ characterizes elements that belong to the area of interest. On the other hand, $-\frac{(Y_{BE}*Y_{EB})}{Y_{EE}}$ is the parcel of $I_B^{eq}$ that tries to illustrate how the external grid behaves in the presence of a disturbance. Therefore, although the Ward approach is able to provide equivalent models, it always needs to have the knowledge of the external network once. Furthermore, the complete characterization of the network equivalent is dependent on the computation of the equivalent injection i.e. $I_B^{eq}$. Following expression (4.4), $I_B^{eq}$ is obtained by subtracting the current injection in the interface nodes - $I_B$ - to a term that shows how the external injections are redistributed through these nodes. To compute this parcel, the injections in the external network - $I_E$ - are necessary. However, these measurements might be unknown in real-time. In such cases, $I_B^{eq}$ can calculated with the following expression:

$$I_B^{eq} = Y_{BB}^{eq} * U_B + Y_{BI} * U_I \tag{4.5}$$

(4.5) states that the equivalent current injection in a border node is simply provided by the sum of the currents in all the admittances connected to that bus i.e. border-border, border-internal grid and border shunts. To achieve these currents, the knowledge of the external grid is mandatory. Otherwise, $Y_{BB}^{eq}$ cannot be computed. In addition, $U_B$ and $U_I$ can easily be obtained through a typical state estimator while $Y_{BI}$ belongs to the data encompassed by the area of interest. Therefore, the dependency on the availability of a real-time measurement is overcome with expression (4.5). Besides this, the usage of (4.5) prevents the propagation of errors to the area of interest caused by imprecisions in the external network characterization. In situations like this, matrix $Y_{BB}^{eq}$ is inaccurately calculated. However, if the correct state of the area of interest - $U_B$ and $U_I$ - is considered, the reduced model will correctly reproduce the operating point of this part of the grid. Thus, the equivalent injections in the border nodes are

the responsible to automatically compensate the arising errors. Figure 19 provides a graphical representation of the network equivalent that is achieved using the linear approach proposed by Ward.

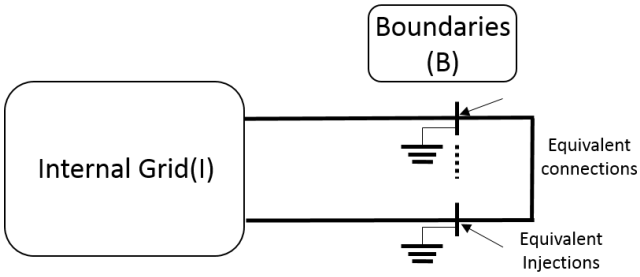


**Figure 19 – Linear Ward equivalent model**

The method previously described ensures the development of an accurate network equivalent model. However, when in the presence of systems with a considerable number of nodes, the computation of the equivalent admittances through (4.3) becomes impractical. In [117], the Gauss elimination method is used to overcome this problem and shows considerable advantages.

### 4.2.2 Non-Linear Ward equivalent model

The aforementioned Ward equivalent follows a linear process. Therefore, for applications in which the external network can be represented by its linear model, this equivalent leads to the exact same result as when considering the full knowledge of the grid. Nonetheless, there are several different types of studies in which loads and/or generating sources need to be represented by constant power. In such cases, a non-linear model of the external network must be considered. Although still possible through a slightly different approach, the obtained equivalent only leads to approximated results. Nevertheless, these approximations are usually acceptable for the majority of studies.

In order to develop an equivalent network that considers the non-linear behavior of the external grid, two steps need to be carried out – computation of the equivalent admittances and of the equivalent active and reactive power injections. On the one hand, the equivalent admittances are calculated following the same procedure already described in the linear Ward model. On the other hand, the active and reactive power injections are computed through expressions (4.6) and (4.7):

$$P_k^{eq} = V_k^0 \sum_{m \in K} V_m^0 * (G_{km}^{eq} * \cos\theta_{km}^0 + B_{km}^{eq} * \sin\theta_{km}^0) \tag{4.6}$$

$$Q_k^{eq} = V_k^0 \sum_{m \in K} V_m^0 * (G_{km}^{eq} * \sin\theta_{km}^0 - B_{km}^{eq} * \cos\theta_{km}^0) \tag{4.7}$$

Where $V^0$ and $\theta^0$ define the state variables of the base case, $K$ is the set of nodes (border and internal nodes) connected to the $k$ node and $G_{km}^{eq} + jB_{km}^{eq}$ is an element of the nodal admittance matrix - $Y^{eq}$ – of the reduce network.

$$Y^{eq} = \begin{bmatrix} \boldsymbol{Y_{BB}^{eq}} & \boldsymbol{Y_{BI}} \\ \boldsymbol{Y_{IB}} & \boldsymbol{Y_{II}} \end{bmatrix}$$

$P_{km}^{eq} + jQ_{km}^{eq}$ simply correspond to the sum of the power flows between $k$ node and each one of the nodes belonging to $K$ set. The influence of the shunt element is also considered for the computation of this complex power. Therefore, the execution of an AC power flow on the top of the reduced model - Figure 19 – allows to obtain the equivalent active and reactive power injections. During this study, the boundaries would be considered the references nodes thus demanding for the specification of the voltage magnitudes and angles. These would be equal to the ones of the base case - $V_k^0$ and $\theta_k^0$.

In the presented approach, the existence of PV nodes in the external network is disregarded. As it is known, PV nodes have the capability to provide significant reactive power support in situations such as contingency events. Thus, treating them as PQ nodes lead to inaccurate grid equivalents in terms of reactive power. Bearing this in mind, there are available in the literature two different options to take into account this important effect:

- Retain the external PV nodes that are electrically close to the boundaries. In other words, the PV nodes are included in the final equivalent model, but they are excluded from the external network reduction procedure

- An extended version of this non-linear Ward equivalent, in which a fictitious PV node is connected to each boundary

### 4.2.3 Ward equivalent with PV nodes retention

This approach to compute equivalent models is characterized by the retention of PV nodes belonging to the external grid. Usually only the PV nodes that are electrically close to the boundaries are retained. In the presence of a disturbance in the area of interest, these would be the ones providing higher levels of reactive power support.

The procedure to obtain the equivalent network through this method is very similar to the one presented for the non-linear variant and is also composed of two steps: calculation of the equivalent admittances and of the equivalent active and reactive power injections. However, within these two steps, some differences arise. The equivalent admittances are – as in the aforementioned approaches – computed through the Gauss elimination method. In this case,

the PV nodes are also considered as boundary nodes since they are retained. In addition, the computation of the equivalent injections is carried out as follows:

- Perform a power flow study considering the network between the boundary nodes and the retained PV nodes. Based on it, is possible to obtain the voltage angle in the PV nodes. As in the non-linear Ward equivalent approach, the boundaries would be considered the references nodes with voltage magnitude and angle equal to the base case - $V_k^0$ and $\theta_k^0$

- With the knowledge of the current network state – area of interest and retained PV nodes – expressions (4.6) and (4.7) can be computed

The described process assumes that *P* and *V* of the retained PV nodes are known. This is normal since these variables are specified for nodes of type PV.

Figure 20 shows an illustration of the non-linear Ward equivalent considering the retention of external PV nodes.

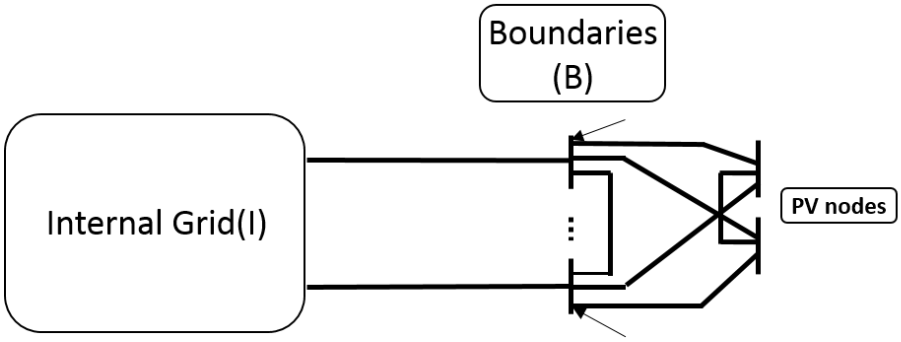


**Figure 20 -** Network equivalent with PV nodes retained

4.2.4 Extended Ward equivalent

The extended version of the Ward equivalent does not retain the original PV nodes of the external grid. Contrary to what happens in the approach previous detailed, the original PV nodes are not included in the final equivalent model. However, the impact associated to the existence of PV nodes is not disregarded. A mechanism of reactive power compensation is carried by fictitious PV nodes that are added to the model and connected to the boundary nodes. Figure 21 shows the configurations and characteristics of this Ward equivalent variant.

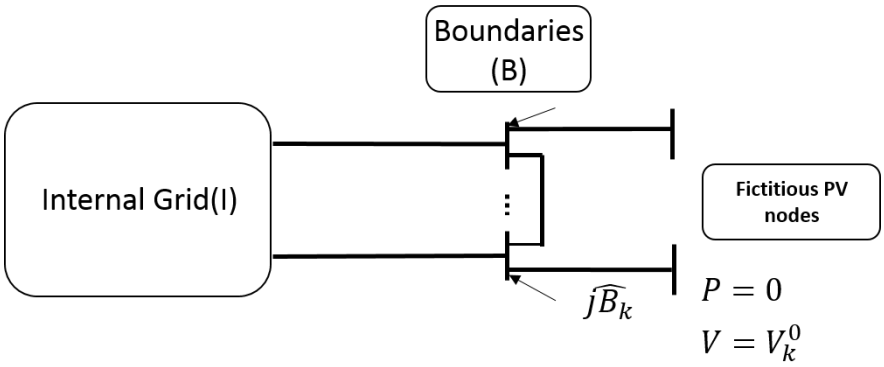


**Figure 21 - Extended Ward equivalent**

The equivalent admittances as well as the equivalent active and reactive power injections are obtained following the same procedure presented for the non-linear Ward equivalent. Regarding the introduced fictitious PV nodes, the voltage magnitudes and active power injections need to be specified. While the former assumes the same value as the boundary nodes, the latter is equal to zero. Therefore, the power flows in the fictitious connections are inexistent unless a perturbation on the area of interest occurs. In such cases, the fictitious PV nodes reply to changes on the voltage magnitude of the boundary nodes by injecting or consuming reactive power. Therefore, the effect of the original PV nodes for the reactive power compensation process is taken into account. The amount of reactive power that is injected/consumed in response to a perturbation in the area of interest is computed using the following expression:

$$\Delta Q_k = V_k * \widehat{B_k} * \Delta V_k \tag{4.8}$$

where $\Delta V_k$ illustrates the voltage variation in the boundary nodes when comparing the cases with and without perturbations. $\widehat{B_k}$ represent the susceptances between the boundaries and the fictitious PV nodes. Their value is obtained by computing $B''_{reduced}$, which defines the susceptances between the entire external network and the boundaries. $B''_{reduced}$ is characterized by two components:

- $\widehat{B_k}$, which is the result of summing all the elements of line $k$ of $B''_{reduced}$
- The equivalent susceptances between the boundary nodes, which correspond to the elements outside the main diagonal of $B''_{reduced}$.

The definition of $B''_{reduced}$ is dependent on the reduction of matrix $B''$. Once again, the Gauss elimination method can be employed to achieve this purpose. With the knowledge of $B''_{reduced}$ is then possible to describe the complete reactive reaction of the external system to a change on the area of interest - $\Delta Q^{reduced}$.

$$\frac{\Delta Q^{reduced}}{V} = B''_{reduced} * \Delta V \tag{4.9}$$

Similarly to expression (4.8), $\Delta V$ points out to the voltage magnitude deviations in the boundary nodes.

## 4.3 Transmission network equivalents – a novel algorithm only dependent on historical data availability

The exploitation of the aforementioned non-linear variants of the Ward equivalent is aligned with one of the dissertation objectives. Particularly, the two last versions allow to capture an interesting set of characteristics that describe the transmission network operation. Therefore, the inclusion of their network equivalents with the distribution grid model provides the necessary conditions to carry an accurate estimation of the flexibility ranges in multiple TSO-DSO connections. However, all the described methods require the full knowledge of the network model in order to compute the grid equivalents. This type of information is only available to the network owners due to confidentiality reasons. Bearing this in mind, the presented approaches would be applicable in a scenario where only the TSO would have access to the transmission network model. This is not the case of the problem addressed in this thesis, which focus on an increasing cooperation between the TSO and the DSO. In an environment characterized by information exchange processes, ensuring the data privacy becomes a topic of utmost importance. Within this context, this thesis proposes a novel algorithm that provides reliable network equivalents to support flexibility estimation services without using confidential data.

The suggested approach is only based on the availability of historical data concerning AC quantities at the TSO-DSO interfaces - $V, \theta, P, Q$. Such data should encompass a considerable time horizon e.g., one-year so that the different operation conditions of the transmission network are taken into account e.g., peak and valley hours considering seasonality. In the proposed approach, the historical information represents the target data. This way, the main goal is to define a network equivalent capable to lead to results that should be close as possible to the target ones. The proposed equivalent model is illustrated in Figure 22 and a metaheuristic approach is applied to fine-tune its parameters - $V_g, r, x, b$.

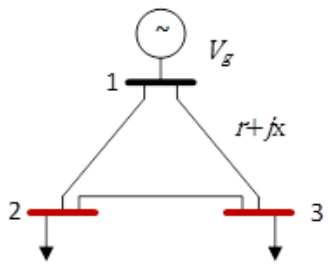


**Figure 22 – Network equivalent model with the respective TSO-DSO interfaces**

The Evolutionary Particle Swarm Optimization (EPSO) [118][119] algorithm was chosen to carry the fine-tuning process of the voltage set-point at the slack bus as well as the line electrical

parameters. The reason for this choice is detailed together with the EPSO description in the following section.

The procedure carried by the EPSO is based on an iterative adjustment of the aforementioned parameters so that the AC load flow in the network equivalent minimizes the fitness function defined in (4.10).

$$Fitness\ f. = 1 \times 10^{10} \sum_{t=1}^{T} \left( \sum_{i=1}^{CN} \left(V_i^{Equiv} - V_{i,t}\right)^2 + \sum_{i=1}^{CN-1} \left( \left(\theta_i^{Equiv} - \theta_{i+1}^{Equiv}\right) - \left(\theta_{i,t} - \theta_{i+1,t}\right) \right)^2 \right) \quad (4.10)$$

where $T$ represents the number of operation scenarios and $CN$ the number of TSO-DSO interfaces. Consequently, $V_i^{Equiv}$ and $\theta_i^{Equiv}$ denote the voltage magnitude and angle at interconnection $i$ as a result of the AC load flow run considering the transmission network equivalent. $V_{i,t}$ and $\theta_{i,t}$ have the exact same meaning, but concern to each $t$ operation scenario of the target data. The angles are measured in radians while the voltage magnitudes follow the pu unit system.

The defined fitness function (4.10) only states the minimization of the squared errors of the voltage magnitude and angle at the TSO-DSO interfaces. Thus, not all the aforementioned AC quantities are considered in the fitness analysis. In fact, the active and reactive power flows in the boundary nodes are imposed in the AC load flow calculations. A careful analysis of (4.10) also highlights that the voltage angle error is computed considering the angle difference between the TSO-DSO interfaces. In other words, $\theta_i^{Equiv}$ and $\theta_{i,t}$ might substantially differ when the fine-tuning process is over. This does not affect the equivalent network accuracy since the coupling between the TSO-DSO boundaries remain unchanged. In addition, the arising of large flows in the equivalent model aiming to create the angle differences between the reference and the interface nodes is avoided. Flows with such magnitudes might contribute to models with a lower quality. Figure 23 provides a high-level view of the fine-tuning process carried by the EPSO.

The results presented in the forthcoming sections clearly show the need for a transmission network equivalent in order to achieve a reliable view of the active and reactive power flows that can be exchanged at the TSO-DSO interfaces. Moreover, the results highlight that a single transmission network equivalent is usually not enough to map all the different grid operation conditions. In other words, an equivalent that is accurate in one operating scenario might lead to an erroneous analysis in other scenarios. Depending on the season and hour of the day (peak or valley), the operation conditions of the transmission network may experience significant changes.


**Figure 23 – EPSO applied to the fine-tune the equivalent model**

This becomes even more evident when the generation technologies available on the transmission side are considerably different from each other. A very simple and illustrative example is to think on a transmission network characterized by a mix of RES and conventional generation. The variable pattern associated to RES may lead to an entirely different redistribution of the active and reactive power flows throughout the several TSO-DSO connections. Therefore, in such cases, it is necessary to have more than one transmission network equivalent. In order to define the optimal number of equivalents to be developed, a clustering procedure was carried. This process aims to group into clusters the different operation scenarios of the transmission grid. To do so, it takes as starting point a set of variables that typically characterize the transmission network. In addition to the already mentioned $V, \theta, P, Q$ in the TSO-DSO interfaces, historical data of Hydro and Wind active power injection as well as the total active and reactive power produced in the transmission side is considered. These new input variables are usually publicly available and/or can be easily obtained without disclosing confidential information.

Prior to the clustering procedure, an additional step should be carried in order to enable an efficient and meaningful analysis. Independently of the historical data content, it is common the existence of outliers that introduce noise in the clustering approach. Bearing this in mind and considering that the main goal of the entire process is to identify significant data trends, these outliers should be detected and removed. To cope with this pre-requirement, data analysis features available on Matlab® are used. Particularly, the *rmoutliers* function is applied for the outlier removal. Departing from this refined dataset, a clustering technique - *k*-means – is employed so that the available *n* observations are assigned to *k* mutually exclusive clusters. The allocation of observation $i$ to one of the *k* clusters is based on the distance minimization

between this dataset point and the mean of the cluster. The *k*-means function is also available on Matlab® within its statistics and machine learning toolbox. Prior to the application of *k*-means, it is necessary to define the number of *k* clusters that this function should consider. In cases where the data to be clustered contains natural divisions, it is easy to define such a number. However, several times, these clear distinctions do not exist or are unknown, thus demanding for a function that determines how well the data fit into a specific number of clusters. The *evalclusters* Matlab® function performs this assessment via one of the following methods: Davies-Bouldin, Gap or Silhouette.

The employment of the aforementioned steps thus constitutes an efficient strategy to define the optimal number of network equivalents that allow to map the different operation scenarios of the transmission grid. Besides this, such a procedure allows to reduce the initial *T* operation scenarios (4.10) into one scenario per cluster. Using only the centroid of each cluster as the target data proved to be an intelligent approach. The parameter tuning of the network equivalent carried within the EPSO became much faster without compromising the reliability of the final result.

The development of the transmission network equivalents can be regarded as an offline process since only relies on historical data. The online part only arises when these reduced models need to be used in the network daily operation. Their successful exploitation is dependent on the knowledge of which network equivalent should be used considering the current operating scenario. To fulfil this mandatory condition, a binary decision tree for classification is employed - *fitctree* Matlab® function. In the perfect scenario, the decision tree would be trained with the same variables that compose the historical data. Nevertheless, this is not always possible since in real-time the data availability is much more constrained. Therefore, within the set of eight variables that compose the historical data, only the ones that are usually public available in near real-time are considered i.e. hydro and wind active power injection, total active and reactive power produced in the transmission grid. The constructed decision tree is then used to predict the cluster to which a specific operation scenario belongs. Figure 24 provides a high-level overview of this entire process.

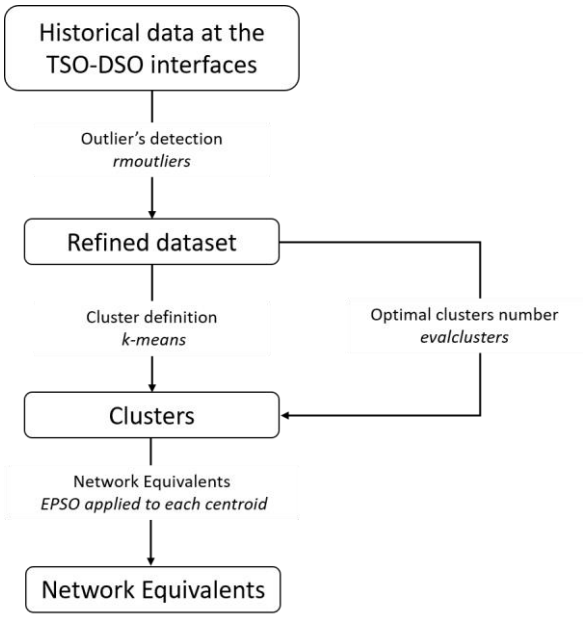


**Figure 24 – Clustering procedure and the transmission network equivalents**

### 4.3.1 Evolutionary Particle Swarm Optimization (EPSO)

Before going into detail concerning EPSO characteristics, it is important to explain why this algorithm was chosen to support in the definition of the transmission network equivalents. The first reason is that EPSO is a population-based metaheuristic, thus maintaining and improving multiple candidate solutions. Contrary to what happens with single-based methods, the population-based allows for a broader inspection of the search space. A global search is carried encouraging the search outside the current zone being explored. As such, a significant contribution is provided by population-based metaheuristics to avoid getting trapped in local optima. Although their space-covering features are of utmost importance, this type of methods encompass a higher number of fitness function evaluations per generation. This may become critical when the fitness function to be accessed is computation time consuming. However, this is not the case of the problem described in this thesis. As defined in (4.10), to evaluate the fitness function of each individual it is mandatory to have the knowledge of $V_i^{Equiv}$, $\theta_i^{Equiv}$, $\theta_{i+1}^{Equiv}$. To do so, simple AC load flow studies need to be run. Therefore, a population-based metaheuristic seems to fit with the problem characteristics and goals. This metaheuristics variant has already a vast state of the art and some of the available methods were highlighted in Chapter 2. However, none of them is EPSO and so the question remains: why EPSO? As well as other approaches (e.g., PSO, Evolution Strategies (ES) [120]), EPSO relies on the Darwin's natural selection paradigm to promote search towards the optimum. Concepts such as mutation and recombination of the current population and selection via stochastic tournament are applied. The search is influenced by inertia, memory and cooperation weights, which aim to emulate the existing social interaction between groups of animals. In addition, EPSO does not disregard the novelties of other metaheuristics. On the one hand, it embeds the self-adaption typical techniques of ES, which decrease the dependence on the defined strategic parameters

and improves the ability to avoid local optima. Thus, the strategic parameters are mutated and evolve throughout the process. On the other hand, EPSO inherits the PSO capabilities to speed-up the search without an excessive parameter tuning. While maintaining these important features, EPSO introduces some new interesting ideas. The Stochastic Star Communication Topology is one of them [119]. This technique intends to promote pure cognitive movements during the search to allow a higher level of local search by each particle, eliminate disturbing noise and avoid premature convergence. To do so, a communication probability defines the amount of information that is exchanged between the swarm and the global best position found so far. This EPSO characteristic of getting together state-of-the art techniques and new features, which have proved their ability to promote the search towards the global optimum, is the main reason for this choice.

The core of the EPSO formulation lies on two expressions that govern the movement rule - (4.11) and (4.12). A new particle position - $\mathrm{X}_t$- is always dependent on the position of its ancestor - $\mathrm{X}_{t-1}$- and on the so-called velocity of the particle - $V_t$. This term is originated from a couple of other parameters, namely: the inertia weight - $w_i^*$ - which is associated to the ancestor velocity, the memory weight - $w_m^*$ - which impacts on the difference between the best ancestor position - $X_b$ - and the ancestor position and the cooperation weight - $w_c^*$ - whose influence falls upon the difference between the best position found so far - $X_{gb}^*$ - and the ancestor position. Moreover, this last term is also affected by a diagonal matrix of Bernoulli variables – $C$ - with success communication probability *P*. A new matrix C is sampled in every *t* generation.

$$\mathrm{X}_t = \mathrm{X}_{t-1} + \mathrm{V}_t \tag{4.11}$$

$$V_t = w_i^* V_{t-1} + w_m^*(X_b - X_{t-1}) + w_c^* C\left(X_{gb}^* - X_{t-1}\right) \tag{4.12}$$

Among the aforementioned weights, $w_m^*$ and $w_c^*$ obviously intend to provide information concerning the best ancestors' position and the best position found so far. The inertia weight aims to maintain the inertial motion of particles in order to attract the search into other zones of the search space. The movement rule hereby described is very similar to the classical PSO. However, the superscript * refers to a mutation process on the top of the corresponding parameter. Expression (4.13) rules the mutation of a generic weight *w*:

$$w^* = w + \tau \mathrm{N}(0,1) \tag{4.13}$$

where $\tau$ is defined as the mutation rate and $N(0,1)$ represents a sampling process following a Gaussian distribution. These weights must be between 0 and 1 and are also considered during the selection phase. In other words, individuals that become part of forthcoming generations keep their weights. In addition, the best solution ever found is also mutated during the process. Therefore, instead of guiding the population towards a static point in space, $X_{gb}^*$ is "randomly

moved" following a Gaussian distribution. The main goal of this innovative technique is to attract the search into zones outside the current one.

The EPSO algorithm was described in this section. All the mentioned steps can be summarized in the following procedure:

1. ***Initialization*** – A population of ***m*** individuals and the corresponding optimization parameters (***r*** – nº of replicas per individual, ***P*** – communication probability, ***T*** - maximum nº of generations, ***τ*** – mutation rate) are initialized.

2. ***Evaluation*** – The initial population is accessed and, consequently, the initial $X_b$ and $X_{gb}^*$ are defined.

3. ***While*** the convergence criteria are not satisfied – maximum allowed number of generations **or** maximum allowed number of generations without finding better solutions:

   a. ***Replication*** – Each individual ***m*** is **replicated** ***r*** times
   ***b***. ***Mutation*** – Accordingly to (4.13), mutate the strategic parameters ($w_i^*$, $w_m^*$, $w_c^*$, $w_{gb}^*$) of each ***r*** replica
   ***c***. ***Movement*** – Expressions (4.11) and (4.12) are applied to govern the movement of each individual ***m*** and their ***r*** replicas. The movement rule is graphically illustrated in Figure 25.
   d. ***Evaluation and selection*** – Each individual ***m*** and their ***r*** replicas are evaluated against each other via the fitness function (4.10). Among them, the best performing individual of each line of ancestors is chosen to become part of the next generation. The best individual ever found in each line of ancestors is also updated.
   ***e***. ***Update*** – The best individual ever found in the entire population is updated.

From the presented description, it becomes clear that the characterization of each individual position is problem-dependent. In the case under study in this thesis, $V_g, r, x, b$ (Figure 22) are the decision variables that characterize $\mathrm{X}_t$. Thus, these parameters evolve and are mutated along the EPSO procedure in order to minimize the fitness function. However, when looking into the defined fitness function (4.10), these parameters do not allow for a direct computation of it. $V_i^{Equiv}$and $\theta_i^{Equiv}$ are only obtained after running an AC power flow study on the top of each individual (or each set of $V_g, r, x, b$) while imposing the active and reactive power flows in the interface nodes. Therefore, the only constraint in the EPSO algorithm is the one brought by the AC power flow: active and reactive power balance equations.

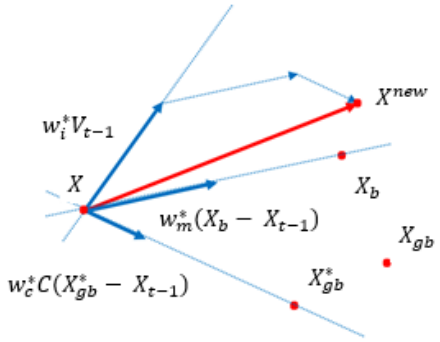


**Figure 25 – EPSO movement rule**

### 4.3.2 Results for the IEEE-RTS 96 (single-area variant)

The effectiveness of the proposed method to develop transmission network equivalents is accessed in this section. More specifically, this innovative approach is tested in the context of the PQ Maps when in the presence of more than one TSO-DSO interconnection. The single-area variant of the IEEE Reliability Test System (RTS) 96 [121] is used for this evaluation process. The one-line diagram of this test system is shown in Figure 26. Throughout this section, it is assumed that buses 1 to 10 belong to the distribution grid while the remaining are part of the transmission network.

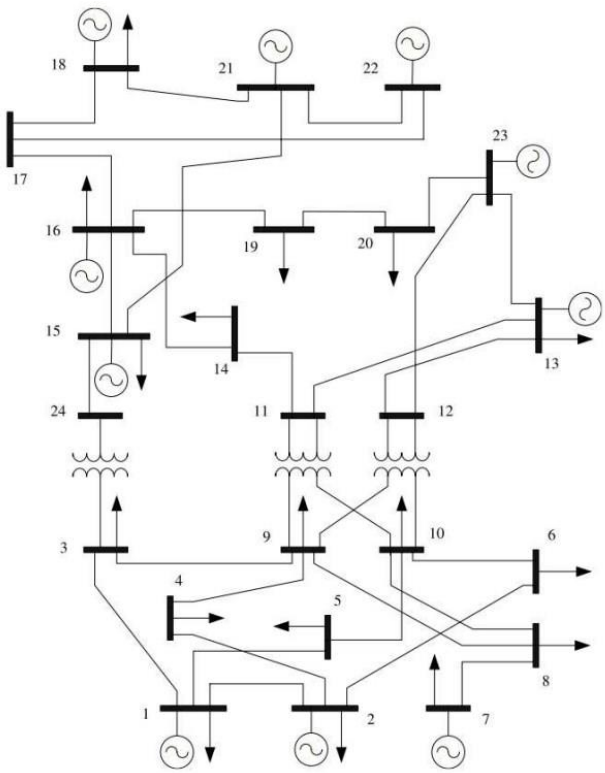


**Figure 26 - Single area IEEE RTS-96**

For the test case purposes, two modifications were employed to the original grid presented in Figure 26. First, the number of TSO-DSO interconnections was reduced to two in order to start the analysis with a simpler test system. To do so, the transformer connecting buses 3 to 24 was removed. Additionally, the transformers connecting buses 11 to 10 and 12 to 9 changed their configuration and now connect buses 11 to 9 and 12 to 10, respectively. In other words, TSO-DSO connections became composed of two parallels of transformers. This last change was necessary due to power flow convergence issues that arose after removing the transformer connecting buses 3 to 24. This modified version of the single area IEEE RTS-96 can thus be characterized as follows:

- 24 grid nodes (10 of them from the distribution grid and 14 belonging to the transmission network)
- 2 TSO-DSO connections (composed of 4 transformers 220/30 kV)
- 54 generating units in the distribution and transmission networks, which can be divided into 7 different types of generation technologies - hydro, wind, PV, nuclear, steam coal and oil and a synchronous compensator.

As referred in the methodology description, the development of the transmission network equivalents is only dependent on the availability of historical data. However, and since a test network is being used to evaluate the algorithm performance, this kind of information is not available. This means that a historical of data needs to be built. To fulfil such task, load and generation time series are necessary. The minimum length of the time window should be of one year in order to capture the different operating scenarios (season-dependent) that characterize the transmission network operation. The National Renewable Energy Laboratory provides this input for the IEEE RTS-96 in its GitHub repository [122]. On the top of these time series, 8760 OPFs are run i.e. hourly OPFs for the all year aiming to construct the aforementioned historical data. Once in the possession of the required AC quantities, - $V, \theta, P, Q$ in the TSO-DSO connections, Hydro and Wind active power injection in the transmission grid and total active and reactive power produced in the TSO side – the approach to develop the grid equivalents can be carried out.

The test plan to access the algorithm effectiveness and reliability is composed of three stages:

- Clustering pre-built historical data;
- Computing transmission network equivalents;
- Computing PQ Maps with three different levels of grid knowledge:
    1. Complete knowledge of the network (transmission + distribution)
    2. Partial knowledge (only distribution)
    3. Partial knowledge plus the grid equivalents (distribution + equivalents).

The comparison between the different PQ Maps is a very important step to show how unrealistic PQ Maps estimation can become when disregarding the impact of the transmission network operation. Moreover, these tests also serve to evaluate the accuracy of the grid equivalents.

After carrying the first stage of the test plan while following the steps stated in Figure 24, four different clusters were obtained. This means that four different sets are enough to cluster an entire year of operation. Although the clustering procedure took into account the already mentioned eight AC variables, some of them had a higher impact than others. Figure 27 shows the dispersion of the dataset points by focusing on two of these variables: $V$ in the two existing TSO-DSO interfaces. It is evident that a well-defined range of voltage magnitudes is associated to three of the four clusters. Cluster 2 is the exception to this evidence, which means that other(s) variables among the defined eight had a higher influence on its emergence.

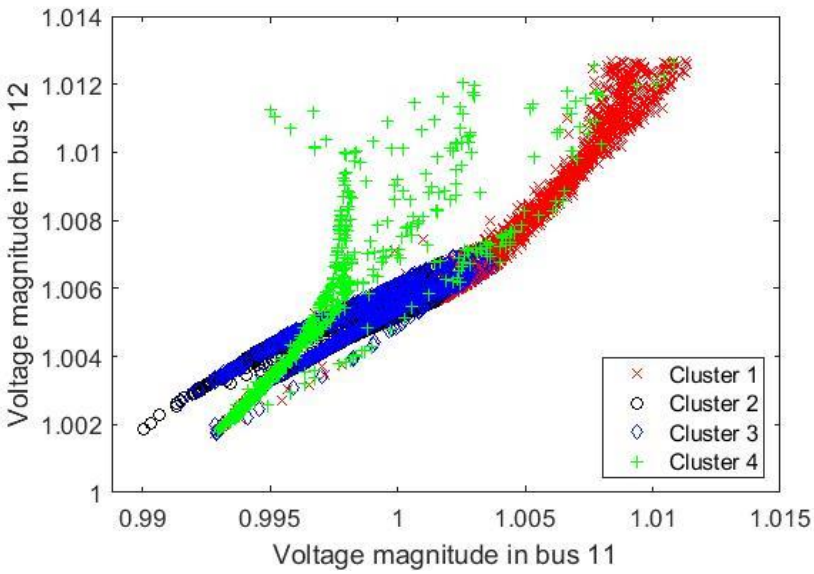


**Figure 27 - Impact of $V_{TSO-DSO}$ in the clustering procedure**

For each one of the obtained clusters is then possible to define the correspondent centroids – Table 5. Their exploitation as representation of four typical operating scenarios of the transmission network is the key to achieve the necessary number of transmission network equivalents.

**Table 5 - Centroids composition**

| V11 (p.u.) | V12 (p.u.) | $\theta 11 - \theta 12$ (Degrees) | P 9-11 (MW) | Q 9-11 (Mvar) | P 10-12 (MW) | Q 10-12 (Mvar) |
|---|---|---|---|---|---|---|
| 0,9979 | 1,0049 | 2,6805 | 203,8809 | 26,2905 | 192,4091 | -44,2483 |
| 1,0051 | 1,0083 | 2,6002 | 290,0649 | 42,1285 | 281,2053 | -29,9945 |
| 0,9978 | 1,0057 | 3,3207 | 304,8866 | 35,0668 | 287,4517 | -35,4316 |
| 0,9987 | 1,0051 | 3,0408 | 217,9157 | 28,0447 | 198,8326 | -43,3914 |

| P Hydro (MW) | P Wind (MW) | P Generation in TSO side (MW) | Q Generation in TSO side (Mvar) |
|---|---|---|---|
| 116,5585 | 59,9882 | 963,4168 | 111,1147 |
| 145,0077 | 55,0283 | 1304,6749 | 270,5550 |
| 144,4088 | 394,2166 | 1366,8750 | 454,7786 |
| 96,2694 | 395,9512 | 990,0313 | 228,9158 |

The four reduced network models were computed in 3m20s using the EPSO algorithm. In every case, the fitness function achieved a zero error, which is understandable since the target data is composed of a single observation – the centroid of each cluster. Table 6 presents the parameters of each transmission grid equivalent. The numeration in the first column refers to the network model shown in Figure 22.

**Table 6 – Parameters of the reduced network models**

| | Cluster 1 | Cluster 2 | Cluster 3 | Cluster 4 |
|---|---|---|---|---|
| Vg 1 (p.u.) | 1,0110 | 1,0008 | 1,0996 | 1,0094 |
| R 1-2 (p.u.) | 0,0018 | 0,0011 | 0,0324 | 0,006 |
| X 1-2 (p.u.) | 0,0021 | 0,0012 | 0,0061 | 0,0176 |
| B 1-2 (p.u.) | 0,2590 | 0,4660 | 0,4998 | 0,4601 |
| R 1-3 (p.u.) | 0,0028 | 0,0010 | 0,0369 | 0,0117 |
| X 1-3 (p.u.) | 0,0184 | 0,0289 | 0,0236 | 0,0448 |
| B 1-3 (p.u.) | 0,2636 | 0,1724 | 0,4579 | 0,2205 |
| R 2-3 (p.u.) | 0,4958 | 0,1896 | 0,2880 | 0,1714 |
| X 2-3 (p.u.) | 0,2177 | 0,0654 | 0,3089 | 0,2096 |
| B 2-3 (p.u.) | 0,0028 | 0,0271 | 0,0451 | 0,0665 |

The two first stages of the test plan are thus completed allowing to move on to the last task. The computation of the PQ maps can now be carried and it will focus on a specific time instant of the historical data - 1st January at 12h. In addition, the flexibility available in the distribution grid will be provided by the two generating units connected to buses 1 and 2. These resources will be willing to change their active and reactive power set-points in both upward and downward directions. The flexibility bands will be defined as $\pm$20% of their current operating point. Figure 28 shows the estimated active and reactive power limits that can be exchanged between transmission and distribution grids (through both TSO-DSO connections)

when considering different knowledge levels i.e. when the transmission grid topology is known and when disregarding that information. In fact, in this second option, a dummy network equivalent is considered. By dummy we mean that no parameter tuning is carried – the impedance and susceptance values of the reduced network model assume very small values and the nominal voltage magnitude is set at the reference bus. The reason for the inclusion of this dummy equivalent is related to how the problem is modelled. If no equivalent was considered, the maximization/minimization of the power flow exchanged between the transmission and distribution networks would be simultaneously performed in the two TSO-DSO connections. As a consequence, direct power flows from one substation to another would arise due to their impact on the network power losses. In other words, the changes on the network power losses would be masked as real flexibility, which would not actually exist. In the opposite direction, when the estimation is carried only maximizing/minimizing the power flow exchanged via the slack bus of the network equivalent, this masked effect disappears and the PQ Map becomes reliable. Nevertheless, the use of this dummy equivalent is similar to not have any knowledge of the transmission network operation. This is why the dummy equivalent is represented by the tag "Only Distribution" when it is used in the forthcoming figures.

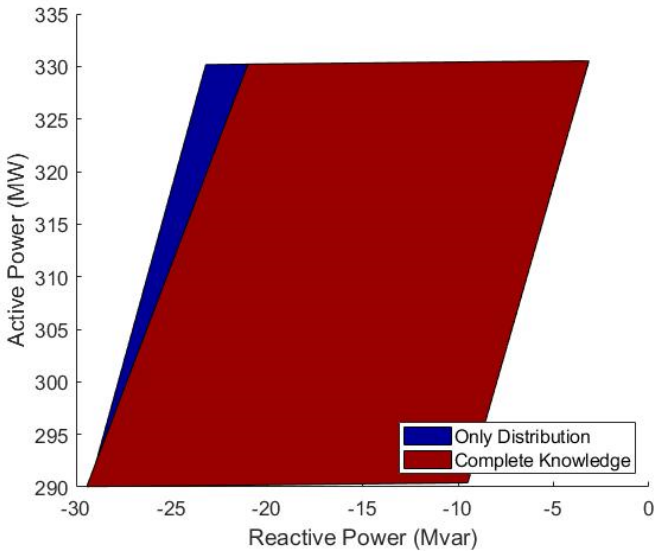


**Figure 28 – PQ limits for all the TSO-DSO connections (Only Distribution)**

The outcome of this test is evident and highlights the fact that no optimization of the reduced model was necessary to achieve a really good estimation of the PQ Map. In fact, the transmission capacity of the HV/MV transformers (also included when only considering the distribution network) proved to be the limiting factor for the power exchanges. Such conclusion may lead the reader to question the value of fine-tuned network equivalents for this application. The following tests should be responsible for clarifying these potential doubts. Figure 29 carries the same comparison as in Figure 28, but focused on the power flow redistribution per TSO-DSO connection. Therefore, these PQ Maps illustrate how the

maximization/minimization of the power flow exchanged between TSO and DSO grids (Figure 28) impact on the power flow of each TSO-DSO interface.

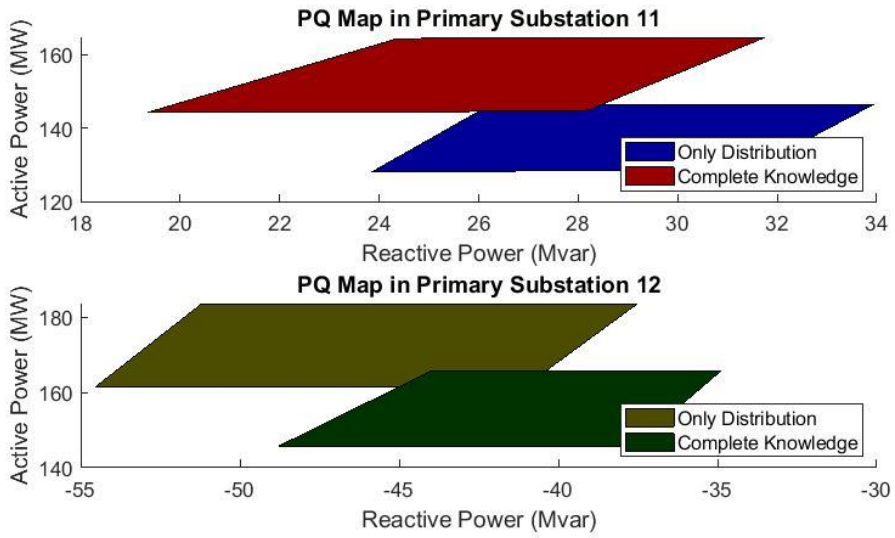


**Figure 29 - PQ limits for each TSO-DSO connection (Only Distribution)**

This test already provides an important clue about the real value of optimized transmission grid equivalents. As depicted in Figure 29, when the transmission network knowledge is disregarded (Only Distribution), an unrealistic estimation of the active and reactive power flows redistribution is performed.

The next step is to add to the previous analysis the PQ Maps when considering the reduced network model computed by the EPSO. Prior to computing these PQ Maps, it is necessary to understand to which cluster the time instant in study belongs. The constructed decision tree should be used to this purpose, as detailed in the methodology description. The fulfilment of this task directly indicates which one of the computed grid equivalents should be used. The result of this analysis was that the 1st January at 12h belongs to cluster Nº4. Figure 30 shows the PQ Maps computed with the defined network equivalent and compares them against the previous approaches. The inclusion of the fine-tuned transmission network equivalent leads to a really good estimation of the power flow redistribution. In fact, the result was almost the same as if the complete knowledge of the transmission network was available. This means that the computed grid equivalent was able to capture the inherent characteristics of the transmission network operation. This way, the PQ Maps methodology is now able to provide more information than only the total PQ power that can flow though the several TSO-DSO connections. It can also deliver important information on how these power flows are redistributed through each one of them.

The set of tests performed not only serve as proof of concept as well as show how valuable the grid equivalents can be in a power systems environment increasingly concerned with confidentiality issues. This innovative methodology empowers both system operators with information of utmost importance concerning the impact that flexibility exploitation has in each one of their physical connections.

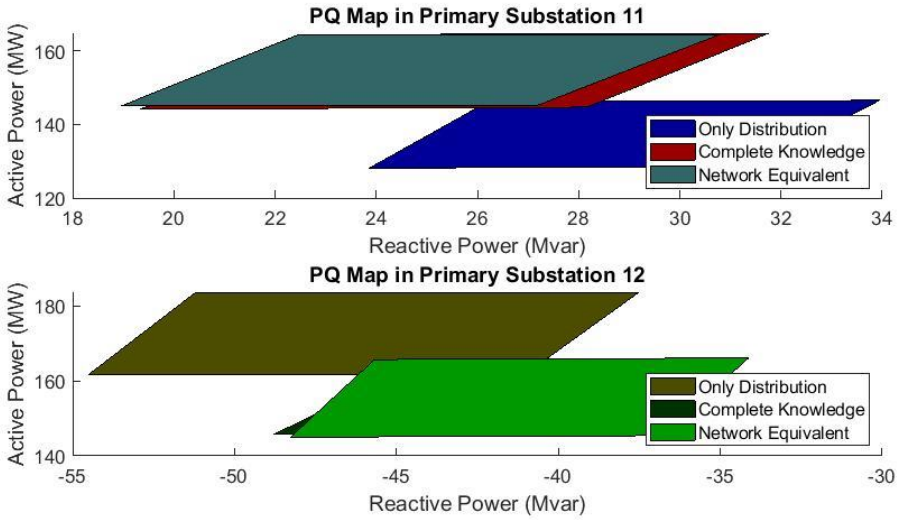


**Figure 30 - PQ limits for each TSO-DSO connection (fine-tuned grid equivalent)**

In order to prove the importance of each step defined in Figure 24, a last test is needed – computing PQ Maps with the network equivalent of other cluster. This test aims to highlight the impact of the clustering procedure in the methodology architecture. Figure 31 compares PQ Maps obtained considering this new network equivalent and the one belonging to cluster N°4 (Real Network Equivalent). A pretty simple conclusion can be extracted from this test: the usage of an inappropriate network equivalent leads to an erroneous estimation of the power flow redistribution. Therefore, the clustering process plays a key role due to its capability to divide into groups the different conditions that the transmission network experience throughout an entire year of operation.

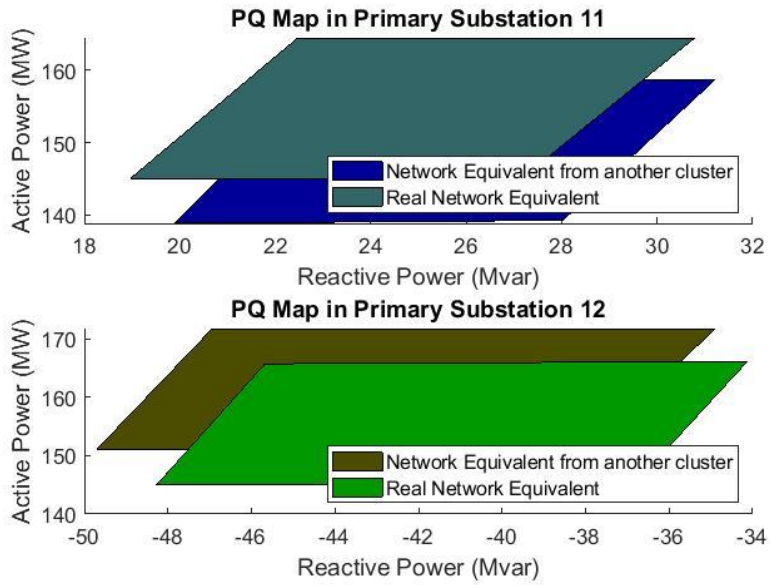


**Figure 31 - PQ limits for each TSO-DSO connection (equivalent of other cluster)**

## 4.4 Contributions to Goal 2

- ***Goal 2:*** to model and integrate a network equivalent for the transmission network to fully tackle the problem of managing the active and reactive power flows in the TSO-DSO boundaries

The fulfilment of *Goal 2* is an important add-on to the practical methodology that this thesis wants to deliver. Contrary to what happens in other research studies where each goal addresses different problems (or the same problem in different perspectives), the goals accessed in this PhD thesis focus on complement each other with the ultimate objective of develop a methodology capable to increase the cooperation between transmission and the distribution network operators. The achievement of such an objective is certainly dependent on the effectiveness and robustness of the proposed methodology, but not exclusively. Aspects such as data confidentiality need to be ensured, particularly when two different parties can benefit from the available information. This becomes even more important when everything that surrounds the topic under study is still under discussion e.g., regulatory frameworks. The proposed methodology is not intended to replace any kind of usual procedure. Instead, it aims to introduce new mechanisms that both TSOs and DSOs are not used to. Therefore, ensuring all the characteristics that can bring comfort to its users is of utmost importance.

*Goal 2* brought the generalization that it is mandatory to have a tool that has the clear goal of supporting the network operator in their daily tasks. As known, it is common the existence of TSO loops among DSO grids. In such cases, the information provided by the algorithm proposed in *Goal 1* would be insufficient. In fact, the network operators would not have the knowledge of the impact that flexibility activation actions would bring to each TSO-DSO connection. Services such as reactive power support and/or reserve management provided by flexible resources would be seen with suspicion due to the lack of knowledge about their impact at the upstream connections. The development of the transmission network equivalents allows to overcome this barrier without disclosing sensitive information. Therefore, the joint result of *Goal 1* and *Goal 2* is a step towards a reinforced cooperation between TSO and DSO and a potential way to improve system security, in a context of increasing penetration of DRES. The flexibility information can thus be graphically provided to the TSO without providing sensitive information such as the flexibility provider or the DSO network data. In addition, the development of the grid equivalents is completely independent from the availability of the transmission network topology.

The enhanced methodology was (and it still is being) accessed under the scope of the EU-SysFlex Project. With the support of two German DSOs (Innogy and Mitnetz), several tests were already carried as reported in the following articles.

- *Test trials carried together with Innogy and Mitnetz (German DSOs):*

    - S. Stock, L. Lower, S. Wende-von Berg, M. Braun, Z. Wang, W. Albers, C. Calpe, M. Staudt, B. Silva, F. Retorta, J. Silva and L. Carvalho, "Operational optimization framework improving DSO/TSO coordination demonstrated in real network operation," presented at the CIRED 2020, Berlin, Germany, 22-23 September, 2020.

    - M. Staudt, M. Pfeiffer, Z. Wang, S. Wende-von Berg, B. Silva, F. Retorta, J. Silva, L. Carvalho, L. Lower, S. Stock, W. Albers and C. Calpe, "Processes and Systems for Using Flexibility from Distribution Grid to Integrate a High Share of RES in a Resilient, Stable and Efficient Operated Energy Supply System," presented at the 18th Wind Integration Workshop 2019, Dublin, Ireland, 16-18 October, 2019.

During 2021, a demonstration phase will run, which aims to highlight the main impact of achieving *Goal 2*: the generalization of the method. In other words, the goal is to show that the aforementioned add-on enables the application of the proposed methodology to any distribution grid i.e. with or without loops through the transmission side.

This thesis focuses on the estimation of the flexibility areas and, for that reason, the network equivalent method was only applied to that purpose. However, this methodology can provide contributes to a much broader scope. In theory, it can support any power system study that demands to know how the upstream grid behaves. This topic, although outside the scope of this PhD thesis, is being studied and will probably lead to further publications.

# Chapter 5

# The impact of discrete variables in the flexibility area

The work presented in the two previous chapters proposed an approach capable to estimate the active and reactive power flexibility ranges at the TSO-DSO interfaces. The usage of such a tool only makes sense in a power systems environment with flexibility at the distribution level. As mentioned in Chapter 1, there are a significant set of providers that can contribute to this whole new paradigm – the so-called flexible DER. Among them, the *modus operandi* can vary between a continuous and a discrete behavior. Demand response services, particularly when settled by an aggregator, can easily provide a sort of continuous range of flexibility. With a similar behavior, DG sources such as cogeneration plants or storage devices are able to control their power output in a continuous pattern. On the other hand, OLTC and capacitor banks are characterized by their discrete operation. This means that their impact in the flexibility provision is ruled by their step length, which is a technical characteristic of these resources.

The method proposed in this thesis deals with both types of resources, regardless of their *modus operandi*. However, when a discrete behavior is followed by a specific resource, the correspondent decision variable in the optimization algorithm has a particular way to be managed - discrete variables are approximated by continuous variables within their corresponding ranges. This approximation of integrality constraints is removed after the fulfilment of the convergence criteria by replacing the continuous value obtained with the closest discrete position. The convergence criteria are re-checked and, if fulfilled, the solution for the optimization problem is obtained. It is not difficult to realize that such approximations, together with the fact that the shape of the flexibility area is defined by the envelope of the vertex points, can lead to over-estimations. The discrete set-points that this type of resources can take are responsible for discontinuities between feasible regions of PQ points. Following the current approach, these discontinuities are included in the flexibility area. Therefore, the proposed methodology based on simple approximations and relaxation of variables may lead to unrealistic estimations. Since this emergence of disjoint areas does not allow to assure that the flexibility domain remains convexly connected, nor to guarantee that it remains connected, a new goal to deal with this problem needs to be formulated.

The inaccuracy brought to the final result when in the presence of discrete variables is much dependent on the step size length of these resources. As an example, OLTC that usually have a low step size may lead to a minor impact on the accuracy of PQ Maps. On the other

hand, capacitor banks can be characterized by considerable step sizes. Other topic that must be discussed when analyzing the importance of considering (or not) the discrete behavior of some flexible resources concerns to their influence in the grid daily operation. It is true that most of the resources available in a power system environment can follow a continuous pattern. It is also true that the traditional capacitive compensators such as static var compensators will be, in short/medium term, replaced by FACTS, which are capable to generate/absorb reactive power within a continuous range of values by controlling the voltage magnitude. However, it cannot be slighted the fact that OLTC and capacitor banks are nowadays one of the main sources used by DSO to control the voltage level in their grids. These resources are usually owned by the DSO and therefore their contribution for the flexibility provision cannot be neglected.

The provision of reliable flexibility areas, even in the presence of discrete variables, is therefore the main topic of this chapter. Two different solutions would be capable of accomplishing such a requirement: an exhaustive procedure, where all the combinations of discrete variables would be inspected or the implementation of a new optimization process aiming to maximize the feasible area found. Obviously, the first option would easily become unpractical. The problem under study has combinatorial characteristics and would take huge dimensions with the growth of the decision variables number. The second solution departs from the idea that the user, when in the presence of the continuous flexibility area i.e. PQ Map obtained via the methods proposed in *Goal 1* and 2 (relaxation of integrality constraints), already knows which region of set-points they want to settle. Based on that first hint given by the user, an optimization procedure would be implemented focused on finding the largest feasible area available in that region. A single solution-based metaheuristic seems to be an appropriate mean to carry this optimization while respecting the traditional non-functional requirements of daily network operation e.g., computational time efficiency. Questions such as *what single solution method would be chosen?* or *why not a population-based metaheuristic?* are addressed in the following sections. *Goal 3* of this dissertation can be formulated as follows:

- ***Goal 3:*** Implementation of a single-solution based metaheuristic to ensure the feasibility of each and every PQ set-point inside the flexibility area.

## *5.1 The arising of disjoint flexibility areas*

The reasons behind the emergence of disjoint flexibility areas were clearly described in the previous section. Nevertheless, there is no better way to ensure the full understanding of the problem in study than a graphical visualization. As mentioned in the test case carried in Chapter 3, the tap changing capability was not considered and the capacitor bank was replaced by a synchronous compensator so that the analysis regarding the discrete variables impact could be done latter. Therefore, the same distribution grid - 210 MV distribution network - was used to

start the analysis. The only exceptions concern to the discrete variables that were included – OLTC with 3 tap positions separated by a step length of 5% and a 1 Mvar capacitor bank with ON/OFF modes.

In order to obtain a clear picture of the effect caused by the introduction of discrete variables, the analysis should be performed in two stages:

1. Running the approach proposed in *Goal 1* ($\theta_{tol}$ =3 degrees) for each one of the six possible discrete variables combinations;

2. Running the approach proposed in *Goal 1* ($\theta_{tol}$ =3 degrees) and approximate the continuous value(s) obtained to the closest discrete position. This illustrates the relaxation of integrality constraints.

Step Nº1 lies on an enumeration process, which should be regarded as a trial that exclusively aims to highlight the problem that this thesis wants to tackle. Moreover, it would be impractical to follow this type of procedure if considering a high number of tap positions and capacitor bank sections. Figure 32 shows the outcome of this step.

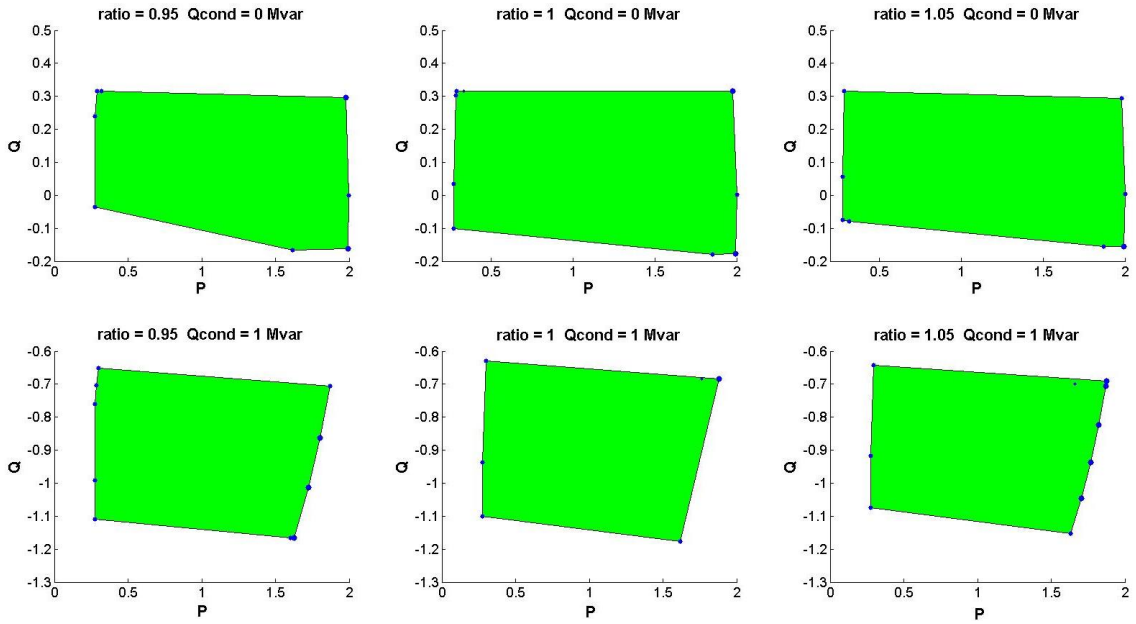


**Figure 32 - Flexibility areas fixing each one of the discrete variable combinations**

The union of the areas presented in Figure 32 compose the feasible flexibility domain at the TSO-DSO interface of the test network. The fulfillment of step Nº2 does not give margin to doubts concerning the potential over-estimations of the flexibility domain when disregarding the true effect of discrete variables.

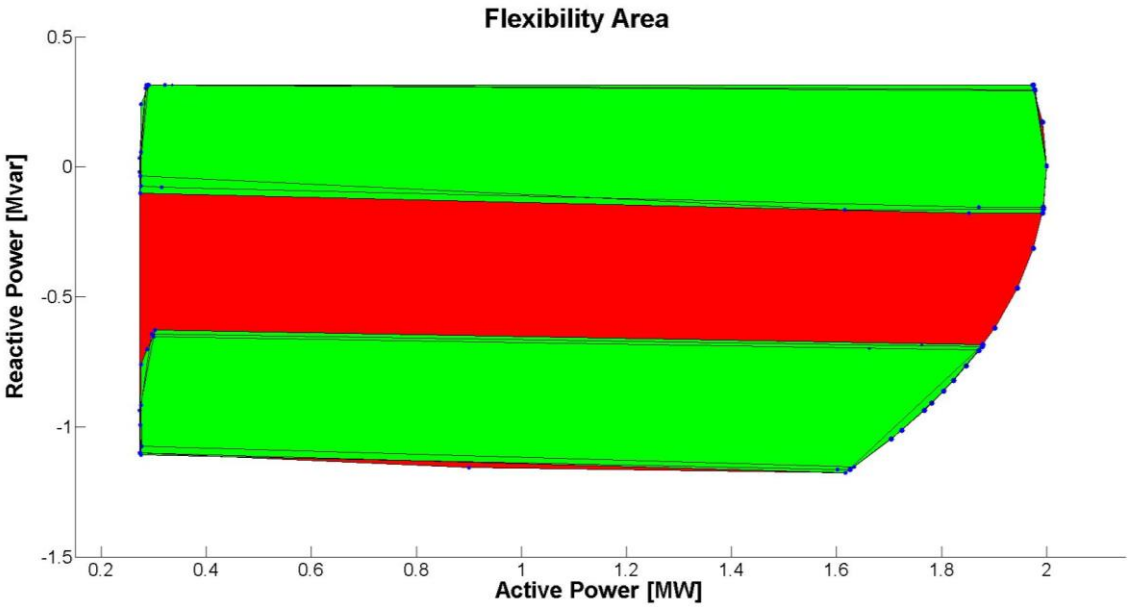


**Figure 33 – Comparison of flexibility areas (step Nº1 – green areas vs step Nº2 – red area)**

Figure 33 is very intuitive – the observable red area refers to an unfeasible region that is provided to the user. This region is associated to capacitor bank sections and/or tap positions that do not belong to the discrete sets of these resources. This way, this is a serious warning against optimistic, but over-estimated flexibility areas.

Conclusions of the test carried in this section can be synthetized as follows: when considering discrete variables, searching only for the vertex points of the flexibility area might lead to a domain larger than the feasible domain. Thus, the definition of the active and reactive power ranges at the TSO-DSO connections by the envelope of the vertex points is completely valid only when considering continuous variables.

## *5.2 Searching for sub-areas of flexibility via a metaheuristic approach*

*Goal 3* mentions the application of a single solution-based metaheuristic to address the problem of finding feasible areas inside the continuous PQ Map provided by *Goal 1* and *2*. One of the first questions that might come to the reader's mind is why not a population-based metaheuristic to tackle this topic. The answer is simple and is related to the computational efficiency of the algorithm. As the name itself highlights, a population-based method relies on the existence of a population of individuals. This means that, at each iteration, all these individuals need to be evaluated via the defined fitness function. Although the description of this function is carried in a forthcoming section, the evaluation object can already be presented – the size of the flexibility area. Therefore, if following a population-based metaheuristic, a flexibility area would need to be computed for each individual. On the one hand, it is true that the employed sparse matrix techniques enable for fast OPF runs. However, it is also true that when the number of OPF increase exponentially (each PQ MAP = several OPFs), the

computational burden can become a problem. This way, the application of a single solution-based metaheuristic arises as an interesting solution to achieve a good trade-off between finding the optimal solution and the computational efficiency. This decision matches with the guiding lines of this PhD work, which were described in the introduction section: finding an actual answer to an innovative topic while never neglecting the minimum requirements of an industrial solution. This means that although a population-based method could probably lead to better results and/or be more effective in avoiding local optima valleys, the required computational effort would prevent the solution deployment at an industrial level.

Among the available single solution-based metaheuristics, the choice fell on the Variable Neighborhood Search (VNS) [125]. As already stated for the Interior Point method in Chapter 3, it is not possible to claim that the VNS is the most suitable method to the topic under analysis. To do so, it would be necessary to carry a benchmarking analysis. Although important, this type of study is not referred to in the thesis objectives and should be considered as a future step. As such, the decision took place after a careful literature review that highlighted some interesting characteristics of the VNS (e.g., parametrization requirements) capable of supporting an effective and feasible path to the final goal: searching for sub-areas of flexibility.

One of the topics that have been more studied in the metaheuristics field throughout the years is the development of approaches to overcome the local optima problem. Local Search [123][124], which is probably the oldest and simplest metaheuristic method is well-known by its convergence characteristics towards local optima when the objective function of the optimization problem is highly multimodal. Therefore, several alternative techniques started arising during the 80s, which can be divided into four different categories:

- *Iterating from different initial solutions* – Approaches characterized by manipulating the initial solution of optimization problems;

- *Accepting non-improving neighbors* - Approaches characterized by accepting uphill movements of the current solution during the search procedure;

- *Changing the neighborhood* - Approaches characterized by changing the structure of the neighborhood during the search procedure;

- *Changing the objective function or the input data of the problem* - Approaches characterized by transform the problem e.g., penalizing the objective function, changing the landscape.

Figure 34 shows how the different techniques to escape from local optima are grouped within these four categories. In order to better understand the choice for the VNS, one method from each category is described in the following sections.

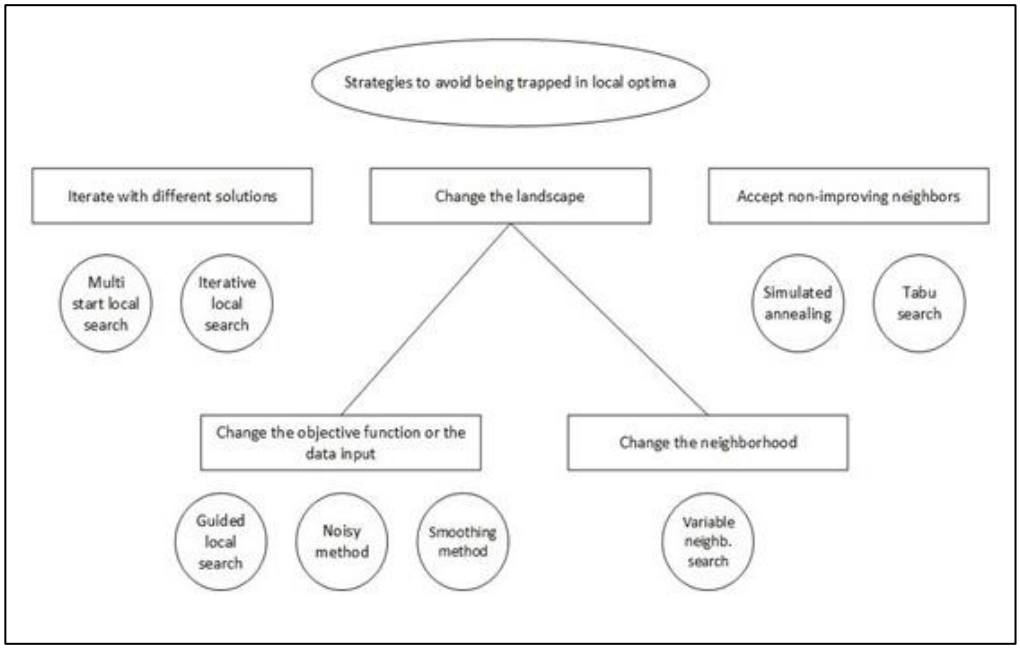


**Figure 34 – Algorithms to escape from local optima**

### 5.2.1 Iterated local search

The origin of the Iterated Local Search (ILS) is closely related to the fact that the quality of the solution obtained by a local search method is highly dependent on the initialization process. The ILS improves the classical multi-start local search by perturbing the current local optima and using this perturbed solution to redirect the search. Therefore, within an ILS implementation, different solutions are iteratively considered since a perturbation is always employed to the current local optima. This perturbation procedure is the key of the method not to become trapped in local optima solutions. The first ILS application is reported in [126], while [127] and [128] have then generalized the approach.

The original ILS framework is divided into four stages: initialization, perturbation, search and acceptance criteria. In the initialization step, a given local search algorithm is applied to the initial solution, which can be randomly defined. This "*a priori* search" intends to provide the ILS with a better initial solution than the one randomly obtained. Afterwards and at each iteration, a perturbation is applied to the local optima – $local\ optima\ at\ iteration\ 0 = initial\ solution$. This step should lead to a large random move of the current solution. However, the definition of the perturbation operator is much dependent on the problem in analysis. Theoretically, the perturbed solution should acquire new characteristics while maintaining some parts of the solution from which it was originated. This stage should thus be responsible for moving the current solution to another basin of attraction. Many biased perturbation

methods can be designed according to the perturbation type: fixed, variable or random. In the first option, the perturbation length is defined *a prior* and is kept constant throughout the search. On the other hand, the application of the variable variant is associated to perturbation lengths that are updated during the process Lastly, the random approach is characterized by a Markovian chain, which means that every move is generated randomly in the neighborhood. Independently from the type, a good balance must be found for the biased perturbation. While a too small perturbation may restrict the exploration of other basins of attraction, a large one may erase the good properties of the current solution. To the perturbed solution computed at each iteration, a search method is then applied. Any single solution metaheuristic would fulfil the purpose of this step e.g., simulated annealing. The acceptance criteria state whether or not a new local optimum is found. It is also responsible to define a ratio between intensification and diversification during the search. In one of the extremes of this ratio, the objective function value is the unique responsible for accepting (or not) a new solution. On the other extreme, any solution is accepted independently from their quality. More conservative approaches are also available in the literature such as the probabilistic acceptance criteria e.g. Boltzmann distribution in the simulated annealing. Figure 35 provides a high-level view of the ILS main steps.

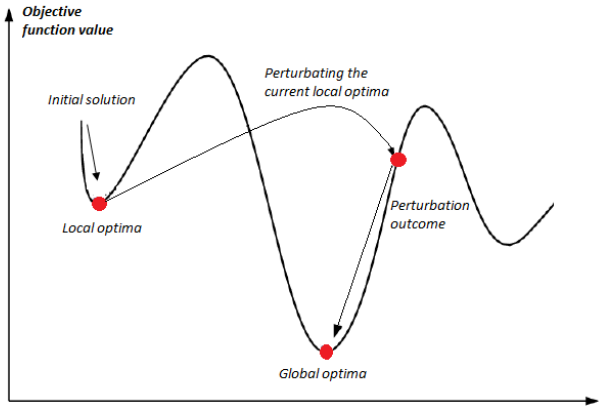


**Figure 35** - Illustration of the ILS principles

The effectiveness of the ILS application to a specific optimization problem is much dependent on the perturbation definition. A deep understanding of what is being studied is usually needed in order to define a proper perturbation method. A blind choice would much probably lead to an infinite loop always getting back to the same local optima.

### 5.2.2 Smoothing methods

The smoothing methods apply modification techniques to the landscape of the optimization problem [129][130] with the goal of escaping from local optima. By smoothing the landscape, the number of local optima is reduced as well as the depth of the basins of attraction. The entire process is carried while the region of the global optimum is maintained. Figure 36

illustrates this idea. For the same search space, the values that the objective function can take are different when compared to the original problem.

Smoothing actions can be applied *n* times depending on the problem in study. Such actions represent no more than the transformation of the original problem into a sequence of sub-problems with different landscapes. These sub-problems are then solved, starting from that with a simpler landscape and finishing with the one with a rougher landscape. The last instance solved is in fact the original problem. Any single-solution metaheuristic can be exploited to solve this sequence of simpler problems. The crucial point of this method is that the solution of smoothed problems is used to guide the search in more rugged landscapes. This means that the initial solution of a more complex problem is the solution to the previously solved problem.

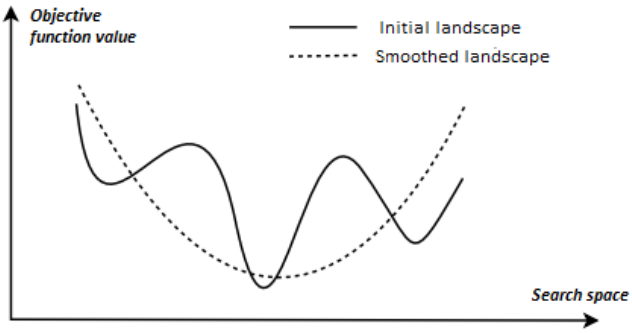


**Figure 36** – Search space smoothing

The smoothing methods thus claim that the probability to find the global optimum of the original problem may increase when considering as initial solution the global optimum of the sub-problems (smoothed landscapes). This happens because the probability to avoid local optima valleys increases. Figure 37 provides a graphical view on how the smoothing techniques affect the landscapes and on how can this procedure support the search for the global optimum.

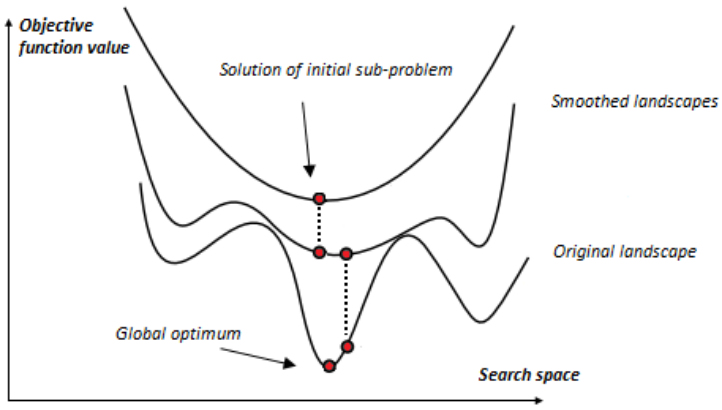


**Figure 37** - Illustration of the smoothing methods principles

The main challenge concerning the application of smoothing techniques is the parametrization of the smoothing factor and its corresponding control strategy. This factor is responsible for defining the strength of the smoothing process. The larger the initial value of

the smoothing factor is, the flatter the landscape becomes. However, the computational effort of the algorithm also increases. Therefore, the parametrization procedure needs to consider this trade-off.

### 5.2.3 Simulate annealing

The application of Simulated Annealing (SA) to optimization problems emerged during the 80's in two innovative works carried by S. Kirkpatrick *et al.* [131] and V. Cerny [132]. Its simplicity and effectiveness in solving combinatorial problems led to a quick and wide spreading phenomenon [133][134][135]. The inspiration behind SA comes from the statistical mechanics, in which the annealing process is based on a slowly cooling schedule so that a strong crystalline structure can be achieved. If during this procedure the rate of cooling metals is not properly defined, an imperfect crystal structure might be obtained. As an example, a very fast cooling schedule has a high probability to lead to situations like this.

SA is a stochastic approach that accepts the degradation of the current solution under some conditions. Therefore, the goal is the same as in the crystallization process – to allow for a slow convergence to the global optimum (perfect crystal structures) by avoiding local optima solutions (crystals with imperfections). After setting an initial solution, SA generates a random neighbor at each iteration. In case this neighbor corresponds to an improvement of the fitness function, it is always accepted as the new current solution. Otherwise, its acceptance is dependent on a probability function, which follows, in general, the Boltzmann distribution:

$$P(\Delta E, T) = e^{-\frac{f(s')-f(s)}{T}} \tag{5.1}$$

where $\Delta E = f(s') - f(s)$ illustrates the objective function difference between the current solution and the generated neighbor and $T$ is a control parameter, named temperature, which intends to control the acceptance level of non-improving neighbors during the search. Thus, the probability of accepting this type of neighbors is inversely proportional to the variation in the fitness function $\Delta E$ and proportional to the temperature $T$. While $\Delta E$ is a direct result of comparing two values of the objective function, $T$ is an unknown parameter that needs to be defined by the user as well as its update procedure. Once again, the analogy with the annealing process is used since a proper formation of crystals begins with an initial high temperature, which is then decreased following a cooling schedule. Therefore, at the beginning of SA procedure, a high temperature is defined to promote diversification movements. This initial temperature is then gradually reduced such that few non-improving solutions are accepted at the end of the process. The SA procedure is also characterized by keeping in memory only the best solution found since the beginning of the search. Any other memory structure to store information gathered throughout the search is employed. Figure 38 provides an overview of how the cooling schedule impacts on the search towards the global optimum.

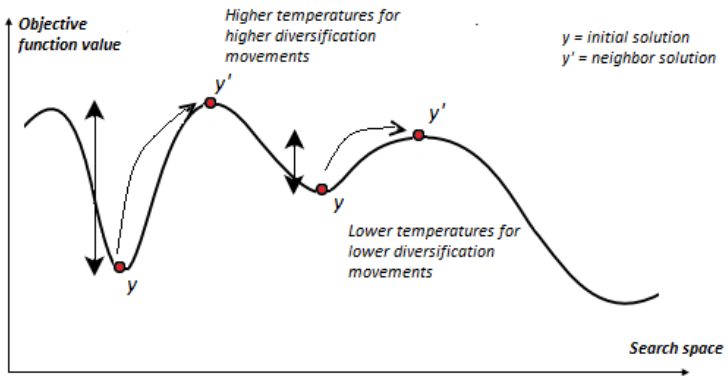


**Figure 38 -** Illustration of the SA principles

The details provided concerning SA implementation point out to a simple heuristic method, which efficiency and effectiveness is closely related to the cooling schedule. The characterization of this schedule can be divided in four different definitions: initial temperature, cooling function, equilibrium state and stopping criteria. Deciding which should be the initial temperature might be a tough task. If a very high value ($T = \infty$) is chosen, all non-improving neighbors are accepted and the SA becomes a random local walk throughout the search space. On the other hand, if a very low value ($T = 0$) is set, only solutions that improve the objective function are accepted thus leading to a first improvement approach (e.g., hill climbing). Different methods to find the equilibrium between these two extreme situations are available in the literature, most of them based on preliminary experiments [136][137]. The initial temperature is then gradually decreased according to a cooling schedule. The rate of this decrease has a great impact on the success of the SA. Once more, a trade-off must be obtained since a very low cooling process leads to better solutions, but with computational times that are not suited with the operational reality. Among the several state-of-the-art schemes to define cooling schedules, three should be highlighted: logarithmic, geometric and non-monotonic. The first one is related to the theoretical study of the asymptotic convergence of SA [138]. Such a cooling schedule is ruled by the following expression:

$$T_i = \frac{T_0}{\log(i)} \tag{5.2}$$

where $i$ illustrates the number of steps that compose the cooling schedule and $T_0$ is the initial temperature. There is a mathematical proof of convergence towards the global optimum when following this schedule. However, it is an asymptotic convergence, which means that the solution would be obtained only after an infinite number of iterations. The geometric schedule is controlled by a parameter $\alpha$ as follows:

$$T_i = \alpha T \tag{5.3}$$

This is one of the most popular approaches to control the temperature during the search. Experience has shown the achievement of very good results for $0.5 < \alpha < 0.99$. In the non-monotonic technique, the temperature can be raised in some stages of the SA, allowing for more diversification movements. Independently of the type chosen for the cooling schedule, this defines the different temperatures that SA implementation faces. However, this does not define when the change between temperature steps should occur. Theory suggests that the equilibrium state at each temperature might be reached after a number of exponential iterations to the problem size. Since in terms of computational time this idea would represent a huge effort, other solutions were studied. One of them relies on a static strategy, in which the number of iterations at each temperature is defined *a priori* and is constant. An example could be a proportion $x$ of the neighborhood size $N_{size}$. Other strategies rely on the characteristics of the search to define when the equilibrium state is achieved. Some of them even employ non-equilibrium conditions e.g. the next temperature step is set if an improving neighbor arises. The stopping criteria is usually associated to the definition of the final temperature $T_f$, which should follow low values $(T_f = 0.01)$. This illustrates that the search should stop when the probability to accept diversification movements is very low. Although this is the common practice with regard to SA stopping criteria, other approaches are available on the literature e.g., stopping the search after a predetermined number of iterations without changes on the best solution found.

SA has a vast application to a wide spectrum of optimization problems. Although it is a simple algorithm to be implemented and, by far, more effective than a simple local search, the required parameterizations may not be an easy task. The definition of the cooling schedule is the key to this method and it can constitute a design issue to be added to the list of common issues present in single solution-based metaheuristics - initial solution and neighborhood definition.

### 5.2.4 Variable neighborhood search

VNS is one of the most recent metaheuristics among the ones presented in Figure 34. It was proposed by P. Hansen and N. Mladenovic [125] and is based on the idea that different neighborhoods lead to different landscapes [139]. Such variation of landscape may generate different local optima solutions thus not allowing the VNS to become stuck in one of them. By exploring several different local optima, the probability of finding the best solution increases – $a\ given\ local\ optimum = global\ optimum$.

Although only one paragraph has been written concerning the VNS, it is already possible to understand that the exploration of successive different neighborhoods only make sense if they are complementary. This means that the local optimum of neighborhood $N_i$ should not be the same as the one from $N_h$. Figure 39 shows in a graphical way the main idea of the VNS.

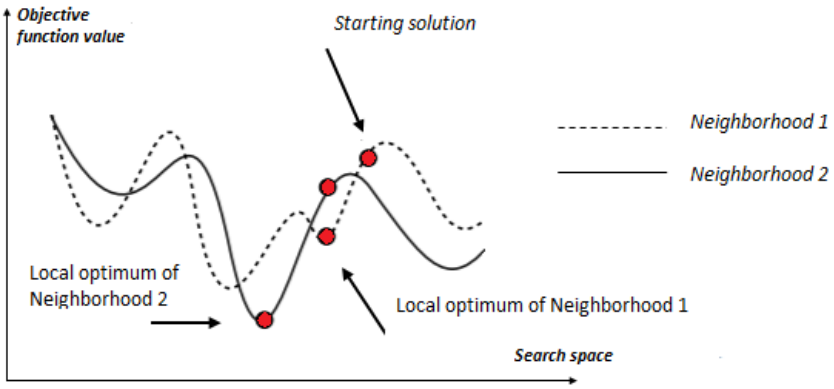


**Figure 39 -** Illustration of the VNS principles

VNS belongs to the family of stochastic algorithms and can be divided into three different phases: shaking, local search and move. Prior to these steps, the different neighborhood structures $N_k$ $(k = 1, \dots, n)$ must be defined. In fact, much of the effectiveness of a VNS implementation lies on this *a priori* step. In addition, the initial solution is generated. It represents the current optimum $x$ at the beginning of the process. After providing these inputs to the algorithm, and at each iteration, a shaking action is carried in the current neighborhood $N_k(x)$. Therefore, a random solution $x'$ is picked from the $k^{th}$ neighborhood of $x$. A simple local search method is then applied to $x'$ to obtain the solution $x''$. This local search procedure can be replaced by more complex approaches such as the Variable Neighborhood Descent, which is a deterministic version of the VNS. The goal of such replacement is to increase the probability of avoid local optima. Nevertheless, the trade-off optimality-computational effort needs to be considered in this decision. In case the solution $x''$ leads to an improvement of the objective function (i.e. $f(x'') < f(x)$), the current optimum $x$ is replaced with this new solution. The search process is then repeated departing from $x''$ in neighborhood $N_1$. The VNS only moves to the next neighborhood $N_{k+1}$ if $x''$ constitutes a worse solution than $x$ (i.e. $f(x'') > f(x)$). The search stops when $N_k = N_n$; however, the entire process can be restarted (from the current solution) depending on the number of generations to be considered.

As well as in other approaches described in this brief state-of-the-art, VNS employs diversification moves to attract the search to potentially better regions of the search space. In the case of the VNS, this is done by exploring different neighborhoods. Since the trade-off intensification-diversification always need to be considered, the choice of the neighborhoods as well as their number are of utmost importance for the success of a VNS implementation. Their proper definition usually demands for a considerable knowledge of the problem in study. Nonetheless, this knowhow is also a necessary condition for the success of other metaheuristics, even if considering a single neighborhood structure. The sensitivity acquired while setting the first neighborhood may provide important guidelines to define the remaining ones. Therefore,

the VNS is a very simple algorithm, whose effectiveness does not depend on complex parametrization schemes. In addition, the results of a VNS run can be very explanatory on how the neighborhood evolution is impacting on the final solution. This visible correlation can contribute to more sophisticated VNS implementations i.e. definition of better neighborhood structures. Establishing this kind of links may not be so straightforward in other metaheuristics e.g., using the solution of a SA implementation to re-define the cooling schedule. The authors of the VNS also carried a comparison between the characteristics of this approach and a list of a desirable properties of a metaheuristic [140]. It was concluded that VNS possesses, to a large extend, the mentioned properties.

All the described metaheuristics while pursuing the same goal have their own pros and cons. Considering this, it cannot be stated that the VNS is the best method to deal with the sub-areas problem. Nevertheless, the characteristics associated to the VNS help to understand why it was the chosen method to tackle it. Among them, the fact that the VNS parametrization only relies on the definition of the neighborhood structures highlights itself. For the problem in study, this definition is concrete and not abstract as it would be the parametrization of a cooling schedule (SA characteristic). Each neighborhood should guide the search to different basins of attraction. As an example, by simply increasing the tap position of OLTC in one step, this objective is fulfilled.

The application of VNS to power systems problems is not as common as in the operational research field [141][142][143]. Notwithstanding, in [144] this metaheuristic is explored to solve a distribution network reconfiguration problem with variable demand and fixed topology. The author claims the achievement of very good results in finding a single optimal topology to operate in the different load levels while trying to reduce the grid power losses. The next section of this dissertation focuses on the application of VNS to the sub-areas problem.

## *5.3 Ensuring the feasibility of the flexibility domain using a VNS*

The search for the sub-areas of flexibility leads to some updates in the original architecture defined in *Goal 1 and 2*. This section focus on this framework changes as well as on the VNS implementation in this specific problem. The following step-by-step description illustrates the path to achieve a feasible flexibility domain:

1. Following the approach proposed in *Goal 1*, a continuous PQ map is provided to the user. The word “continuous” intends to state that the PQ map is the outcome of several optimization procedures in which the discrete variables are optimized within their corresponding operating ranges;

2. Depending on the user's final objective (e.g., reactive power support actions), they might be interested in checking the feasibility of a specific region inside this continuous PQ map. Based on it, the user defines a PQ point in that region. The feasibility of the chosen PQ point is then checked by running a classical OPF algorithm with two additional constraints - $P_{TSO-DSO} = P_{user}$ and $Q_{TSO-DSO} = Q_{user}$. The result of such analysis leads to one of the following conclusions:

    a. The OPF does not converge, which means that there is no combination of discrete variables capable to lead to that PQ point at the TSO-DSO interface. Moreover, the chosen PQ point is not encompassed by any sub-area of flexibility;

    b. The OPF converges, which tells to the user that there is, at least, one combination of discrete variables capable of leading to that PQ point at the TSO-DSO interface. However, and since this thesis claims the development of a decision support approach, the user expects to get a feasible domain, which will then help him to take the final decision according his goals. The combination of discrete variables obtained in the OPF run would already lead to a feasible domain, but probably not to the largest one that encompasses the chosen PQ point;

3. The VNS uses as initial solution the combination of discrete variables obtained in the OPF run and starts the search for the largest sub-flexibility area in that region.

This new architecture is user-guided in the sense that the method knows which region of the continuous PQ map needs to be explored. A different option, not dependent on an input from the user, could be followed: search for the largest sub-area of flexibility in the whole continuous PQ map. Such an approach would lead to the largest feasible domain available. Notwithstanding, that area could be located on a region without significant value to the user. This could arise for example due to $\tan\varphi$ limits. Therefore, this new framework seems to be the best choice to avoid an enumerative and non-oriented procedure. Step nº3 deserves a more detailed explanation since it illustrates the main part of *Goal 3*. The following description intends to guide the reader throughout the different stages of the VNS implementation:

1. **Initialization -** Independently from the employed metaheuristic, an initial solution $x$ to the problem needs to be computed. The state-of-the-art documents two main strategies to the initialization step: random approaches and greedy algorithms. While the former represent a quick process, the latter often lead to better solutions

to start the search. However, using these better solutions as the initial ones does not necessarily mean that a better local optimum is obtained in the end of the process. The way how the initial solution should be designed is much dependent on the metaheuristic properties. As an example, the larger the neighborhood, the lower is the impact of the initial solution to the search performance. To overcome this dependency, the literature also presents hybrid approaches. For instance, considering a pool of initial solutions where some of them are the result of greedy algorithms and others were randomly generated. Indeed, all the presented methods have their own advantages and disadvantages. Nevertheless, there is one characteristic of the greedy algorithms that should be highlighted. In some constrained problems where there are no feasibility insights, these algorithms ensure a feasible initial solution. They start from an empty solution and construct it step-by-step (i.e. assigning values to one decision variable at a time) while locally minimizing the objective function. Although the aforementioned options can be applied to the problem in study, none of them was followed in this thesis since a feasible solution is already known at this stage. As previously mentioned, the OPF execution that checks the feasibility of the PQ point defined by the user already provides a viable combination of discrete variables. Therefore, running an instance of the method proposed in *Goal 1* using such combination leads to a feasible domain encompassing that PQ point. Such solution thus constitutes the best one in the beginning of the search process. Moreover, the dimension of the sub-area of flexibility defines the initial value of the objective function.

2. **Neighborhood structures definition** – This is the unique step that demands for parametrization actions. The definition of these structures provides the basis to construct the shaking neighborhoods. In this thesis, the two defined structures employee changes of one and two positions (upward and downward) on the discrete variables of the current best solution $x$. Therefore, each shaking neighborhood $N_k$ $(k = 1, \dots, n)$ is composed of $2 * N_{Discrete} = 2 * (N_{OLTC} + N_{shunt})$ neighbors – Figure 40. When comparing each neighbor with the current best solution, differences arise only in one of the discrete variables since the aforementioned changes are independent from each other's. Although this structure definition led to interesting results, other architectures may achieve similar outcomes (or even better). Nonetheless, the trade-off between optimality and computational effort should always be considered in this decision.

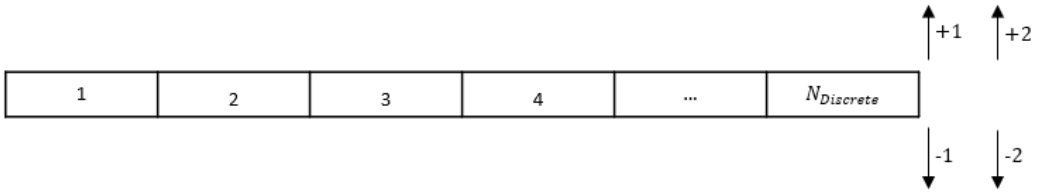


**Figure 40** - Changes applied on the discrete variables to create shaking neighborhoods

3. **Shaking phase** - In this stage, a random solution $x'$ is picked from the current $k^{th}$ neighborhood $N_k(x)$ of $x$. To do so, a pseudo-random integral number between $1$ and $2 * N_{Discrete}$ is generated - Figure 41.

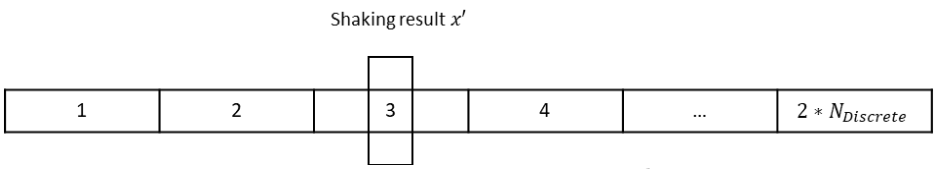


**Figure 41** - Random solution extracted from the $\boldsymbol{k^{th}}$ neighborhood $\boldsymbol{N_k(x)}$

4. **Local Search** - A local search is then applied to $x'$ in order to find the solution $x''$. The employment of a local search procedure is dependent on the definition of neighborhood structures, which is usually independent from the shaking neighborhoods $N_k$ defined in step nº2. These new neighborhoods can be constructed following a single-level or a multi-level approach. The Variable Neighborhood Descent (VND) is an example of this last category. When the VND is used in this step, the VNS becomes a Variable Neighborhood Decomposition Search (VNDS) [145]. In this PhD thesis, the neighborhood (single-level) is iteratively built and not the result of an *a priori* definition. At each iteration, one of the decision variables that compose $x'$ is perturbed leading to a new neighbor $x'''$. If $f(x''') > f(x')$, the following perturbation is applied on the top of $x'''$ and this process continues until all the decision variables are perturbed. The existence of a memory vector ensures that each decision variable is perturbed only one time. Therefore, the number of decision variables is what defines the size of these neighborhoods. Solution $x''$ is the best improving neighbor found throughout this local search procedure. Other criterions such as the first improvement, in which the search ends right after a better solution is found, could also be applied. The option here followed was not this one since the neighborhood usually has a size that does not take huge dimensions (OLTC and Capacitor banks are most of times only associated to the HV/MV substations). The way the decision variables are perturbed is also a topic that demands for an explanation. This process is mainly composed of two sub-steps and is illustrated in Figure 42:

a. Creation of a pseudo-random integral number between 1 and $N_{Discrete}$ to define which decision variable is going to be perturbed

b. The decision concerning increasing or decreasing (in one step size) this variable is dependent on the application of a uniform distribution

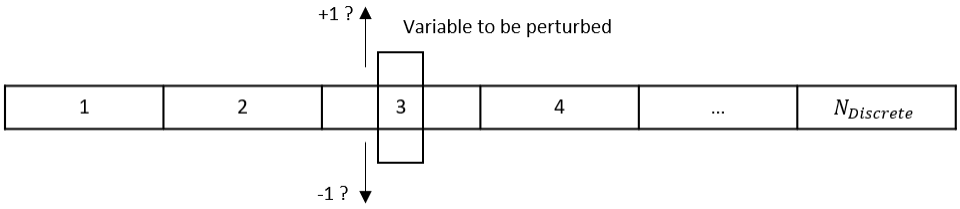


**Figure 42** - Perturbation process during the local search

5. **Fitness function** $f(x)$ - In each iteration of step nº4, two solutions need to be evaluated: the current best solution within the local search $(x')$ and the perturbed solution $(x''')$. Consequently, PQ Maps following the combination of discrete variables defined by $x'$ and $x'''$ are computed. This means that two instances of the method proposed in *Goal 1* take place, but with the discrete variables fixed to the values that characterize $x'$ and $x'''$. $f(x)$ are then responsible for computing the area of these PQ Maps as described in (5.3). The goal is to find the largest sub-flexibility area that encompasses a specific PQ point i.e. the PQ Map with higher $f(x)$.

$$f(x) = \frac{1}{2}\left|\sum_{i=1}^{n-1} P_i * Q_{i+1} + P_n * Q_1 - \sum_{i=1}^{n-1} P_{i+1} * Q_i - P_1 * Q_n\right| - C \qquad (5.3)$$

Expression (5.3) illustrates the Shoelace formula [146], which allows to compute the area of a polygon as long as the coordinates are ordered e.g. clockwise. In the PQ Maps case, these coordinates correspond to the *P* and *Q* values that characterize the extreme points of the flexibility areas. The parameter $C$ is a penalization factor that assumes a very high value in two situations: if the computed PQ Map does not encompass the chosen PQ point or if the combination of discrete variables of $x'/x'''$ leads to an unfeasible solution. An automatic process to check if a PQ point is within a PQ Map was developed. In any other case, $C = 0$. Each local search procedure leads to $N_{Discrete} + 1$ evaluations of the fitness function. $N_{Discrete}$ corresponds to the number of accessed neighbors while the remaining one corresponds to $x'$. However, this is the maximum number since a vector is kept in memory to avoid unnecessary computations of PQ Maps. Therefore, if a combination of discrete variables was already tested, the memory vector directly defines the corresponding area. In the end of the entire process, $x''$ is obtained.

6. **Acceptance criteria -** A strong selection criteria is then applied. If $f(x'') > f(x)$, a new solution is selected as the current best one ($x = x''$). Therefore, a new local optimum is defined only if there is a flexibility area with a larger dimension than the one originated by $x$. The evaluation of the fitness function of $x$ can be performed in any of the mentioned steps. The result of the comparison between $f(x'')$ and $f(x)$ is also decisive to define which shaking neighborhood $N_k$ should be explored in the next iteration of the VNS. If a better solution is found, the search should get back to $N_1$. Otherwise, a diversification strategy should be applied, thus moving the search towards $N_{k+1}$. The entire process is repeated until $k = k_{max}$ and for a specific number of generations defined by the user.

The framework of the implementation of a VNS approach to the sub-areas problem was detailed. By applying a simple and effective metaheuristic that relies on systematic neighborhood exchanges together with local search techniques, it is expected to highly contribute to a more accurate information exchange procedure between TSO and DSO. In which concerns the local search approach followed in this VNS implementation, a more detailed explanation should be given to support such a choice. As mentioned in step nº4 of the architecture, the composition of each neighbor is dependent on previous comparisons between other neighbors and the current best solution within the local search. If a specific perturbation contributes to a better fitness function, it is kept throughout the local search. This procedure intends to intensify the search in a specific direction of the neighborhood. Therefore, an intensification characteristic is brought to a method – VNS - that relies on diversification techniques to avoid the local optima problem. Although the results shown in the following section support the use of the defined architecture, other variants could be applied, probably also leading to interesting levels of effectiveness e.g. VND during the local search phase.

### 5.3.1 Results for the IEEE-RTS 96 (single-area variant)

The effectiveness of the approach hereby described was accessed using a similar test grid and following the same assumptions as in Chapter 4 – the IEEE RTS. Changes on the transformer's characteristics and the addition of capacitor banks were the only adaptions. Such modifications intended to challenge and test the limits of the proposed algorithm. More particularly, the existing four transformers acquired TAP change capability (21 positions each separated by a step of 1%). Also, one ON/OFF 75 Mvar capacitor bank was connected to the MV side of the TSO-DSO interconnections. Thus, if only focusing on the existing discrete variables, the updated grid is characterized by a huge number of different status. This number corresponds to the combinations between the OLTC's and capacitor bank set-points. Unlike the illustrative example provided in the beginning of this Chapter (Figure 33), the number of combinations is

now much higher. Therefore, this test-case is at the same time impractical for an enumerative search and challenging for the proposed goal. Its definition was based on typical characteristics of distribution grids: OLTC's and capacitor banks are commonly available at the primary substations in order to control the voltage levels in the entire distribution network and provide reactive power support actions.

Considering the context of the topic discussed in this Chapter, the focus on the transmission grid side is no long necessary. This way, the following tests were carried only on the top of the distribution grid observable in Figure 26. Moreover, all the analysis, figures and conclusions presented in this Chapter focus on the total PQ Map i.e. flexibility limits considering both interconnections and not divide per TSO-DSO interface as in the previous Chapter.

The estimation of the continuous PQ map for the updated IEEE RTS was the first step to be carried out since all the remaining analysis depends on it. To do so, the methodology described in *Goal 1* was used and the result is presented in Figure 43. In addition to the OLTC's and capacitor bank, flexibility is being provided by the two generating units connected to buses 1 and 2. The degrees of flexibility are the same as in the test-case conducted in Chapter 4 i.e. $Flexibility\ bands = \pm 20\% * Current\ set - point$.

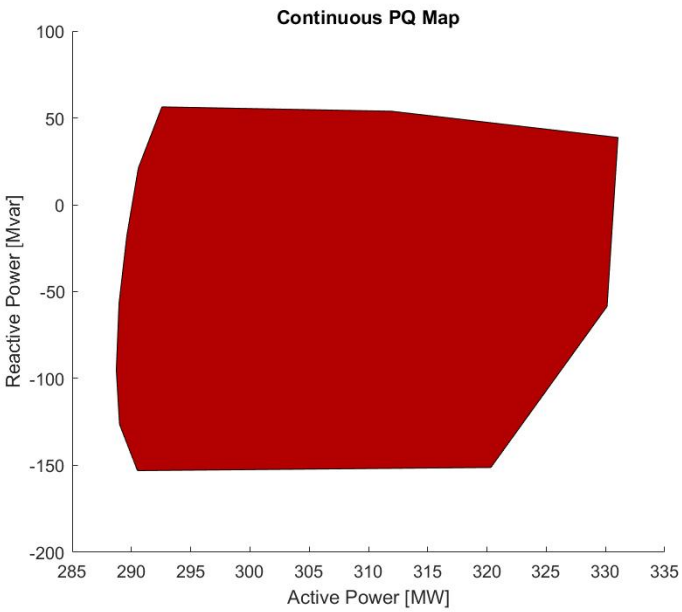


**Figure 43** – Continuous PQ Map for the updated IEEE RTS

The flexibility area shown in Figure 43 lacks of accuracy due to the presence of resources that follow a discrete operation pattern. Nevertheless, it is an interesting starting point for a more reliable analysis. Since the user is already informed about the flexibility limits, which are well defined by the continuous PQ Map, he is in conditions – with the support of a proper methodology - to investigate the potential existence of unfeasible regions. The triggering event is the choice of a $PQ_{TSO-DSO}$ point inside the flexibility area of Figure 43. The algorithm will not only tell if that point is feasible but also will provide the maximum feasible area that encompasses it.

In the real-world environment, the $PQ_{TSO-DSO}$ usually needs to be kept within some limits, which are defined in the national regulatory frameworks of each country. In Portugal, the DSO must maintain the reactive energy within a specific range imposed by the TSO, otherwise a penalty for violating the limits is applied ($-0.3 \leq \tan\varphi \leq 0.3$). In order to comply with the Portuguese regulatory framework, this test-case considers $P_{TSO-DSO} = 320\ MW$ and $Q_{TSO-DSO} = 20\ Mvar$.

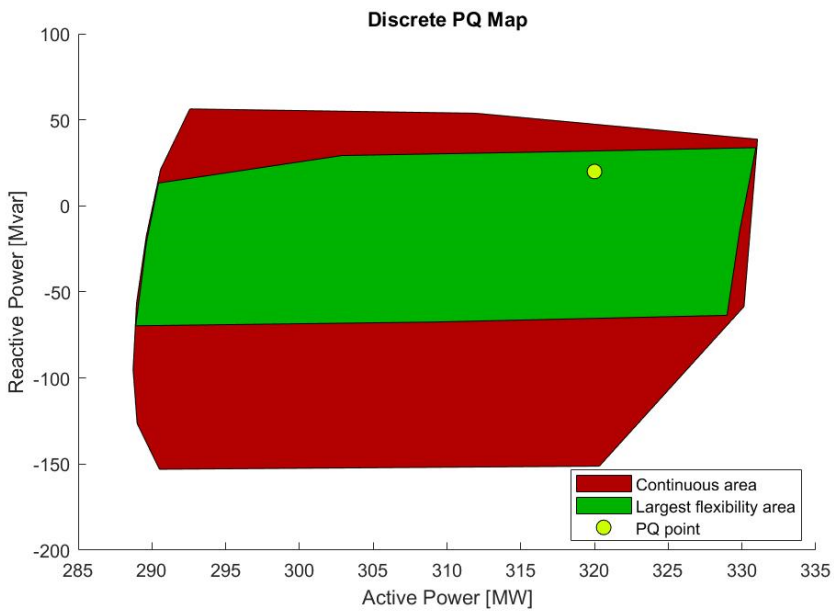


**Figure 44 -** Largest sub-flexibility area encompassing $\boldsymbol{PQ_{TSO-DSO}}$

Figure 44 shows a first result of the VNS application. With this novel input, the network operator knows that any PQ point inside the green area can be set in the TSO-DSO interconnections. Unlike the flexibility area of Figure 43, this PQ Map provides the largest feasible flexibility margins that surround $PQ_{TSO-DSO}$. In addition, the network operator becomes aware of the combination of set-points that should be followed to achieve these flexibility margins. This type of information has a high value since DSOs are usually the owners of resources such as OLTCs and capacitor banks. In this specific test-case, the combination of set-points is shown in Table 7.

**Table 7 -** Combination of discrete variables for the largest sub-flexibility area

| | **Final set-point** |
|---|---|
| OLTC 1 ratio | 1.02 |
| OLTC 2 ratio | 0.97 |
| OLTC 3 ratio | 0.99 |
| OLTC 4 ratio | 0.98 |
| CB 1 (Mvar) | 0 |

Although the aforementioned results correspond to the final outcome of the VNS, they do not validate the effectiveness of the algorithm. The analysis of the characteristics associated to how the search evolved may give an important contribution to this topic. Figure 45 shows the fitness function value in each iteration.

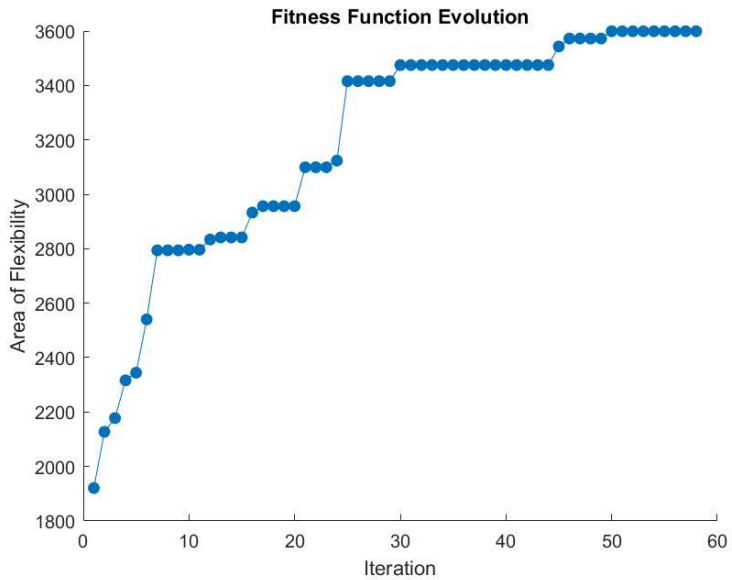


**Figure 45 –** Fitness function evolution during the search

It becomes clear that the implemented procedure guided the search towards the maximization of the feasible flexibility area. Although not possible to ensure that such area corresponds to the maximum – there is no methodology that ensures it – this method allowed an increase of 87,4% in the area magnitude when comparing with the first computed area. The whole process took 42 seconds to be completed. This was exactly the intention of the metaheuristic inclusion – to find a non-exhaustive method capable of maximizing the feasible flexibility area within a computational time aligned with the operational requirements.

The conclusions extracted in this Chapter support the idea that the two main goals were successfully achieved: feasibility and maximization. If the aim was only to provide a feasible area encompassing the chosen $PQ_{TSO-DSO}$, the method could be much less refined. In fact, it would be enough to follow three simple steps: running a classical OPF algorithm to find a combination of discrete variables capable to fulfill the pre-defined $PQ_{TSO-DSO}$, fixing it and running the method proposed in *Goal 1* on the top of it. This idea would provide one of the N areas that encompass $PQ_{TSO-DSO}$, but not the largest one. Figure 46 provides a graphical view that allows to compare the flexibility area associated to this simple process and the area achieved using the proposed approach. The reliability of the information provided to the network operator is the same, but not its content. Having in his possession the information provided by the green area, the operator is empowered with $PQ_{TSO-DSO}$ margins that give them a higher flexibility to define potential control-actions.

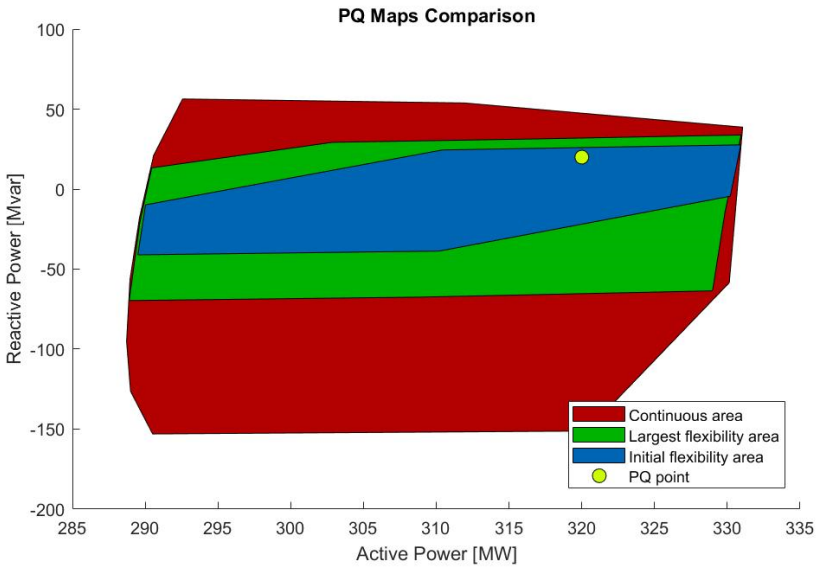


**Figure 46** – Impact of maximizing the feasible flexibility area

The test-case presented in this Chapter could have taken a different direction thus leading to additional conclusions. With a different $PQ_{TSO-DSO}$, the result could be infeasible. In fact, the discrete variables that characterize the test grid lead to discontinuities in the continuous PQ Map. In the impossibility of graphically show all the PQ Maps computed during the metaheuristic in a clear way, Figure 47 presents the regions where these areas arose.

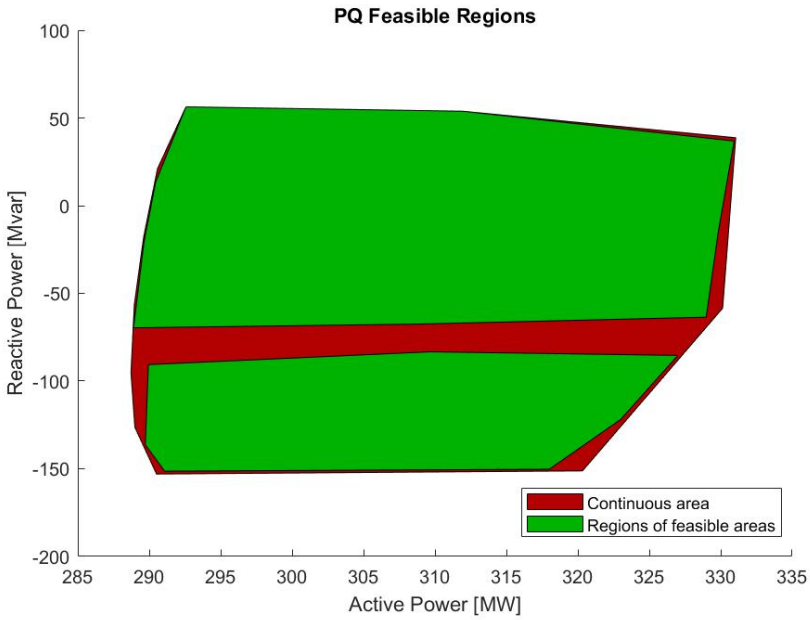


**Figure 47 -** Feasible regions within the continuous flexibility area

The areas shown in Figure 47 only intend to provide a graphical idea where the feasible PQ Maps are located since they do not correspond to real flexibility areas. With this result, the analysis that was carried can be closed. Contrary to what was discussed in the beginning of this Chapter, there is currently a mechanism capable of avoiding the problems brought by the discrete controls.

## 5.4 Contributions to Goal 3

- ***Goal 3:*** Implementation of a single-solution based metaheuristic to ensure the feasibility of each and every PQ set-point inside the flexibility area

If *Goal 3* had a slogan, it would be something such as "Tomorrow is too late to start cooperation". Although this is a PhD work and not a slogan contest, this shows to the reader the exact idea behind the achievement of *Goal 3*. The timespan between a research study and its deployment at an industrial level is usually considerable, particularly when the topics under discussion do not belong to the BaU. This is the case of end-users participating on grid management tasks by providing flexibility. Although under an intensive discussion, it is not possible to state that a complete roll out of this model has already taken place. Therefore, it is crucial that the contributions provided by this work also include some of the mechanisms network operators use nowadays to manage their grids. If it is true that the energy transition process is introducing new ways of providing voltage control support, it also cannot be neglected that OLTCs and capacitor banks are still one of the main sources to achieve such purposes. However, the inclusion of this type of resources in the optimization procedures was a challenging task, as reported in the following article.

- *Analyzing the challenges posed by the flexibility area estimation:*

    - J. Silva, J. Sumaili, R.J. Bessa, L. Seca, M.A. Matos and V. Miranda, "The challenges of estimating the impact of distributed energy resources flexibility on the TSO/DSO boundary node operating points," *Computers & Operations Research, vol. 96*, pp. 294-304, Aug., 2018.

The emergence of disjoint flexibility areas is a non-static problem i.e. varies accordingly with the current network conditions. This justifies even more the need of providing reliable information to the network operator at each time instant. Thus, a novel algorithm was presented aiming to mitigate the impact caused by the discrete nature of OLTCs and capacitor banks on the flexibility area's feasibility. The results highlight that *Goal 3* was accomplished. Both the TSO and the DSO have now a powerful mechanism in hands that will support in managing a future flexible power system, but which can also have an immediate impact. By exploiting the availability of BaU assets, a strong and direct contribution towards a highly cooperative environment is provided.

# Chapter 6

# Conclusions

This chapter intends to summarize the research work that has been carried out during this PhD thesis. Moreover, additional research lines that aim to bring new features to this topic of the TSO-DSO coordination are outlined.

## *6.1 Meeting the goals*

The PhD thesis hereby presented was built up on the top of a real problematic. By the time this dissertation started, the research work on this topic was scarce, but now there has been an increasing interest on it. Therefore, it is possible to state that the "TSO-DSO cooperation" is nowadays a hot topic.

The growth of RES penetration across distribution grids together with their uncertain injection pattern has been contributing to an increase of technical problems in both transmission and distribution systems. However, the benefits behind this RES growth are incomparably greater than the problems brought by it. First, because the solution to the aforementioned technical problems can lie on the exact some source that creates them. RES and other types of DER can answer external signals and thus modify their injection and/or consumption typical profiles. This is what in the literature is called Flexibility. In addition, this flexible environment brings a vast set of other system services that can be provided to both TSO and DSO e.g., reactive power support provided by the DSO to the TSO. Although the potential of this exploitation is clear, it is also obvious the need of a high level of coordination between system operators. Otherwise, it would be difficult to predict the impact that some action in the distribution side would have for the transmission grid. To achieve this cooperation, the first step is to overcome the lack of power flow coordination at the system operator's interface. This idea was, therefore, the first focus of this dissertation and consequently led to *Goal 1*:

- ***Goal 1:*** Formulation of an optimization problem that, iteratively, changes its own objective function in such an intelligent way that allows to estimate the entire flexibility area perimeter.

The estimation of the decision margins for changing the operating point at the TSO-DSO interface is of the utmost importance regarding added system security and lower operational

costs. This dissertation provided a novel and innovative contribute in this field by proposing a decision-aid method capable to effectively answer to the flexibility recognition problem. By reaching the definition of the flexibility area hull - even when non-convex – a clear add-on to the current state-of-the-art was provided. The bidirectional exchange of information that this methodology promotes can lead to a safer and sustainable growth of the RES hosting capacity in the distribution grids.

The proposed methodology was compared against the first approach available on the literature that tried to address this specific problem. The results were clear: the employment of a random sampling method to tackle this topic leads to an under-estimation of the flexibility area. Moreover, it requires a considerably higher computational effort to reach flexibility margins with lower levels of accuracy.

The development of this thesis had an interesting characteristic: the way how it was built was based on analyzing the on-going work, try to capture its weaknesses and find solutions to them. In other words, the lessons learned during the research work were the source of the remaining goals. The main objective was always to address a challenging topic in terms of scientific and theoretical background while trying to provide a practical and operation tool to the industry. One of the major drawbacks of the method described in *Goal 1* was its application to meshed distribution grids with loops between primary substations in the transmission side. The approach considered an assumption that although simple was not completely realistic: the estimation of the flexibility area in a TSO-DSO interface is possible if the PQ operating points in the remaining interconnections are known. Since this assumption may be unrealistic, *Goal 2* tackled it:

- ***Goal 2:*** to model and integrate a network equivalent for the transmission network to fully tackle the problem of managing the active and reactive power flows in the TSO-DSO boundaries.

The reason why the method proposed in *Goal 1* could lead to an inaccurate estimation of the flexibility ranges in more than one interconnection is clear: in meshed grids the redistribution of the active and reactive power flows per each TSO-DSO interface is dependent on the operation in the transmission side. In the absence of a complete knowledge of the transmission grid topology, which is usually confidential, the consideration of a grid equivalent model was therefore mandatory. As reported in this thesis, several options were available to fulfill this requirement. After analyzing them, it became clear that a contribution to the state-of-the art could also be provided in this matter. Considering the fact that the information of the grid topology is very sensitive, a data-driven approach that only relies in historic variables was proposed. The effectiveness of the method when applied to the flexibility areas was well-documented in Chapter 4, but it is expected that its application can be implemented in a variety of other problems e.g., contingency analysis.

The idea of achieving a highly accurate method always guided the course of this PhD thesis, as easily observable throughout the storyline. *Goal 3* continued that path by trying to study the impact that resources with a discrete behavior could have for that accuracy.

- ***Goal 3:*** Implementation of a single-solution based metaheuristic to ensure the feasibility of each and every PQ set-point inside the flexibility area.

It became proved that the exploration of the vertex points of the flexibility area would lead to over-estimations when in the presence of resources such as OLTCs or capacitor banks. This type of resources is usually owned by the DSOs and, therefore, their contribution should not be neglected. The fulfillment of *Goal 3* allowed to overcame this drawback by enabling a search for the larger feasible flexibility area that encompasses a specific PQ set-point. Although it cannot be considered an add-on to the literature as the previous goals – since is the application of an existing method to the flexibility area recognition problem – it is certainly an important contribution to a more complete, robust and operational tool for the future of the control rooms.

This PhD thesis will likely provide very helpful contributes for both TSO and DSO e.g., definition of interchange conditions that are actually feasible and can be fulfilled through DER flexibility activations, avoid the exceed of regulated operational limits in the TSO-DSO interconnections.

## *6.2 Thesis main impacts*

Thesis and any research work in general usually provide multiple types of contributions, which can differ in their impact. They can range from theoretical approaches on how to address a specific problem to more practical solutions that aim to achieve higher Technology Readiness Levels. Between these two extremes, there are several steps that need to be fulfilled, which can also have their own impacts e.g., improving an existing methodology in terms of its computational effort so that it can be used in an operational environment. The PhD thesis hereby presented made all the path between the two extremes and this is possibly one of the most important conclusions to be extracted.

From a theoretical point view, this dissertation addressed an innovative topic with a limited background available in the literature and proposed groundbreaking solutions to tackle it. As a result, a total of 9 articles were published (two of them in peer reviewed journals). Moreover, Chapter 4 and 5 still have interesting material to feed two additional journal publications, which are currently being prepared. The number of citations of the published articles already achieved the significant number of 90, which is a very good metric to evaluate the impact of this study to the state-of-the-art. The theoretical scope of this PhD thesis was also on the basis

of several European projects, some of them still on-going – the FP7 evolvDSO [11], the H2020 EU-SysFlex [147] and the H2020 TDX-ASSIST [148]. As such, all the methods described in this dissertation were also accessed by external stakeholders. This allowed not only to re-validate the concepts as well as to perform real-world implementations. The pre-requisites of this type of demonstrations are of utmost importance when there is the objective of achieving a practical tool ready to be deployed. Although important, the algorithm itself is not enough if several non-functional requirements are not fulfilled e.g., integration with TSO/DSO systems, maximum computational effort needed. Thanks to the aforementioned projects, four demonstration trials involving three different DSOs were ran thus allowing to build an effective, robust and practical tool. The technical reports referred in the annex show how close this theoretical approach may be of becoming a guidance tool to the network operators.

The topics discussed in this thesis are still up-to-date and therefore new studies and methods will continue to arise, probably allowing to achieve even better results (or more complete) than the ones presented in this thesis. But that's exactly what science and research represents – an evolving process. In which refers to this PhD thesis, its goal was never to carry a benchmarking analysis of the flexibility recognition problem. Rather than that, it was focused on discussing a completely new topic, proposing solutions to tackle it and provide new research lines.

## *6.3 Impact on the state-of-the-art*

In Chapter 2 a revision of the state-of-the-art was performed, which somehow illustrated the works and research studies that inspired the dissertation hereby presented. However, almost 5 years separate the beginning of this thesis and the moment when I am writing these paragraphs. Therefore, the state-of-the-art has naturally evolved. The reason why these new contributions are not addressed in Chapter 2 is related to the fact that there is a clear distinction in the state-of-the-art prior and after the contributions provided by this dissertation. This represents a qualitative and important measure of the impact brought by this work. As such, the most relevant studies that arose during these 5 years are below detailed.

In [149] the authors, inspired by the methods presented in this thesis, propose a similar approach to compute the flexibility areas, but using a linearized version of the optimization problem. The authors claim that, by doing so, a significant decrease in the computational effort is achieved. Although it is not possible to deny that the linearization of the optimization problem naturally leads to a decrease in the computational effort, the comparison made in this work considers an over-estimated time for the non-linear version – 1 flexibility area = 15 minutes. In fact, if taking advantage of the sparse characteristics of the problem, a flexibility area can be extracted in 1 second. In addition, the linearization procedure has a natural cost in terms of accuracy. It is mentioned in [149] that the linearization error is directly proportional

to the distance of the PQ point within the map to the initial PQ operating point. The consideration of the discrete variables is carried using a brute-force approach i.e. the algorithm is run for every discrete variable position. An important contribution of this study is the implementation of advanced models to better characterize the flexibility provided by different DER, not restricted to the typical maximum/minimum limits in terms of active and reactive power. The same authors continued their research work concerning this topic in [150][151][152]. First, they exploited a random-sampling approach to validate the flexibility ranges obtained when using the linearized version [150]. The results showed that a good trade-off between accuracy and computational effort is achieved. Even more interesting to the state-of-the-art was the consideration of a random-sampling method that is able to find the extreme values of the operating regions. Although this is an enhancement in terms of accuracy when compared to [24], the computational time problem still remains. The impact of grid topology and tap positions on the flexibility provision was accessed in [151]. Although similar in context to the studies carried in this dissertation, the procedure to evaluate such impact was different. By considering all the possible combinations of discrete variables, the study compares the area that is transversal to all the feasible combinations against the larger area that is obtained. The flexibility areas computation is based on an enumeration process and the results highlight that the capacity to provide flexibility is higher in meshed grids due to the homogenization of the power flows through the transmission lines. In [152], the time domain was brought to the discussion, associating typical time series to each DER. The flexibility ranges assessment is also performed in an enumeration fashion way i.e. for each timestamp the algorithm is executed. An interesting outcome is achievable by normalizing the obtained flexibility areas. By doing so, is possible to determine the probability of a specific PQ point remain feasible throughout the entire time-horizon. The impact of time-variant flexibility is also accessed in [153], but here introducing the forecasting errors as a new topic for the analysis. A random number of scenarios are generated according to the forecast of time-variant influencing factors (e.g., wind speed, PV irradiation) and the probability density functions of forecast errors. Each scenario is evaluated using a Monte Carlo simulation, which requires a significant computational effort. As an outcome, a metric $r$ that illustrates the probability of a particular PQ point of being feasible in a future time is calculated. The paper wrote by Florian Capitanescu [154] is a proof of how the TSO-DSO cooperation has become a hot topic in the last years. In this work, the exact same idea that is behind this dissertation was explored. The author refers that while was writing his contributions, similar approaches arose in the literature (papers associated to this thesis). The main differences between the approaches are here described from the point-of-view of [154]: 1) Rectangular coordinates are used instead of polar voltage coordinates since there are empirical evidences that they can lead to slightly better computational performances; 2) The methodology is less refined in terms of convergence criteria however the perimeter points can be extracted in parallel; 3) Voltage dependent load models are considered; 4) Maximum cost

for flexibility purchase is not taken into account. From the same authorship, [155] considers that the idea proposed in this thesis is a pre-requisite for increasing the TSO-DSO cooperation. According it, the information provided by the flexibility area to the TSO constitutes a significant improvement when compared to the traditional assumption of a constant power exchange with the distribution systems. This way, this research study proposes an OPF formulation that already embeds the information brought by the flexibility area limits. [156] picks on the idea detailed in this dissertation and, based on it, defines a new method to estimate the capability curve of a virtual power plant. Although the authors acknowledge that is not possible to achieve a more accurate result than the one provided by the method hereby described, they believe that there is an excessive extraction of perimeter vertex points. However, similarly to [149], the work considers an over-estimated vision of the method – extraction of 100 vertex points - by do not including the convergence criterions here defined. Nevertheless, [156] brings very interesting inputs considering the geometric understanding behind the study. In a first step, a linear approximation of the capability curve is computed based on linearized network configuration and a polytopic projection algorithm. This preliminary approximation already provides a good notion of what will be the flexibility area shape. In a second stage, the classical OPF is used to map the vertices of the preliminary approximation into PQ points on the capability curve perimeter. The final approximation result is the convex hull of these PQ points. The method described in [157] is similar in context and form to the one described in this thesis to compute non-convex flexibility areas. The extreme points of the area perimeter are found using a rotational angle which defines the search direction of the method. Moreover, the methodology considers the capability limits of different DER. Although the authors do not explicitly acknowledge it, this simple change in the way the extreme points are obtained is of utmost importance to highlight potential non-convexities in the area of flexibility.

In line with the investigation carried in this dissertation, [158] does not neglect the role of the transmission side to the definition of the flexibility ranges. The exercise developed in this publication argues that the definition of the TSO-DSO flexibility area needs to comprise the transmission system ability to accept the feasible margins presented by the DSO grid. As such, the concept of TSO desirability surfaces is introduced, which can be computed with the algorithm presented in this thesis while considering TSO criteria for safe and economical operation of the transmission system. The resulting surface can then be compared to the ones detailed in this thesis and two meaningful coefficients can be extracted to access how valuable the flexibility available in the distribution system can be to the TSO. Another work of great interest arises in [159] by distinguishing between feasibility and flexibility operating regions. According to the authors, they are only similar if all the flexibility resources have a sub-second response time. Since in most cases this is not true, it is necessary to define operating regions that consist on the set of PQ points that are achievable in a given amount of time. Therefore, DER characteristics such as activation times or ramp rates need to be considered.

Other works tackled the topics discussed throughout this thesis in different perspectives. In [160], flexibility is exploited in order to address potential grid technical problems that arise as a result of the day-ahead market-clearing. Thus, an ex-post re-dispatch mechanism to manage flexibility from local DER including demand response units and their inherent rebound effect is proposed. Different optimization techniques are investigated and the results demonstrate that the dispatch of the asymmetric blocks associated to demand response actions differs when applying linear approximations or considering an exact convex relaxation of the AC-OPF model. Therefore, such linearization procedures should be used with caution in these cases. Also focusing on the importance of demand response, [161] analyses the capability of this type of actions to provide ancillary services both at the local level – distribution grids - and system-wide – transmission system. Having in mind that a coordination scheme is necessary to enable that all the players take advantage from the available flexibility, this work suggests the incorporation of local demand response market models in the context of a stochastic energy/reserve market. In that sense, a stochastic multi-period bi-level programming problem to optimally coordinate the operation of local and central markets is presented. While the upper-level of this bi-level model determines the TSO flexibility requirements in each load bus, the lower-level is responsible to clear the demand response markets at each load bus considering the needs of all the buyers. Different coordination schemes for TSO and DSO were also the topic of discussion in the SmartNet project, as already mentioned in Chapter 2. The final outcomes of the project allowed to conclude that the proper coordination scheme is much dependent on the scenario in which it is applied [162]. To investigate such dependency, several scenarios were built based on three reference countries (Italy, Denmark and Spain) and their foreseen 2030 electrical evolution. In addition to highlight these dependencies, the simulations showed that a common market model for both TSO and DSO where all the technical constraints are considered allows to find the optimal solution and it is characterized by high economical performances. Nevertheless, there is a need for high cooperation levels between TSO and DSO and the market-clearing algorithms can represent a problem in terms of computational efficiency. Still in the context of *how flexibility available in the distribution grids should be exploited* and *who has priority in accessing to that flexibility*, [163] describes a fix-term contract market for the DSO. Based on that, the distribution operator can procure and establish contracts for flexibility products with demand response aggregators, still leaving room for those aggregators to sell the flexibility left to other players such as the TSO. This type of contract scheme allows the DSO to optimally reserve flexibility, but it might not be the best design for the whole electricity system. The type of aggregators that are expected to be active and how to fairly pay them are also matters of discussion. In [164], the future of Advanced Distribution Management Systems and corresponding applications is analyzed considering three different time-horizons 1) Applications already available and implemented at an industrial level; 2) Applications to be implemented in a short-term horizon (1-5 years); 3) Applications to be

implemented in a mid-term horizon (5-10 years). Although there is not a direct reference to the integration of features that estimate the aggregated flexibility at the TSO-DSO interconnection points, there are some clues that allow to believe that they will be required by the operators in a mid-term horizon. On the one hand, the added complexity and heterogeneity of proactive and controllable assets will impose the adoption of centralized model-based optimization methods instead of the classical rule-based or local management methodologies. On the other hand, and as the publication refers "From the transmission system operator's perspective, the primary interest is the behavior at the transmission/distribution interface (e.g., requiring a specific power factor), and it may be sufficient to obtain only aggregated information at the corresponding substations."

In a more direct or indirect form, [165] and [166] bring significant contributes to the subject discussed in Chapter 4. Although [165] does not focus on developing reduced models for the transmission grids, it carries a comprehensible analysis on how clustering procedures should be employed. A hierarchical spectral clustering method, which uses the eigenvalues and eigenvectors of the Laplace matrix, is applied to partition a power system into a set of parts. The decomposition can follow different criteria (e.g., lines admittances, active and reactive power flows) and the main goal is to improve the computational efficiency in solving power systems problems when applying parallelization techniques. On the other hand, [166] presents a new method to develop equivalent grid models that still requires the topological knowledge of the grid to be reduced. Built on the top of a clustering method that combines spatial data (network structure) with the temporal metadata (e.g., generation time-series), the approach determines the clusters of nodes that are similar in their time-series, and they are connected. The final outcome is an equivalent grid model with new time-series.

## *6.4 Future research lines*

Given the few years of research considering the topics discussed in this dissertation, it is possible to propose a substantial number of research opportunities that might inspire other authors. If some of them are associated to new ideas to improve the proposed algorithms, others focus on applying the concepts of different fields of study (e.g., data science) to this same topic.

***Definition of new goals:***

- To constrain the flexibility areas to other parameters rather than the cost e.g., inclusion of RES uncertainty levels in the PQ maps;

- The development of conditional flexibility maps. The main idea would be to study the impact of defining a PQ set-point in a specific TSO-DSO interface upon the remaining interconnections;

- To study, define and apply the necessary adaptations to move from a single-period approach to a multi-temporal analysis thus adding a third dimension to the current problem. This will also lead to interesting visualization challenges concerning the flexibility ranges;

- To incorporate inter-temporal characteristics in the flexibility recognition problem thus trying to include the behavior of other resources such as storage devices;

- To explore the impact of flexibility exploitation on different variables rather than the power flows at the TSO-DSO interfaces. TSOs and DSOs might be interested in visualizing other types of variables (e.g., voltage) in order to properly define interchange conditions;

- To apply the proposed methodology to MV/LV substations. This could help aggregators to define flexibility margins provided by LV customers thus also promoting their contribution to the grid operation and management;

- To apply and test the methodology to compute transmission grid equivalent models in different contexts e.g., contingency analysis.

***Exploring other research fields:***

- Some of the processes described in this thesis demand significant computational efforts e.g., inspection of sub-areas of flexibility. Such requirements will exponentially increase in the case of a multi-temporal analysis. Therefore, it is of utmost importance to explore how to maintain the computational efficiency above the minimum requirements set by the operational constraints. The usage of Graphical Processing Units (GPU) should thus be considered due to their acceleration capabilities when applied to problems that can be parallelized;

- The algorithms proposed in this PhD thesis will be one additional (and new) source of data available in the network operator's systems. As such and considering the advances that data science has undergone in recent years, it will be also an opportunity to extract knowledge from these new sets of data. One interesting idea would be to apply pattern

recognition approaches to the flexibility areas. As an example, these algorithms could explore if there is a correspondence between the value of the discrete variables and the shape of the sub-areas of flexibility;

- Investing on the interface human-machine is also an important topic to be explored. Since the flexibility areas intend to work as a decision-support tool to the network operators, it is not possible to neglect the importance of how this information is presented. The network operators should be perfectly able to understand and interact with it. Therefore, the application of science visualization techniques will also be necessary, particularly when additional dimensions (e.g., time) are considered.

# References


[1] Eurelectric. (2014, Jan.). Flexibility and Aggregation Requirements for their interaction in the market. Eurelectric. Brussels,Belgium.[Online].Available:http://www.elecpor.pt/pdf/14_01_2014_tf_bal_agr_report_final_je_as_2014.pdf

[2] Ea Energy Analyses. (2013, Nov.). Activating electricity demand as regulating power - FlexPower - Testing a Market Design Proposal. Ea Energy Analyses. Copenhagen, Denmark. [Online]. Available: http://www.eurisco.dk/images/1027_flexpower_activating_electricity_demand_as_regulating_power.pdf

[3] Y. Ding, L. H. Hansen, P. D. Cajar, P. Brath, H. W. Bindner, C. Zhang and N. C. Nordentoft. (2013, March). Development of a DSO-Market on Flexibility Services. SPIR iPower Project. [Online]. Available:http://www.danskenergi.dk/~/media/Analyse/Projekter/iPower/Development_of_a_DSO-market_on_flexibility_services.ashx.

[4] Expert Group 3. (2015, Jan.). Regulatory Recommendations for the Deployment of Flexibility. Smart Grids Task Force. [Online]. Available: http://ec.europa.eu/energy/sites/ener/files/documents/EG3%20Final%20-%20January%202015.pdf

[5] CEER. (2017, March). Guidelines of Good Practice for Flexibility Use at Distribution Level. CEER. Brussels, Belgium. [Online]. Available:http://smartnet-project.eu/wp-content/uploads/2017/05/C16-DS29-03-Flexibility-Paper-_-final-version.pdf

[6] H. Brunner and A. Zegers. (2014, Sept.). An Overview of current interaction between transmission and distribution system operators and an assessment of their cooperation in Smart Grids. ISGAN. Seoul, South Korea. [Online]. Available: http://smartgrids.no/wp-content/uploads/sites/4/2016/01/ISGAN-TSO-DSO-interaction.pdf

[7] E. Rivero, D. Six and H. Gerard. (2016, Dec.). Basic schemes for TSO-DSO coordination and ancillary services provision. EU Horizon 2020 SmartNet Project. [Online]. Available: http://smartnet-project.eu/wp-content/uploads/2016/12/D1.3_20161202_V1.0.pdf

[8] NY State Department of Public Service. (2014, Apr.) Reforming the Energy Vision – Case 14-M-0101. NY State Department of Public Service. Albany, NY. [Online]. Available: http://documents.dps.ny.gov/public/Common/ViewDoc.aspx?DocRefId=%7B9CF883CB-E8F1-4887-B218-99DC329DB311%7D.

[9] USEF Foundation. (2015, Nov.). USEF: The Framework Explained. USEF Foundation. Arnhem, Netherlands. [Online]. Available: https://www.usef.energy/download-the-framework/#

[10] GridWise Architecture Council. (2015, Jan.). GridWise Transactive Energy Framework. Pacific NW National Lab. Richland, WA. [Online]. Available: http://www.gridwiseac.org/pdfs/te_framework_report_pnnl-22946.pdf.

[11] E. Rivero, D. Six and H. Gerard. (2015, Oct.). Assessment of future market architectures and regulatory frameworks for network integration of DRES – the future roles of DSOs. EC FP7 evolvDSO Project.

[12] Eurelectric. (2013, Feb.). Active Distribution System Management: A key tool for the smooth integration of distributed generation. Eurelectric. Brussels, Belgium.[Online].Available: http://www.eurelectric.org/media/74356/asm_full_report_discussion_paper_final-2013-030-0117-01-e.pdf

[13] Expert Group 3. (2013, Jan.). Options on handling Smart Grids Data. Smart Grids Task Force. [Online]. Available:https://ec.europa.eu/energy/sites/ener/files/documents/xpert_group3_first_year_report.pdf

[14] P. Oosterkamp, P. Koutstaal, A. Welle, J. Joode, J. Lenstra, K. Hussen and R. Haffner. (2014, Apr.). The role of DSOs in a Smart Grid environment. Ecorys. Rotterdam, Netherlands. [Online].Available: https://ec.europa.eu/energy/sites/ener/files/documents/20140423_dso_smartgrid.pdf

[15] ENTSO-E. (2013, Sept.). Network Code on Operational Planning and Scheduling. ENTSO-E. Brussels, Belgium.[Online].Available:https://www.entsoe.eu/fileadmin/user_upload/_library/resources/OPS_NC/130924-AS_NC_OPS_2nd_Edition_final.pdf

[16] SP Energy Networks. (2016, Oct.). SPEN DSO Vision. ScottishPower Group. Scotland, United Kingdom. [Online].Available:https://www.spenergynetworks.co.uk/userfiles/file/SPEN%20DSO%20Vision%20210116.pdf

[17] T. Esterl and C. Gutschi. (2017, Jun.). hybrid-VPP4DSO: Providing flexibility from distributed resources under consideration of the needs of the DSO. AIT Austrian Institute of Technology. Vienna, Austria. [Online]. Available: http://www.grazer-ea.at/hybridvpp4dso/upload/workshop_170609/hybrid-vpp4dso_workshopsi_projectdescription.pdf

[18] INESC TEC. (2015, Aug.). European Electricity Market Reference Model Assessment & SmarterEMC2 Positioning. EU Horizon 2020 SmarterEMC2 Project. [Online]. Available: http://www.smarteremc2.eu/wp-content/uploads/2016/08/D2.1-European-Electricity-Market-Reference-Model-Assessment-SmarterEMC2-Positioning.pdf

[19] CEER. (2016, Sept.). CEER Position Paper on the Future DSO and TSO Relationship. CEER. Brussels, Belgium. [Online]. Available: https://www.ceer.eu/documents/104400/3731907/C16-DS-26-04_DSO-TSO-relationship_PP_21-Sep-2016.pdf/e8532c60-56d5-17bf-cecb-b4f9594fe0c4

[20] ACER. (2014, Sept.). Energy Regulation: A Bridge to 2025 Conclusions Paper. ACER. Ljubljana, Slovenia. [Online]. Available: http://www.acer.europa.eu/official_documents/acts_of_the_agency/sd052005/supporting%20document%20to%20acer%20recommendation%2005-2014%20-%20%20energy%20regulation%20a%20bridge%20to%202025%20conclusions%20paper.pdf

[21] EDSO for smart grids. (2015, May). Coordination of transmission and distribution system operators: a key step for the Energy Union. EDSO for smart grids. Brussels, Belgium. [Online]. Available: https://www.edsoforsmartgrids.eu/wp-content/uploads/public/Coordination-of-transmission-and-distribution-system-operators-May-2015.pdf

[22] ENTSO-E, CEDEC, GEODE, EURELECTRIC and EDSO for Smart Grids. (2016, July). TSO-DSO data management report. ENTSO-E, CEDEC, GEODE, EURELECTRIC and EDSO for Smart Grids. Brussels, Belgium. [Online]. Available: http://www.edsoforsmartgrids.eu/wp-content/uploads/TSO-DSO_Data-management-Report-2.pdf

[23] ENTSO-E. (2016, Oct.). ENERGY STORAGE AND STORAGE SERVICES. ENTSO-E. Brussels, Belgium. [Online].Available:https://www.entsoe.eu/Documents/Publications/Position%20papers%20and%20reports/entsoe_pp_storage_web.pdf

[24] M. Heleno, R. Soares, J. Sumaili, R. J. Bessa, L. Seca and M. A. Matos, "Estimation of the Flexibility Range in the Transmission-Distribution Boundary," in *Proc. IEEE Eindhoven PowerTech*, Eindhoven, 2015, pp. 1685-1691.

[25] Entidade Reguladora dos Serviços Energéticos, "Despacho n.º 7253/2010", in *Diário da República*, 2.ª série, nº80, Abril 2010 (*In Portuguese*).

[26] L. Lo Schiavo. (2015, Nov.). Regulatory incentives for smart grids demonstration and deployment in Italy, within the European framework. Presented at 6th International Conference on Integration of Renewable and Distributed Energy Resources. [Online]. Available: http://www.nedo.go.jp/english/ired2014/program/pdf/s5/s5_3_luca_lo_schiavo.pdf

[27] H. Farhangi. (2010, Jan.). The path of the smart grid. *IEEE Power and Energy Magazine. vol. 8(1),* pp. 18-28.

[28] C.S. Gouveia, D. Rua, F.J. Soares, C. Moreira, P.G. Matos and J.A. Peças Lopes. (2015, March). Development and implementation of Portuguese smart distribution system. *Electric Power Systems Research. vol. 120,* pp. 150-162.

[29] L. Zhao, W. Zhang, H. Hao and K. Kalsi. (2017, Feb.). A Geometric Approach to Aggregate Flexibility Modeling of Thermostatically Controlled Loads. *IEEE Trans. Power Systems. vol. PP(99).*

[30] R. Schneider, "Convex Bodies: The Brunn-Minkowski Theory," in *Encyclopedia of Mathematics and its Applications*, 1st ed. Cambridge, United Kingdom: Cambridge Press, 1993.

[31] H. Hao, A. Somani, J. Lian and T. E. Carrol, "Generalized aggregation and coordination of residential loads in a smart community," in *Proc. IEEE International Conf. Smart Grid Communications*, Miami, Flo., 2015, pp. 67-72.

[32] J. F. Nash. (1950, Apr.). The bargaining problem. *Econometrica, vol. 18*(2), pp. 155–162.

[33] E. Polymeneas and S. Meliopoulos, "Aggregate Modeling of Distribution Systems for Multi-Period OPF," in *Proc. Power Systems Computation Conf.*, Genoa, 2016, pp. 1224-1232.

[34] H. Nosair and F. Bouffard. (2015, July). Flexibility Envelopes for Power System Operational Planning. *IEEE Trans. Sust. Energy. vol. 6(3),* pp. 800-809.

[35] H. Nosair and F. Bouffard. (2016, Nov.). Energy-Centric Flexibility Management in Power Systems. *IEEE Trans. Power Systems, vol. 31(6),* pp. 5071-5081.

[36] J. Zhao, T. Zheng and E. Litvinov. (2016, Jan.). A Unified Framework for Defining and Measuring Flexibility in Power System. *IEEE Trans. Power Systems. vol. 31(1),* pp. 339-347.

[37] M. A. Bucher, S. Delikaraoglou, K. Heussen, P. Pinson and G. Andersson, "On Quantification of Flexibility in Power Systems," in *Proc. IEEE Eindhoven PowerTech,* Eindhoven, 2015, pp. 1626-1632.

[38] T. Kornrumpf, J. Meese, M. Zdrallek, N. Neusel-Lange and M. Roch, "Economic Dispatch of Flexibility Options for Grid Services on Distribution Level," in *Proc. Power Systems Computation Conf.*, Genoa, 2016, pp. 157-164.

[39] M. A. Bucher, S. Chatzivasileiadis and G. Andersson. (2016, March). Managing flexibility in multi-area power systems. *IEEE Trans. Power Systems, vol. 31(2),* pp. 1218-1226.

[40] S. Mathieu, D. Ernst and B. Cornéiusse, "Agent-based analysis of dynamic access ranges to the distribution network," in *Proc. IEEE PES Innovative Smart Grid Technologies Conf. Europe*, Ljubljana, 2016, pp. 105-111.

[41] D. Pudjianto, C. Ramsay, and G. Strbac. (2007, March). Virtual power plant and system integration of distributed energy resources. *IET Renewable Power Generation. vol. 1(1)*, pp. 10-16.

[42] R. Schwerdfeger and D. Westermann, "Storage management algorithm for schedule based DSO system operation with respect to TSO's system responsibility," in *Proc. Power Systems Computation Conf.*, Wroclaw, 2014.

[43] J. Carpentier. (1962, Aug.). Contribution à l'étude du dispatching économique. *Bull. Soc. Francaise Elect. vol. 8*, pp. 431-447.

[44] D.W.Wells. (1968, Aug.). Method for economic secure loading of a power system. *Proc. of the Institution of Electrical Engineers. vol.115(8)*, pp. 1190-1194.

[45] G. B. Dantzig, in *Linear Programming and Extensions*, 1st ed. New Jersey: Princeton University Press, 1963.

[46] C. M. Shen and M. A. Laughton. (1970, Nov.). Power-system load scheduling with security constraints using dual linear programming. *Proc. of the Institution of Electrical Engineers. vol.117(11)*, pp. 2117-2127.

[47] B. Stott and E. Hobson. (1978, Sept.). Power System Security Control Calculation Using Linear Programming - Parts I and II. *IEEE Trans. Power Apparatus and Systems. vol. PAS-97(5),* pp. 1721-1731.

[48] E. Housos and G. Irisarri. (1983, May). Real and Reactive Power System Security Dispatch Using a Variable Weights Optimization Method. *IEEE Power Engineering Review. vol. PER-3(5),* pp. 42-43.

[49] S. A. Farghal, M .A. Tantawy, M .S. Abou-Hussein, S. A. Hassan and A. A. Abou-Slela. (1984, May). Fast Technique for Power System Security Assessment Using Sensitivity Parameters of Linear Programming. *IEEE Trans. Power Apparatus and Systems. vol. PAS-103(5)*, pp. 946-953.

[50] O. Alsac, J. Bright, M. Prais and B. Stott. (1990, Aug.). Further developments in LP-based optimal power flow. *IEEE Trans. Power Systems. vol. 5(3),* pp. 697-711.

[51] H. W. Dommel, W .F. Tinney. (1968, Oct.). Optimal Power Flow Solutions. *IEEE Trans. Power Apparatus and Systems. vol. PAS-87(10)*, pp. 1866-1876.

[52] C. M. Shen and M. A. Laughton. (1969, Feb.). Determination of optimum power-system operating conditions under constraints. *Proc. of the Institution of Electrical Engineers. vol.116(2)*, pp. 225-239.

[53] A. M. Sasson. (1969, Oct.). Combined Use of the Powell and Fletcher - Powell Nonlinear Programming Methods for Optimal Load Flows. *IEEE Trans. Power Apparatus and Systems. vol. PAS-88(10)*, pp. 1530-1537.

[54] O. Alsac and B. Stott. (1974, May). Optimal Load Flow with Steady-State Security. *IEEE Trans. Power Apparatus and Systems. vol. PAS-93(3)*, pp. 745-751.

[55] R. Divi and H. K. Kesavan. (1982, Sept.). A Shifted Penalty Function Approach for Optimal Load-Flow. *IEEE Trans. Power Apparatus and Systems. vol. PAS-101(9)*, pp. 3502-3512.

[56] J. Zhu and J. A. Momoh. (2001, Aug.). Multi-area power systems economic dispatch using nonlinear convex network flow programming. *Electric Power Systems Research. vol. 59(1),* pp. 13-20.

[57] G. F. Reid and L. Hasdorff. (1973, Nov.). Economic Dispatch Using Quadratic Programming. *IEEE Trans. Power Apparatus and Systems. vol. PAS-92(6)*, pp. 2015-2023.

[58] B. F. Wollenberg and W. O. Stadlin. (1974, Sept.). A Real Time Optimizer for Security Dispatch. *IEEE Trans. Power Apparatus and Systems. vol. PAS-93(5)*, pp. 1640-1649.

[59] R. C. Burchett, H. H. Happ, D. R. Vierath and K. A. Wirgau. (1982, Feb.). Developments in the Optimal Power Flow. *IEEE Trans. Power Apparatus and Systems. vol. PAS-101(2)*, pp. 406-414.

[60] M. R. Hestenes. (1969, Nov.). Multiplier and gradient methods. *Journal of Optimization Theory and Applications. vol. 4(5)*, pp. 303-320.

[61] M. J. D. Powell, "A method for nonlinear constraints in minimization problems," in *Optimization*, 1st ed. New York: Academic Press, 1969, pp. 283-298.

[62] R. C. Burchett, H. H. Happ and D. R. Vierath. (1984, Nov.). Quadratically Convergent Optimal Power Flow. *IEEE Trans. Power Apparatus and Systems. vol. PAS-103(11),* pp. 3267-3275.

[63] G. C. Contaxis, B. C. Papadias and C. Delkis. (1983, Sept.). Decoupled Power System Security Dispatch. *IEEE Trans. Power Apparatus and Systems. vol. PAS-102(9),* pp. 3049-3056.

[64] X. Lin, A. K. David and C. W. Yu. (2003, May). Reactive power optimisation with voltage stability consideration in power market systems. *IEE Proc. - Generation, Transmission and Distribution. vol. 150(3),* pp. 305-310.

[65] A. Berizzi, M. Delfanti, P. Marannino, M. S. Pasquadibisceglie and A. Silvestri. (2005, Aug.). Enhanced security-constrained OPF with FACTS devices. *IEEE Trans. Power Systems. vol. 20(3),* pp. 1597-1605.

[66] B. Cova, G. P. Granelli, M. Montagna, A. Silvestri, M. Innorta and P. Marannino. (1987, July). Large-scale applications of the Han–Powell algorithm to compact models of static and dynamic dispatch of real power. *Int. Journal of Elect. Power Energy Syst., vol. 9(3),* pp. 130–141.

[67] A. M. Rashed and D. H. Kelly. (1974, Sept.). Optimal Load Flow Solution Using Lagrangian Multipliers and the Hessian Matrix. *IEEE Trans. Power Apparatus and Systems. vol. PAS-93(5),* pp. 1292-1297.

[68] H. H. Happ. (1974, May). Optimal Power Dispatch. *IEEE Trans. Power Apparatus and Systems. vol. PAS-93(3),* pp. 820-830.

[69] L. K. Kirchmayer and G. W. Stagg. (1952, Jan.). Evaluation of Methods of Co-ordinating Incremental Fuel Costs and Incremental Transmission Losses. *Trans. of the American Inst. Electrical Engineers Part III: Power Apparatus and Systems. vol. 71(1),* pp. 513-521.

[70] S-Der. Chen and J-Fuh. Chen. (1997, Feb.). A new algorithm based on the Newton -Raphson approach for real-time emission dispatch. Electric Power Systems Research. vol. 40(2), pp. 137-141.

[71] A. Monticelli, M. V. F. Pereira and S. Granville. (1987, Feb.). Security-Constrained Optimal Power Flow with Post-Contingency Corrective Rescheduling. *IEEE Trans. Power Systems. vol. 2(1),* pp. 175-180.

[72] D. I. Sun, B. Ashley, B. Brewer, A. Hughes and W. F. Tinney. (1984, Oct.). Optimal Power Flow by Newton Approach. *IEEE Trans. Power Apparatus and Systems. vol. PAS-103(10),* pp. 2864-2880.

[73] O. Crisan and M. A. Mohtadi. (1992, Sept.). Efficient identification of binding inequality constraints in optimal power flow Newton approach. *IEE Proc. C - Generation, Transmission and Distribution. vol. 139(5),* pp. 365-370.

[74] R. S. Ferreira, C. L. T. Borges and M. V. F. Pereira. (2014, Sept.). A Flexible Mixed-Integer Linear Programming Approach to the AC Optimal Power Flow in Distribution Systems. *IEEE Trans. Power Systems. vol. 29(3),* pp. 2447-2459.

[75] G. C. Contaxis, C. Delkis and G. Korres. (1986, May). Decoupled Optimal Load Flow Using Linear or Quadratic Programming. *IEEE Trans. Power Systems. vol. 1(2),* pp. 1-7.

[76] K. R. Frisch, "The logarithmic potential method of convex programming," Univ. Institute of Economics, Oslo, Norway, Memorandum, May, 1955.

[77] A. V. Fiacco and G. P. McCormick, "Interior Point Unconstrained Minimization Techniques," in *Nonlinear Programming: Sequential Unconstrained Minimization Techniques,* 1st ed. New Jersey: John Wiley & Sons, 1968.

[78] N. Karmarkar. (1984, Dec.). A new polynomial-time algorithm for linear programming. *Combinatorica. vol. 4(4)*, pp. 373-395.

[79] P. E. Gill, W. Murray, M. A. Saunders, J. A. Tomlin and M. H. Wright. (1986, Jun.). On projected Newton barrier methods for linear programming and an equivalence to Karmarkar's projective method. *Mathematical Programming, vol. 36(2)*, pp. 183-209

[80] R. E. Marsten, M. J. Saltzman, D. F. Shanno, G. S. Pierce and J. F. Ballintijn. (1989, Nov.). Implementation of a dual affine interior point algorithm for linear programming. *ORSA Journal on Computing, vol. 1(4)*, pp. 287-297.

[81] R. Saigal, "Interior Point Methods," in *Linear Programming: A Modern Integrated Analysis,* 1st ed. New York: Springer US, 1995.

[82] N. Megiddo, "Pathways to the optimal set in linear programming," in *Progress in Mathematical Programming,* 1st ed. New York: Springer-Verlag New York, 1989.

[83] C. C. Conzaga. (1992, Jun.). Path following methods for linear programming. *SIAM Review, vol. 34(2)*, pp. 167-224.

[84] R. D. C. Monteiro and I. Adler. (1989, May). Interior path following primal-dual algorithms. Part I and II. *Mathematical Programming, vol. 44(1-3)*, pp. 27-66.

[85] S. Mizuno and A. Nagasawa. (1993, Feb.). A primal-dual affine-scaling potential-reduction algorithm for linear programming. *Mathematical Programming, vol. 62(1-3)*, pp. 119-131.

[86] R. Polyak. (1992, Feb.). Modified barrier functions (theory and methods). *Mathematical Programming, vol. 54(1-3)*, pp. 177-222.

[87] S. Mehrotra. (1992, Nov.). On the implementation of a primal-dual interior point method. *SIAM Journal on Optimization, vol. 2(4)*, pp. 576-601.

[88] J. Gondzio. (1996, Sept.). Multiple centrality corrections in a primal-dual method for linear programming. *Computational Optimization and Applications, vol. 6(2)*, pp. 137-156.

[89] K. A. Clements, P. W. Davis and K. D. Frey, "Power system state estimation with inequality constraints," in *IEEE International Symp. On Circuits and Systems*, Singapore, 1991.

[90] L. S. Vargas, V. H. Quintana and A. Vannelli. (1993, Aug.). A tutorial description of an interior point method and its applications to security-constrained economic dispatch. *IEEE Trans. Power Systems, vol. 8(3)*, pp. 1315-1324.

[91] S. Granville. (1994, Feb.). Optimal reactive dispatch through interior point methods. *IEEE Trans. Power Systems, Vol. 9(1)*, pp. 136-146.

[92] G. L. Torres and V. H. Quintana. (1998, Nov.). An interior point method for nonlinear optimal power flow using voltage rectangular coordinates. *IEEE Trans. Power Systems, vol.13(4)*, pp. 1211-1218.

[93] G. L. Torres and V. H. Quintana. (2001, May). On a nonlinear multiple-centrality-corrections interior-point method for optimal power flow. *IEEE Trans. Power Systems, vol.16(2)*, pp. 222-228.

[94] W. Yan, J. Yu, D. C. Yu and K. Bhattarai. (2006, Feb.). A new optimal reactive power flow model in rectangular form and its solution by predictor corrector primal dual interior point method. *IEEE Trans. Power Systems, vol.21(1)*, pp. 61-67.

[95] T. S. Chen and Y. Z. Li. (2000, Aug.). A hybrid GA approach for OPF with consideration of FACTS devices. *IEEE Power Engineering Review, vol.20(8)*, pp. 54-57.

[96] Z-Lee. Gaing and R-Fang. Chang, "Security-constrained optimal power flow by mixed-integer genetic algorithm with arithmetic operators," *in Proc. IEEE PES General Meeting*, Montreal, 2006, pp. 1-8.

[97] R. Storn and K. Price. (1995, March). Differential Evolution - A simple and efficient adaptive scheme for global optimization over continuous spaces. International Computer Science Inst. Berkley, CA. [Online].Available:http://citeseerx.ist.psu.edu/viewdoc/download?doi=10.1.1.67.5398&rep=rep1&type=pdf

[98] H. R. Cai, C. Y. Chung and K. P. Wong. (2008, May). Application of Differential Evolution Algorithm for Transient Stability Constrained Optimal Power Flow. *IEEE Trans. Power Systems, vol.23(2)*, pp. 719-728.

[99] M. A. Abido. (2002, Oct.). Optimal power flow using particle swarm optimization. *Int. Journal of Elect. Power Energy Syst., vol. 24(7)*, pp. 563–571.

[100] P. E. O. Yumbla, J. M. Ramirez and C. A. C. Coello. (2008, Feb.). Optimal Power Flow Subject to Security Constraints Solved With a Particle Swarm Optimizer. *IEEE Trans. Power Systems, vol.23(1)*, pp. 33-40.

[101] M. R. AlRashidi and M. E. El-Hawary. (2007, Nov.). Hybrid Particle Swarm Optimization Approach for Solving the Discrete OPF Problem Considering the Valve Loading Effects. *IEEE Trans. Power Systems, vol.22(4)*, pp. 2030-2038.

[102] S. H. Low. (2014, March). Convex Relaxation of Optimal Power Flow—Part I: Formulations and Equivalence. *IEEE Trans. Control of Network Systems, vol.1(1)*, pp. 15-27.

[103] S. H. Low. (2014, Jun.). Convex Relaxation of Optimal Power Flow—Part II: Exactness. *IEEE Trans. Control of Network Systems, vol.1(2)*, pp. 177-189.

[104] V. H. Quintana, G. L. Torres and J. Medina-Palomo. (2000, Feb.). Interior-point methods and their applications to power systems: a classification of publications and software codes. *IEEE Trans. Power Systems, vol.15(1)*, pp. 170-176.

[105] V. H. Quintana, G. L. Torres, "Introduction to Interior-Point Methods," IEEE PES Task Force on Interior-Point Methods Applications to Power Systems, 1997.

[106] Y. Zhang and Z. Ren. (2005, Aug.). Optimal reactive power dispatch considering costs of adjusting the control devices. *IEEE Trans. Power Systems, vol.20(3)*, pp. 1349-1356.

[107] A. Madureira, "Coordinated and optimized voltage management of distribution networks with multi-microgrids," Ph.D. Thesis, Dept. of Electro. and Computers Eng., Faculty of Eng. of the Univ. of Porto (FEUP), Porto, Portugal, 2010.

[108] Ministério da Economia, da Inovação e do Desenvolvimento, "Portaria n.º 592/2010", in *Diário da República*, 1.ª série, nº146, Julho 2010 (*In Portuguese*).

[109] Ministério do Ambiente, Ordenamento do Território e Energia - Direção-Geral de Energia e Geologia, "Despacho n.º 8810/2015", in *Diário da República*, 2.ª série, nº154, Agosto 2015 (*In Portuguese*).

[110] P. Cuffe. (2016, Oct.). Impact assessment of tools at international level. EC FP7 evolvDSO Project.

[111] N. Fonseca, J. Silva, A.C. Silva, J. Sumaili, L. Seca, R.J. Bessa, J. Pereira, M. Matos, P. Matos, C. Morais, M. Caujolle and M. Sebastian-Viana, "evolvDSO grid management tools to support TSO-DSO cooperation," in *Proc. CIRED 2016 Workshop*, Helsinki, 2016, pp. 287-291.

[112] A. C. Silva, J. Sumaili, J. Silva, L. Carvalho, L. Seca, M. Matos, R.J. Bessa, G. Schaarschmidt and R. Hermes, "Assessing DER flexibility in a German distribution network for different scenarios and degrees of controllability," in *Proc. CIRED 2016 Workshop,* Helsinki, 2016, pp. 805-809.

[113] V. Giordano, I. Onyeji, G. Fulli, M. S. Jiménez and C. Filiou. (2012, Apr.). Guidelines for conducting a cost-benefit analysis of Smart Grid projects. Joint Research Centre. Luxembourg. [Online]. Available:https://ec.europa.eu/energy/sites/ener/files/documents/20120427_smartgrids_guideline.pdf

[114] J. B. Ward. (1949, July). Equivalent Circuits for Power-Flow Studies. *Trans. of the American Institute of Electrical Engineers, vol. 68(1)*, pp. 373-382.

[115] A. Monticelli, S. Deckmann, A. Garcia and B. Stott. (1979, March). Real-Time External Equivalents for Static Security Analysis. *IEEE Trans. Power Apparatus and Systems, vol. PAS-98(2)*, pp. 498-508.

[116] S. Deckmann, A. Pizzolante, A. Monticelli, B. Stott and O. Alsac. (1980, Nov.). Studies on Power System Load Flow Equivalencing. *IEEE Trans. Power Apparatus and Systems, vol. PAS-99(6)*, pp. 2301-2310.

[117] A. Monticelli, "Fluxo de carga em redes de energia eletrica", 1st ed. E. Blucher, 1983.

[118] V. Miranda and N. Fonseca, "EPSO – Best-of-Two-Worlds Meta-Heuristic Applied to Power System Problems", in *Proc. WCCI/CEC – World Conference on Computational Intelligence, Conference on Evolutionary Computation*, Honolulu (Hawaii), 2002.

[119] V. Miranda, H. Keko, and A.J. Duque, "EPSO: Evolutionary particle swarms", *in Jain L.C., Palade V., Srinivasan D. (eds) Advances in Evolutionary Computing for System Design. Studies in Computational Intelligence,* vol 66. Springer-Verlag Berlin Heidelberg, 2007

[120] I. Rechenberg, "Evolutionstrategie, Optimierung Technisher Systeme nach Prinzipien des Biologischen Evolution", Fromman-Hozlboog, Stuttgart, 1973.

[121] C. Grigg *et al.* (1999). The IEEE Reliability Test System 1996. A report prepared by the reliability test system task force of the application of probability methods subcommittee. *IEEE Trans. on Power Systems, vol. 14(3)*, pp. 1010-1020.

[122] C. Barrows *et al.*, Reliability Test System - Grid Modernization Lab Consortium, (2017), GitHub repository. [Online] https://github.com/GridMod/RTS-GMLC

[123] E. H. L. Aarts and J. K. Lenstra, *in Local Search in Combinatorial Optimization*. New York: John Wiley & Sons, 1997.

[124] C. H. Papadimitriou, "The complexity of combinatorial optimization problems," MSc. Thesis, Princeton University, New Jersey, USA, 1976.

[125] M. Mladenovic and P. Hansen. (1997, Nov.). Variable neighbourhood search. *Computers & Operations Research, vol.24(11)*, pp. 1097-1100.

[126] O. Martin, S.W. Otto and E.W. Felten. (1991). Large-Step Markov Chains for the Traveling Salesman Problem. *Complex Systems., vol.5(3)*, pp. 299-326.

[127] H.R. Lourenco, O. Martin and T. Stutzle, "Iterated Local Search," in *Handbook of Metaheuristics. International Series in Operations Research & Management Science*. Boston: Springer, 2003.

[128] T. Stutzle, "Local search algorithms for combinatorial problems: Analysis, algorithms and new applications," PhD. Thesis, Technische Universitat¨ Darmstadt, Sankt Augustin, Germany, 1999.

[129] F. Glover and C. McMillan. (1986). The general employee scheduling problem. An integration of MS and AI. *Computers & Operations Research, vol.13(5)*, pp. 563-573.

[130] J. Gu and X. Huang (1994, May). Efficient local search with search space smoothing: a case study of the traveling salesman problem. *IEEE Trans. on Systems Man and Cybernetics, vol. 24(5)*, pp. 728-735.

[131] S. Kirkpatrick, C. D. Gelatt and M. P. Vecchi. (1983, May). Optimization by simulated annealing. *Science, vol.220(4598)*, pp. 671-680.

[132] V. Cerny. (1985, Jan.). Thermodynamical approach to the traveling salesman problem: An efficient simulation algorithm. *Journal of Optimization Theory and Applications, vol.45(1)*, pp. 41-51.

[133] A. Dekkers and E. H. L. Aarts. (1991, March). Global Optimization and simulated annealing. *Mathematical Programming, vol.50(1-3)*, pp. 367-393.

[134] M. Locatelli. (2000, Jan.). Simulated annealing algorithms for continuous global optimization: Convergence conditions. *Journal of Optimization Theory and Applications, vol.29(1)*, pp. 87-102.

[135] L. Ozdamar and M. Demirhan. (2000, Aug.). Experiments with new stochastic global optimization search techniques. *Computers & Operations Research, vol.27(9)*, pp. 841-865.

[136] E. H. L. Aarts and R. J. M. Van Laarhoven, "Simulated annealing," in *Simulated Annealing: Theory and Applications*. Netherlands: Springer, 1987.

[137] M. D. Huang, F. Romeo and A. L. Sangiovanni-Vincentelli, "An efficient general cooling schedule for simulated annealing", *in Proc. IEEE International Conf. on Computer-Aided Design*, Santa Clara, CA, 1986, pp. 381-384.

[138] C. Koulamas, S. R. Anthony and R. Jaen. (1994, Jan.). A survey of simulated annealing application to operations-research problems. Omega, vol.22(1), pp. 41-56.

[139] T. Jones, "Evolutionary algorithms, fitness landscapes and search" PhD. Thesis, University of New Mexico, Albuquerque, USA, 1995.

[140] M. Mladenovic and P. Hansen, "Variable neighborhood search," in *Handbook of Metaheuristics. International Series in Operations Research & Management Science.* Boston: Springer, 2003.

[141] D. J. Aloise, D. Aloise, C. T. Rocha, C. C. Ribeiro, J. C. Ribeiro Filho and Luiz S. S. Moura. (2006, Apr.). Scheduling workover rigs for onshore oil production. *Discrete Applied Mathematics, vol.154(5),* pp. 695-702.

[142] O. Braysy. (2003, Nov.). A Reactive Variable Neighborhood Search for the Vehicle-Routing Problem with Time Windows. *Informs Journal on Computing, vol.15(4),* pp. 347-368.

[143] E. K. Burke, P. I. Cowling, R. Keuthen, "Effective Local and Guided Variable Neighbourhood Search Methods for the Asymmetric Travelling Salesman Problem", *in Boers E.J.W. (eds) Applications of Evolutionary Computing. EvoWorkshops 2001. Lecture Notes in Computer Science,* vol 2037. Springer, Berlin, Heidelberg, 2001.

[144] L. H. Possagnolo, "Reconfiguração de sistemas de distribuição operando em vários níveis de demanda através de uma meta-heurística de busca em vizinhança variável," MSc. Thesis, Universidade Estadual Paulista Júlio de Mesquita Filho, São Paulo, Brasil, 2015.

[145] M. Mladenovic, P. Hansen and D. Perez-Brito. (2001, July). Variable Neighborhood Decomposition Search. *Journal of Heuristics, vol.7(4)*, pp. 335-350.

[146] B. Braden. (1986, Sept.). The Surveyor's Area Formula. *The College Mathematics Journal, vol.17(4)*, pp. 326-337.

[147] EU-SysFlex Consortium. (2018). *EU-SysFlex Project*. Retrieved from https://eu-sysflex.com/

[148] TDX-ASSIST Consortium. (2018). *TDX-ASSIST Project*. Retrieved from http://tdx-assist.eu/

[149] D. A. Contreras and K. Rudion. (2018, June). Improved Assessment of the Flexibility Range of Distribution Grids Using Linear Optimization. in Proc. Power Systems Computation Conf., Dublin, 2018, pp. 1-7.

[150] D. A. Contreras and K. Rudion. (2019, June). Verification of Linear Flexibility Range Assessment in Distribution Grids. *in Proc. IEEE Milan PowerTech*, Milan, 2019, pp. 1-6.

[151] D. A. Contreras and K. Rudion. (2019, Sept.). Impact of Grid Topology and Tap Position Changes on the Flexibility Provision from Distribution Grids. *in Proc. 2019 IEEE PES Innovative Smart Grid Technologies Europe (ISGT-Europe)*, Bucharest, 2019, pp. 1-5.

[152] D. A. Contreras and K. Rudion. (2019, Aug.). Time-Based Aggregation of Flexibility at the TSO-DSO Interconnection Point. *in Proc. Power & Energy Society General Meeting (PESGM) 2019 IEEE*, Atlanta, 2019, pp. 1-5.

[153] D. Mayorga Gonzalez, J. Hachenberger, J. Hinker, F. Rewald, U. Hager, C. Rehtanz and J. Myrzik. (2018, June). Determination of the Time-Dependent Flexibility of Active Distribution Networks to Control their TSO-DSO Interconnection Power Flow. *in Power Systems Computation Conf.*, Dublin, 2018.

[154] F. Capitanescu. (2018, Oct.). TSO-DSO Interaction: Active Distribution Network Power Chart for TSO Ancillary Services Provision. *Electric Power Systems Research, vol. 163*, pp. 226-230.

[155] F. Capitanescu, "OPF Integrating Distribution Systems Flexibility for TSO Real-Time Active Power Balance Management" *in Mediterranean Conference on Power Generation, Transmission, Distribution and Energy Conversion (MEDPOWER 2018)*, Cavtat, 2018.

[156] T. Zhenfei, Z. Haiwang, W. Xuanyuan and T. Honghai. (2020, Aug.). An Efficient Method for Estimating the Capability Curve of a Virtual Power Plant. *CSEE Journal of Power and Energy Systems*.

[157] N. Savvopoulos and N. Hatziargyriou, "Estimating Operational Flexibility from Active Distribution Grids", *in 17th European Energy Market Conference (EEM 2020)*, Stockholm, 2020.

[158] S. Stanković, L. Söder, Z. Hagemann and C. Rehtanz. (2021, Jan.). Reactive Power Support Adequacy at the DSO/TSO Interface. *Electric Power Systems Research, vol. 190.*

[159] S. Riaz and P. Mancarella, "On Feasibility and Flexibility Operating Regions of Virtual Power Plants and TSO/DSO interfaces", *in IEEE Milan PowerTech, Milan*, 2019.

[160] A. Hermann, J. Kazempour, S. Huang and J. Østergaard. (2019, Nov.). Congestion Management in Distribution Networks With Asymmetric Block Offers. *IEEE Trans. Power Systems, vol. 34(6)*, pp. 4382-4392.

[161] J. Saebi and D. T. Nguyen. (2020, June). Distributed demand response market model for facilitating wind power integration. *IET Smart Grid, vol. 3 (3)*, pp. 394-405.

[162] M. Rossi, G. Migliavacca, G. Viagnò, D. Siface, C. Madina, I. Gomez, I. Kockar and A. Morch. (2020, December). TSO-DSO coordination to acquire services from distribution grids: Simulations, cost-benefit analysis and regulatory conclusions from the SmartNet project. *Electric Power System Research, vol. 189.*

[163] C. Kok, J. Kazempour and P. Pinson, "A DSO-Level Contract Market for Conditional Demand Response", in *IEEE Milan PowerTech*, Milan, 2019.

[164] A. Dubey, A. Bose, M. Liu and L. Ochoa. (2020, Jan.). Paving the Way for Advanced Distribution Management Systems Applications. *IEEE Power and Energy Magazine, vol. 18 (1)*, pp. 63- 75.

[165] R. J. Sánchez-Garcia, M. Fennelly, S. Norris, N. Wright, G. Niblo, J. Brodzki and J. W. Bialek. (2014, Sept.). Hierarchical Spectral Clustering of Power Grids. *IEEE Trans. Power Systems, vol. 29 (5)*, pp. 2229- 2237.

[166] D. Vankov, I. Zorin and D. Pozo, "Clustering Time Series over Electrical Networks", *in 2020 International Conference on Smart Energy Systems and Technologies (SEST)*, Istanbul, 2020.

# Annex I – List of Publications

## Publications in Peer Reviewed Conferences:

- S. Stock, L. Lower, S. Wende-von Berg, M. Braun, Z. Wang, W. Albers, C. Calpe, M. Staudt, B. Silva, F. Retorta, **J. Silva** and L. Carvalho, "Operational optimization framework improving DSO/TSO coordination demonstrated in real network operation," presented at the CIRED 2020, Berlin, Germany, 22-23 September, 2020.

- M. Staudt, M. Pfeiffer, Z. Wang, S. Wende-von Berg, B. Silva, F. Retorta, **J. Silva**, L. Carvalho, L. Lower, S. Stock, W. Albers and C. Calpe, "Processes and Systems for Using Flexibility from Distribution Grid to Integrate a High Share of RES in a Resilient, Stable and Efficient Operated Energy Supply System," presented at the 18th Wind Integration Workshop 2019, Dublin, Ireland, 16-18 October, 2019.

- T. Simão, P. Gama, M. Louro, L. Carvalho, G. Gloria, R. Pestana, F. Reis and **J. Silva**, " TDX-Assist: Beyond state of art in TSO-DSO interoperability – The Portuguese demonstrator," presented at the CIRED 2019, Madrid, Spain, 3-6 June, 2019.

- M. Sebastian-Viana, M. Caujolle, B. Goncer-Maraver, J. Sumaili, J. Pereira, P. Barbeiro, **J. Silva** and R.J. Bessa, "LV state estimation and TSO-DSO cooperation tools: Results of the French field tests in the evolvDSO project," presented at the CIRED 2017, Glasgow, Scotland, 12-15 June, 2017.

- **J. Silva**, J. Sumaili, R.J. Bessa, L. Seca and M.A. Matos, "Estimation of active and reactive flexibility range in primary substations," presented at the Workshop on Optimization Challenges in the Evolution of Energy Networks to Smart Grids, Coimbra, Portugal, 27-28 Oct., 2016.

- A.C. Silva, J. Sumaili, **J. Silva**, L. Carvalho, L. Seca, M. Matos, R.J. Bessa, G. Schaarschmidt and R. Hermes, "Assessing DER flexibility in a German distribution network for different scenarios and degrees of controllability," presented at the CIRED 2016, Helsinki, Finland, 14-15 June, 2016.

- N. Fonseca, **J. Silva**, A.C. Silva, J. Sumaili, L. Seca, R.J. Bessa, J. Pereira, M. Matos, P. Matos, C. Morais, M. Caujolle and M. Sebastian-Viana, "evolvDSO grid management tools

to support TSO-DSO cooperation," presented at the CIRED 2016, Helsinki, Finland, 14-15 June, 2016.

## Publications in Peer Reviewed Journals:

- **J. Silva**, J. Sumaili, R.J. Bessa, L. Seca, M.A. Matos and V. Miranda, "The challenges of estimating the impact of distributed energy resources flexibility on the TSO/DSO boundary node operating points," *Computers & Operations Research, vol. 96*, pp. 294-304, Aug., 2018.

- **J. Silva**, J. Sumaili, R.J. Bessa, L. Seca, M. Matos, V.Miranda, M.Caujolle, B. Goncer-Maraver and M. Sebastian-Viana, "Estimating the Active and Reactive Power Flexibility Area at the TSO-DSO Interface," *IEEE Trans. Power Systems, vol. 33 (5)*, pp. 4741- 4750, Sept., 2018.

## Technical Reports:

- J. Sumaili, **J. Silva**, R. J. Bessa, M. Matos, L. Seca, D. Clerici *et al.*, "Advanced Methodologies and Tools for Operation and Maintenance of Distribution Grids with DRES," EC FP7 evolvDSO Project, 2015.

- J. Pereira, J. Sumaili, R. J. Bessa, L. Seca, A. Madureira, **J. Silva** *et al.*, "Validation of the Methodologies and Tools Developed for DSO," EC FP7 evolvDSO Project, 2015.

- R. Caire, M. Sebastian-Viana, M.Caujolle, R. J. Bessa, **J. Silva**, A. C. Silva *et al.*, "Data Collection," EC FP7 evolvDSO Project, 2016.

- R. J. Bessa, **J. Silva**, G. Bartolucci, T. Bongers, R. Hermes, B. Prousch *et al.*, "Impact assessment at country level," EC FP7 evolvDSO Project, 2016.

- L. Carvalho and **J. Silva**, "Network Models for Bandwidth Testing," EC H2020 TDX-ASSIST Project, 2018.

- L. Carvalho, J. Gouveia, T. Soares and **J. Silva**, "Improved TSO/DSO Collaboration Domain Tools," EC H2020 TDX-ASSIST Project, 2019.

- **J. Silva** and L. Carvalho, "New Interval Constrained Power Flow," EC H2020 TDX-ASSIST Project, 2019.

- R. Pestana, T. Simão, L. Carvalho, T. Soares, T. Abreu, **J. Silva** *et al.*, "Exchange Evaluations," EC H2020 TDX-ASSIST Project, 2020.

- L. Lower, S. Wende-von Berg, W. Albers, M. Staudt, B. Silva, **J. Silva** *et al.*, "Optimization tools and first applications in simulated environments," EC H2020 EU-SysFlex Project, 2019.

A new paper, which will be submitted to the IEEE Transactions on Power Systems, is being developed with the research reported in Chapter 4.

# Annex II – Load and DRES data

**Table 8 – Load hourly forecast for a specific time instant**

| Bus Number | Active Load (MW) | Reactive Load (Mvar) |
|---|---|---|
| 1 | 0,064 | 0,0064 |
| 2 | 0,016 | 0,0016 |
| 4 | 0,02696 | 0,002696 |
| 5 | 0,056979386 | 0,005697938 |
| 7 | 0,03504 | 0,003504 |
| 9 | 0,02896 | 0,002896 |
| 13 | 0,02496 | 0,002496 |
| 16 | 0,07392 | 0,00736 |
| 17 | 0,00896 | 0,000896 |
| 19 | 0,002 | 0,0002 |
| 20 | 0,42896 | 0,042896 |
| 24 | 0,03296 | 0,003296 |
| 25 | 0,156 | 0,0156 |
| 28 | 0,00696 | 0,000696 |
| 30 | 0,07392 | 0,00736 |
| 33 | 0,03696 | 0,003696 |
| 34 | 0,03024 | 0,00304 |
| 36 | 0,03024 | 0,00304 |
| 37 | 0,005529154 | 0,000552915 |
| 39 | 0,00304 | 0,000304 |
| 40 | 0,02096 | 0,002096 |
| 45 | 0,012 | 0,0012 |
| 46 | 0,028 | 0,0028 |
| 51 | 0,00304 | 0,000304 |
| 53 | 0,036 | 0,0036 |
| 54 | 0,08896 | 0,008896 |
| 56 | 0,06496 | 0,006496 |
| 58 | 0,03104 | 0,003104 |
| 60 | 0,01696 | 0,001696 |
| 61 | 0,067339274 | 0,006733927 |
| 63 | 0,07496 | 0,007496 |
| 64 | 0,002071978 | 0,000207198 |
| 66 | 0,10896 | 0,010896 |
| 71 | 0,07096 | 0,007096 |
| 72 | 0,016575821 | 0,001657582 |
| 73 | 0,00696 | 0,000696 |
| 74 | 0,06496 | 0,006496 |
| 76 | 0,01896 | 0,001896 |
| 77 | 0,022 | 0,0022 |

| | | |
|---|---|---|
| 80 | 0,02 | 0,002 |
| 81 | 0,04704 | 0,004704 |
| 82 | 0,052 | 0,0052 |
| 84 | 0,00096 | 0,000096 |
| 85 | 0,02696 | 0,002696 |
| 86 | 0,00696 | 0,000696 |
| 89 | 0,00696 | 0,000696 |
| 91 | 0,108 | 0,0108 |
| 92 | 0,06496 | 0,006496 |
| 96 | 0,03296 | 0,003296 |
| 101 | 0,01504 | 0,001504 |
| 105 | 0,024 | 0,0024 |
| 109 | 0,026 | 0,0026 |
| 114 | 0,468 | 0,0468 |
| 121 | 0,04096 | 0,004096 |
| 122 | 0,02096 | 0,002096 |
| 123 | 0,052 | 0,0052 |
| 124 | 0,056 | 0,0056 |
| 128 | 0,042 | 0,0042 |
| 130 | 0,01504 | 0,001504 |
| 133 | 0,03296 | 0,003296 |
| 135 | 0,002 | 0,0002 |
| 139 | 0,25 | 0,025 |
| 141 | 0,03 | 0,003 |
| 143 | 0,008 | 0,0008 |
| 144 | 0,01 | 0,001 |
| 149 | 0,016 | 0,0016 |
| 150 | 0,14096 | 0,014096 |
| 154 | 0,03104 | 0,003104 |
| 157 | 0,038 | 0,0038 |
| 158 | 0,022 | 0,0022 |
| 160 | 0,00496 | 0,000496 |
| 163 | 0,004 | 0,0004 |
| 164 | 0,02296 | 0,002296 |
| 169 | 0,006 | 0,0006 |
| 170 | 0,02096 | 0,002096 |
| 171 | 0,04 | 0,004 |
| 172 | 0,00696 | 0,000696 |
| 174 | 0,128 | 0,0128 |
| 175 | 0,05696 | 0,005696 |
| 176 | 0,36288 | 0,03632 |
| 178 | 0,036 | 0,0036 |
| 180 | 0,01696 | 0,001696 |
| 182 | 0,026 | 0,0026 |
| 184 | 0,03104 | 0,003104 |
| 185 | 0,08696 | 0,008696 |
| 190 | 0,322 | 0,0322 |
| 191 | 0,36288 | 0,03632 |
| 192 | 0,01296 | 0,001296 |
| 195 | 0,00496 | 0,000496 |

| | | |
|---|---|---|
| 199 | 0,026365917 | 0,002636592 |
| 205 | 0,11 | 0,011 |
| 207 | 0,02096 | 0,002096 |
| 208 | 0,016 | 0,0016 |
| 209 | 0,02096 | 0,002096 |

**Table 9 - DRES/DG installed capacity**

| Bus Number | Installed Capacity (MW) |
|---|---|
| 3 | 1 |
| 16 | 0,082 |
| 30 | 0,082 |
| 34 | 0,0173 |
| 36 | 0,0173 |
| 45 | 1 |
| 176 | 0,433 |
| 182 | 2 |
| 191 | 0,433 |